

**A REVIEW OF RESEARCH
ON
AERONAUTICAL FATIGUE IN THE UNITED STATES**

2005 – 2007

Compiled by
Dr. Ravi Chona
Air Force Research Laboratory
Wright-Patterson Air Force Base, Ohio, USA

FOR PRESENTATION AT THE MEETING
OF THE
INTERNATIONAL COMMITTEE ON AERONAUTICAL FATIGUE

14-18 MAY 2007

NAPLES, ITALY

TABLE OF CONTENTS

9.1	INTRODUCTION.....	9/5
9.2	OVERVIEWS	9/6
9.2.1	2005-2006 Structural Activities.....	9/6
9.2.2	Stress Corrosion Cracking in 7079-T6 Sheet.....	9/7
9.2.3	Study of In-Flight Flammability and Inerting on a Boeing 747.....	9/8
9.2.4	Development of Advisory Circulars for Thermal Acoustic Insulation Flammability Tests	9/9
9.2.5	An Evaluation of the Flammability of Aircraft Electrical Wiring and the Adequacy of Current FAA Flammability Requirements	9/10
9.2.6	Guidelines for Adhesively Bonded Aircraft Structures	9/11
9.2.7	Improving Usability and Reliability of Aviation Technical Manuals.....	9/12
9.2.8	Best Practices for Tool Calibration.....	9/13
9.2.9	Evaluating Remote On-Ground Ice Detection Systems.....	9/13
9.2.10	New Guidance on Instrumentation for Icing Certification Flights	9/14
9.2.11	Operating Aircraft in Ice Pellet Conditions	9/14
9.2.12	Assessing Wire Separation and Segregation Arc Damage.....	9/15
9.3	DURABILITY AND DAMAGE TOLERANCE.....	9/16
9.3.1	Three Dimensional Effects on Fatigue Crack Closure Under Fully- Reversed Loading	9/16
9.3.2	Further Development of the NASGRO Software for Fracture Mechanics and Fatigue Crack Growth Analysis.....	9/16
9.3.3	Validation of Stress Intensity Factors	9/17
9.3.4	Residual Strength Finite Element Analysis of C-130 Center Wing Box	9/18
9.3.5	Nonlinear Finite Element Analysis of Stiffened Panels, With and Without Dents.....	9/18
9.3.6	Commercialization of Metallic Materials Properties Development and Standardization (MMPDS)	9/19
9.3.7	Fatigue Crack Growth Methods for Rotorcraft Applications.....	9/20
9.3.8	Integrated Electronics Structural Durability Analysis Tool.....	9/20
9.4	REPAIR AND LIFE ENHANCEMENT	9/22
9.4.1	Fatigue Performance of New Aluminum-Lithium Alloys With Cold Expanded Holes.....	9/22
9.4.2	Long-Term Performance of Bonded Composite Repairs to Metallic Aircraft Structure.....	9/22
9.4.3	Negligible Damage Limits for Dents in Fuselage Structure	9/25
9.4.4	Finite Element Analysis of the Influence of Edge Geometry on Shot Peening Process	9/25
9.4.5	A Simplified Modeling Approach for Predicting Global Distortion Caused by the Installation of Interference Fit Bushings.....	9/33
9.5	COMPOSITES.....	9/34
9.5.1	Composites Affordability Initiative	9/34
9.5.2	Performance of an Improved Composite Joining Concept Under Fatigue	9/37
9.5.3	Characterization of Fatigue Damage in Composite Sandwich Hull Materials at Low Temperatures	9/38
9.5.4	Environmental and Aging Effects on Composite Structures	9/39
9.5.5	Training Maintenance and Repair Personnel for Composite Structures	9/39
9.5.6	Flame Retardant Epoxy Resins Containing Phosphorus for Aircraft Structural Applications.....	9/40

9.6	LOADS	9/41
9.6.1.	HC-130H Center Wing Box Monitoring Program.....	9/41
9.6.2.	Helicopter Component Fatigue Life With Usage Monitor.....	9/42
9.6.3.	Helicopter Rotating Component Fatigue Tracking Using Energy Harvesting Wireless Sensors.....	9/42
9.6.4.	Study of Side Load Factors During Aircraft Ground Operations	9/43
9.6.5.	Loads Data for the Boeing 777	9/43
9.6.6.	Structural Loads on Fire-Fighting Aircraft	9/44
9.7	STRUCTURAL TEARDOWN ASSESSMENTS	9/45
9.7.1	T-37 Structural Teardown Analysis Program.....	9/45
9.7.2	C-130 Center Wing Box Structural Teardown Analysis Program.....	9/45
9.7.3	USAF Handbook for Structural Teardown Analysis Programs	9/46
9.7.4	Assessing the Airworthiness of Commercial Aircraft	9/47
9.7.5	Cracking in Acrobatic Aircraft Fleet	9/47
9.8	NONDESTRUCTIVE EVALUATION/INSPECTION (NDE/I).....	9/49
9.8.1	Crack Detection Under Raised Head Fasteners in High Cycle Fatigue Joints.....	9/49
9.8.2	Development of Nondestructive Inspection Methods for Repairs of Composite Aircraft Structures	9/49
9.8.3	Updating Default Probability of Detection Curves for Ultrasonic Inspection of Hard-Alpha Inclusions in Titanium Billet	9/50
9.8.4	Validating Nondestructive Inspection Technologies With Teardown Data.....	9/51
9.9	RISK ASSESSMENTS	9/52
9.9.1	Risk Quantified Structural Assessment	9/52
9.9.2	Further Development of the Darwin Software for Probabilistic Damage Tolerance Analysis	9/52
9.9.3	Electrical Systems Risk Analysis Tool	9/53
9.10	ENGINES.....	9/54
9.10.1	Rapid Fatigue Cracking of a Wing Lift Strut.....	9/54
9.10.2	Enhanced Life Management Process for Damage Tolerance of Engine Components.....	9/54
9.10.3	Uncontained Engine Debris Damage Assessment Model.....	9/55
9.11	MULTIPLE-SITE DAMAGE (MSD).....	9/56
9.11.1	Damage Characterization of a Lap Joint From a Commercial Aircraft at Design Service Goal	9/56
9.11.2	Development of Multiple-Site Damage in Fuselage Structure	9/56
9.12	ADVANCED STRUCTURES	9/58
9.12.1	Advances in Testing and Analytical Simulation Methodologies to Support Design and Structural Integrity Assessment of Large Monolithic Parts	9/58
9.12.2	Advanced Hybrid Structures and Materials	9/59
9.13	FIGURES/TABLES	9/62

9.1 INTRODUCTION

Leading government laboratories, universities and aerospace manufacturers were invited to contribute summaries of recent aeronautical fatigue research activities. Their voluntary contributions are compiled here. Inquiries should be addressed to the person whose name accompanies each article. On behalf of the International Committee on Aeronautical Fatigue, the generous contribution of each organization is hereby gratefully acknowledged.

GOVERNMENT

- **FAA-ATO-P, R&D**
- **NASA – Johnson Space Center**
- **Swedish Defense Research Agency**
- **USAF Research Laboratory – Air Vehicles Directorate**
- **USAF Research Laboratory – Materials & Manufacturing Directorate**

ACADEMIA

- **Georgia Institute of Technology**
- **University of Illinois**
- **USAF Academy**
- **Wayne State University**

INDUSTRY

- **Alcoa Technical Center**
- **Bell Helicopter Textron**
- **C. J. Roberts & Associates, Inc.**
- **Jacobs ESCG**
- **Southwest Research Institute**
- **The Boeing Company – Seattle**

References, if any, are listed at the end of each article. Figures and tables are compiled at the end of the review.

The assistance of Jim Rudd and Charlotte Burns, Universal Technology Corporation, in the preparation of this review is greatly appreciated.

9.2 OVERVIEWS

9.2.1 2005-2006 STRUCTURAL ACTIVITIES

Jon Cutshall, Southwest Research Institute

Commercial Aircraft

For the last 25 years, SwRI has been involved in structural analysis of aging military aircraft. In 2006, we expanded our program to full-scale static and fatigue certification testing of commercial aircraft designs for the Eclipse 500 very light jet. (Figure 9.2-1) We performed Federal Aviation Administration design certification testing for this new class of jet, and we will continue fatigue testing to extend its certification for additional operating conditions.

T-38 Aircraft Structural Integrity Program (ASIP) Activities:

SwRI has been performing ASIP related work for the T-38 trainer for almost 40 years. (Figure 9.2-2) The ASIP activities during the 2005-06 period for the Ogden ALC at Hill AFB, Utah, includes the following activities:

- Force Structural Maintenance Plan (FSMP) Update
- Durability and Damage Tolerance Analysis – Ground Rules Update
- Flight Data Recorder Program
- Over-G Investigation
- ASIP Master Plan Update
- Analytical Condition Inspection (ACI) and Risk Program
- Durability and Damage Tolerance Analysis (DADTA) Update
- Damage Tolerance Analysis (DTA) of Field Repairs
- Damage Analysis – Horizontal Stabilizer
- Damage Limits for the ROLOC Disc
- Probability of Detection (POD) Evaluation for the Rotoscan Replacement Tool

T-38 Full Scale Fuselage Fatigue Test and Component Economic Life Evaluation

The T-38 aircraft has been utilized by the United States Air Force as its advanced trainer since 1960. Over the years, several structural modifications to the fuselage and wing designs have been implemented to extend the T-38 service life. In order to determine the future structural life of the fuselage and identify other fatigue critical locations, a full-scale durability test, teardown and economic life evaluation has been accomplished for the fuselage. The goal of this program is to determine if the T-38 fuselage can be safely and economically flown until calendar year 2025, or beyond. (see ICAF poster presentation for more details). (Figures 9.2-3 and 9.2-4)

A-10 Aircraft Structural Integrity Program (ASIP) Support Activities:

As part of the A-10 Prime Team led by Lockheed-Martin Systems Integration, Southwest Research Institute (SwRI) is working with the USAF and Northrop Grumman to update the required analyses and inspections for the A-10 ASIP. The team worked together to analyze all of the 100+ necessary fatigue critical control points for the various structural configurations. This update required a significant amount of material testing, which allowed the team to refine the procedures for crack growth retardation parameter determination, and gave insights into spectrum, stress, and geometry effects on retardation. The DTA update allowed the team to also produce a new Force Structural Maintenance Plan outlining the aircraft inspection requirements. In order to implement these requirements, SwRI developed a number of new inspections and documented them in a newly updated technical order for use by inspectors.

To modernize maneuver data recording on the A-10 in the early part of the decade, SwRI designed a new data recording system, and is processing data using newly created processing software. The data is being used to assess the current usage of the fleet in comparison to previously recorded usage. SwRI is also supporting the USAF on a number of fleet repair and finite element analysis issues.

Bonded Repairs

SwRI has been involved with bonded repairs since the mid 1990s. Design, analysis and testing of bonded repairs were made in 2005-2006 under contract to Wright-Patterson AFB. The staff has designed, analyzed, tested and installed bonded repairs for various aircraft. SwRI has designed both metallic and composite bonded repairs for wing skin planks, pressurized transport fuselage structure, and complex three dimensional fighter aircraft bulkheads. (Figures 9.2-5 and 9.2-6)

C-5A Destructive Structural Teardown

Under contract to S&K Technologies, Southwest Research Institute (SwRI) performed destructive teardown inspections on a number of large pieces of structure cut from the forward fuselage, inner wing, and wing-fuselage attachment of a retired C-5A. After disassembly of the individual parts, the subsequent inspections revealed locations exhibiting minor fatigue cracking and some evidence of corrosion, particularly in the forward fuselage near the visor hooks for the hinged canopy.

T-37 Flight Data Recording (L/ESS) and Development of New Stress-To-Load Ratio for ASIP

The overall objective of this United States Air Force (USAF) program was to perform a loads/environment spectra survey (L/ESS), and to determine stress/strain levels at specified aircraft locations for the T-37 structure. The program included the analysis of selected strain gages from one aircraft as part of the development of a new stress-to-load ratio for a specific fatigue critical location (FCL) for future spectrum generation.

A total of five aircraft were involved in the data collection program. Installed in each aircraft were a vertical and lateral accelerometer, velocity and altitude pressure transducers, a roll rate sensor, linear potentiometers on the cables for the aileron and elevator control surfaces, a strain gage on the forward banjo fitting, and the flight loads data recorder (FLDR) system. One aircraft had additional strain gages installed on the wing aft lower rear spar caps (left and right). These gages along the aft spar cap were used to develop the new stress-to-load ratio for the FCL.

9.2.2 STRESS CORROSION CRACKING IN 7079-T6 SHEET

Molly Walters, United States Air Force Academy

Abstract

The Center for Aircraft Structural Life Extension (CAStLE) at the United States Air Force Academy has been assigned to study stress corrosion cracking (SCC) in AA7079-T6 as part of the 646th Aeronautical Systems Squadron. CAStLE was introduced to this problem by Lockheed-Martin, the manufacturer of the C-5A, to resolve potential problems in the home station check (HSC) modeling techniques. Currently, models are being generated by data from thick sheet SCC testing which are assumed to be very conservative. Also, a material properties report has been used that was developed by an unknown contractor about thirty years ago. The details of the test are unknown, essentially making the data unusable.

Results generated by CAStLE have justified the short inspection intervals thus far. Various load types and environmental types have been tested. Loads were introduced to the specimen by constant displacement, constant load, and K-controlled tests, where active feedback was used to generate a load command in LabView in conjunction with test frame software. Three environment types were used, also. Deionized water fog, saturated salt bath, and 3.5 mol% NaCl baths were tested.

In each of the salt-containing environments, crack growth rates were faster than those previously published in 1977. The deionized water fog created crack growth rates below the previously published rates. All three load types added worthwhile data to the program and acted similarly on the crack growth rate versus stress intensity scale.

Later in testing, the group was posed with the problem of SCC combined with fatigue, since this would be a more accurate account of in-service cracking. Alternate load methods were used as the crack propagated through the

specimen. It was found these values could be superimposed to obtain the results as if alternate loading had occurred on the specimen.

Background

For this effort, specimens were taken from actual C-5A aft crown skin material, where this problem in the fleet resides. The sheet was then machined by electrical-discharge machining (EDM) into ESE(T) specimens and pre-cracked in accordance with ASTM E647. The schematic for an ESE(T) specimen is Figure 9.2-7.

The specimen was instrumented using a back face strain gage in order to calculate crack opening. Data on the strain gage was taken at regular intervals. Load readings were also done concurrently. This generated data for load and crack opening displacement, which was later reduced to crack growth rate vs. stress intensity data.

Progress

CAStLE will continue to pursue SCC-Fatigue tests, but with a slightly higher stress intensity amplitude. Tests were done at ± 2 ksi $\sqrt{\text{in}}$. Next, ± 4 ksi $\sqrt{\text{in}}$ will be studied. It has been assumed that if specimens are exposed to fatigue at a higher frequency than 10Hz, a state of submersion will not effect the crack growth.

Results

CAStLE designed and built a test frame in-house in order to complete constant displacement tests. Constant load tests were performed on closed loop, computer-controlled servo-hydraulic fatigue test frames. K-controlled tests were done using LabView with active feedback on the same fatigue test frames. Deionized water fog was exposed to the specimen by enclosing it in a clear section of PVC and forcing warm vapor into the chamber. Humidity levels were assumed to be sufficient if condensation was present. Specimens were exposed to a bath by sealing a plastic cup to a specimen with RTV silicone. The seal easily held until the end of the test.

As suspected, the behavior of the samples as a result of the load method was dependent of stress intensity only, see Figure 9.2-8.. Also, the three environments used were least severe to most severe in the following order: deionized water fog, 3.5 mol% NaCl bath, and saturated salt bath. The two salty baths had crack growth rates above the published values, where the deionized water fog exposure led to rates less severe than the published data.

True K_{ISCC} tests were not done, as they take upwards of 1000 days to complete. The closest results to K_{ISCC} that were acquired were slightly higher than the original results. This could be assumed to be an excellent factor of safety if current crack growth rate predictions were based on those lower K_{ISCC} values. Also, it can be noted that no unstable crack growth was measured for any specimens tested. Crack growth rates were measured until failure, but the frequency of data recording most likely was not able to communicate this data. Also, this area of the curve was not in the customer's particular interest.

9.2.3 STUDY OF IN-FLIGHT FLAMMABILITY AND INERTING ON A BOEING 747

William Cavage, Federal Aviation Administration, ATO-P, R&D

Significant emphasis has been placed on fuel tank safety since the TWA Flight 800 accident in July 1996. This prompted the FAA to study methods that could limit the flammability exposure of fuel tanks in the commercial transport fleet. The effort was focused on high-flammability exposure fuel tanks: center wing and body-style fuel tanks. Extensive development and analysis by the Fire Safety Branch has shown that fuel tank inerting during aircraft operation could be cost-effective if air separation modules (ASM) could be integrated into an inert gas generation system in an effective manner. Also, the study of center wing fuel tank ullage flammability through the use of scale experiments and analytical models has been extensively pursued by the FAA. This research has led to a more complete understanding of both the inerting requirements and the factors that affect the flammability exposure for a commercial transport airplane fuel tank.

To demonstrate the use of hollow-fiber membrane ASMs for inerting commercial transport airplane fuel tanks, the FAA, with the assistance of several aerospace companies, developed a prototype onboard inert gas generation

system (Figure 9.2-9) that uses aircraft bleed air to generate nitrogen-enriched air (NEA) at varying flows and purities (NEA oxygen concentration) during a commercial airplane flight cycle. Additionally the FAA developed models and experimental methods to study the progression of flammability of an aircraft fuel tank throughout a typical flight cycle.

In conjunction with NASA aircraft operations personnel, a series of ground and flight tests were performed to evaluate the simplified inerting system and examine the flammability of both the center wing and one inboard wing fuel tank. The FAA inerting system was mounted in the pack bay of the NASA 747 SCA, which is used for transporting the Space Shuttle Orbiter (Figure 9.2-10). During testing the inerting system was operated while fuel tank oxygen concentration and flammability were measured using special instrumentation developed by the FAA. This gave a complete picture of the ability of the inerting system to reduce the flammability exposure of a commercial airplane center wing tank (CWT).

The results of the testing indicated that the FAA inerting system operated as expected. Inerting system warm-up times had no measurable effect on the ability of the system to keep the ullage inert during typical commercial transport flight conditions. (Figures 9.2-11 and 9.2-12) Using a variable flow methodology allowed for a greater amount of NEA to be generated on descent at a higher oxygen concentration (lower purity) as intended and allowed for improved inert gas distribution by decreasing the worst bay oxygen concentration. All assumptions concerning ground operations and aircraft turn-around with an inert ullage were validated. Flammability measurements from both the CWT and the wing tank showed trends consistent with experimental and computational analysis previously performed and allowed for the potential improvement of ullage flammability models.

A description of the flight test program and findings are contained in FAA technical report DOT/FAA/AR-04/41, "Evaluation of Fuel Tank Flammability and the FAA inerting system on the NASA 747 SCA," authored by Mike Burns, William Cavage, Robert Morrison, and Steven Summer.

9.2.4 DEVELOPMENT OF ADVISORY CIRCULARS FOR THERMAL ACOUSTIC INSULATION FLAMMABILITY TESTS

Tim Marker, Federal Aviation Administration, ATO-P, R&D

On September 1, 2003, a new FAA rule was passed pertaining to the flammability of thermal acoustic insulation used in transport category aircraft. The new rule established two new tests, the first aimed at measuring the material's capability of resisting flame spread from a small ignition source, and the second used to determine the ability of the material to resist penetration or burn through from an external fuel fire. A radiant panel is used to conduct the flame spread test, while an oil-fired burner is used to simulate the external fire in the burnthrough test. Both of these tests are significantly more severe than the previous test method used to qualify insulation materials, the vertical Bunsen burner.

Although the new tests have been further developed and refined over the past 2 years, many details still exist with regard to the conduct of these tests and the installation of insulation blankets in an aircraft. In terms of flame propagation, for example, many components of the blanket system such as tape and "hook and loop" fasteners must also be tested, since they are considered part of the blanket system and have been shown to have an influence on whether the material will propagate a fire. In the case of measuring the burnthrough resistance of insulation, although the test is now well established, it is important that a blanket meeting the requirement be properly installed and attached to the aircraft structure in order to recognize the full benefit of its fire resistance. A highly burnthrough resistant blanket will be of no value in a crash accident if it is easily displaced during the fire due to insufficient attachment hardware.

To ensure that all of these additional details are properly addressed, Advisory Circulars (ACs) have been developed for both new test methods based on results from the research. The radiant panel AC, 25.856-1 describes the test methodology and pass/fail criteria for evaluating the flammability of insulation blankets containing sub-components, not just the basic elements such as the thin moisture barrier and encapsulated batting material. The most common sub-components or detail materials include thread, tape, and hook and loop. In addition, damping material that is not part of the traditional insulation blanket assembly must also be tested. Although there is practically an infinite number of possibilities in terms of blanket arrangement, the AC describes a simple plan for reducing the number of

tests, while not compromising safety. Tapes, for example, are used during initial production and also in the process of making repairs to aircraft in service. Since it is not practical to test each possible configuration of tape and film/batting material, a simplified process using strips of tape has been developed. As shown in Figure 9.2-13, four 2-inch strips of tape are installed on the test blanket from right to left, with a one-half inch overlap for successive strips.

In addition to the detail materials integrated into the typical blanket, there are also structural damping materials, which may be considered thermal/acoustic insulation, depending on their specific configuration and use. Although small aluminum sheets bonded directly to the airplane skin would not be considered insulation, materials that include a layer of foam or other material sandwiched between the skin and thin aluminum sheets should be tested. The most important aspect of testing this type of design is to ensure that the interface between the insulating material and the substrate is exposed to the tip of the burner flame.

The burnthrough AC, 25.856-2 describes the appropriate methods of installing the insulation in an aircraft, which is important in fully realizing the benefits of improved materials. To date, numerous thermal/acoustic insulation materials have been successfully tested, and these materials can be classified into three basic categories: batting systems, barrier systems, and encapsulating systems. The AC describes each of the system types, and an appendix lists schematic examples of each.

In addition to these examples, the AC focuses on specific installation aspects, highlighting key areas that include blanket overlap at frame members, horizontal blanket overlap, penetrations, and types of installation hardware. Previous testing has shown that a certain level of blanket overlap at the frame member is essential in maintaining a continuous burnthrough barrier, as shown in Figure 9.2-14. A detailed test methodology for evaluating the burnthrough resistance of two horizontally overlapped blankets is also included in the AC.

Although schematic descriptions of acceptable installation techniques are included, the AC also describes the appropriate test methodology for evaluating system performance in the event that an alternative approach is desired. This methodology includes a description of the test apparatus modifications necessary to fully evaluate any unconventional approach.

In the case of both ACs, this guidance material is primarily aimed at airframe manufacturers, modifiers, foreign regulatory authorities, and FAA type certification engineers and their designees. While these guidelines are not mandatory, they are derived from extensive FAA and industry experience in determining compliance with the relevant regulations.

An electronic version of the radiant panel AC can be found at <http://www.airweb.faa.gov/rg1> Although an electronic version of the burnthrough AC is not yet available, it will also be posted on this site in the near future.

9.2.5 AN EVALUATION OF THE FLAMMABILITY OF AIRCRAFT ELECTRICAL WIRING AND THE ADEQUACY OF CURRENT FAA FLAMMABILITY REQUIREMENTS

Pat Cahill, Federal Aviation Administration, ATO-P, R&D

Life threatening in-flight fires usually originate in hidden areas of the airplane, such as the attic above the cabin ceiling, beneath the floor, in or around the lavatories, or at similar locations that are difficult to access. Because of the occurrence of in-flight fires in recent years, the FAA is examining the adequacy of its flammability test requirements for all hidden materials. The focus will primarily be on thermal acoustic insulation, electrical wiring, and heating, ventilation, and air conditioning (HVAC) ducting.

The genesis for the current FAA flammability test requirement for electrical wiring was Amendment 25-32, effective May 1, 1972, which added a new section 25.1359(d), which applied the flammability requirements of Appendix F of Part 25 to wire insulation used in aircraft. Section 25.1359(d) is now Section 25.869 in 14 CFR Part 25. The mandated test specifies that insulation on electrical wire or cable installed in any area of the fuselage must be self-extinguishing when subjected to the 60° test specified in Part I of Appendix F. The requirements state that the average burn length may not exceed 3 inches and the average flame time after removal of the 3-inch Bunsen burner flame source may not exceed 30 seconds. Drippings from the test specimen may not continue to flame for

more than an average of 3 seconds after falling. This is the only test the FAA mandates for aircraft wire flammability.

TEST PROGRAM

60° Flammability Testing

The results of the 60° flammability tests performed in this program are shown in Table 9.2-1.

The data in Table 9.2-1 shows that all wires and cables passed this test except PVC/nylon wire, which exhibited the longest burn length and after flame time and the zero halogen cable. Note that the zero halogen cable had an average after flame of 60.3 seconds and an average burn length of 3.1 inches, which barely exceeded the 3-inch requirement. These samples did not propagate the flame but continuously burned in place (evolving gases) with no drippings. The 60° test does not discriminate very well between the performance of different materials. For those materials that were compliant with the 60° test requirement, the difference in burn length for the best material (PTFE/polyimide/PTFE) and the worst materials (plenum cable A, riser cable A, and riser cable, CMR CAT 5E) was only 1.3 inches. Only one material exhibited after flame (Spec 2112) and the value was very small (1.7 inches) with no drippings.

Intermediate- Scale Testing

In this phase of testing, 5 of the original 12 types of wire and cable were evaluated. They included PTFE/polyimide/PTFE, Tefzel™, Spec 2112, riser cable (A), and PVC/nylon. These constructions were selected based on the data from the 60° flammability tests and widespread use in commercial and general aviation aircraft. The PTFE/polyimide/PTFE construction was the overall best performer. The Tefzel™ and Spec 2112 constructions were selected because they are widely used. The PVC/nylon construction was included as a worst-case scenario and the riser cable (A) as the only non-aviation grade wire.

Intermediate Scale Testing (Second Configuration)

In order to verify the findings from the first intermediate test, two further tests were run. The PTFE/polyimide/PTFE and the riser (A) cable were chosen because the data showed them as being the best and the worst (disregarding PVC/nylon) in terms of wiring compliance with the 60° test. Also, spacing of the bundles appeared to have a bearing on the degree of flame propagation. In this series of testing, the wire bundle configuration was changed. Instead of intersecting the bundles, they were placed in the lengthwise direction only. Also, the test area was halved. Figure 9.2-15 shows stages of the riser (A) cable burn.

Based on the test data, the 60° flammability test may not disqualify wiring that propagates a fire when subjected to a severe ignition source used by the FAA to upgrade the fire test criteria of hidden fires. The test results are documented in Technical Note, DOT/FAA/AR-TN04/32, "An Evaluation of the Flammability of Aircraft Wiring."

9.2.6 GUIDELINES FOR ADHESIVELY BONDED AIRCRAFT STRUCTURES

Curtis Davies, Federal Aviation Administration, ATO-P, R&D

The FAA undertook a number of activities in 2005 and 2006 to evaluate the adequacy of current certification requirements for adhesive bonded aircraft structures. Adhesive bonding is used in many manufacturing and repair applications for aircraft structures. The technical issues for bonding are complex and require cross-functional teams for successful applications. Researchers looked at bonding composite-to-composite, metal-to-metal, and composite-to-metal structures to acquire knowledge about these construction and repair methods. They conducted a survey to benchmark industry practices and collect information on the safety issues and certification considerations for bonded aircraft structures and repairs. Thirty-eight companies with experience and history in adhesive bond manufacturing and repair practices responded to the survey. After reviewing the survey results, the FAA sponsored workshops to gather additional information. 142 representatives from industry, academia, and governmental agencies representing 70 companies, universities, and governmental agencies attended the first workshop. A second workshop, held in

Europe, provided international input about areas that need to be addressed to enable the safe and reliable application of adhesive bonding in manufacturing aircraft. This cooperative effort of industry, government groups, and academia led to the development of initial guidelines. Future joint efforts by the FAA, industry, and academia will lead to recommendations on standardization, engineering guidelines, shared databases, and focused research for bonded structures.

9.2.7 IMPROVING USABILITY AND RELIABILITY OF AVIATION TECHNICAL MANUALS

Michael Vu, Federal Aviation Administration, ATO-P, R&D

Aviation maintenance technical manuals have been in use from the earliest days of flight. Technical manuals have grown in volume and weight as aviation systems have become more complex and sophisticated. The process for making page-by-page changes to these manuals has grown increasingly cumbersome and expensive.

There is a growing body of evidence that the current generation of technical manuals may contain an unacceptable level of built-in errors generated from within the publication process. Tasks that are inadequately or incorrectly described are likely to generate process errors. Process errors, in turn, can lead to equipment failure and costly rework.

The NTSB Accident and Incident database contains instances where technical manuals were a primary or contributing cause. For example, one instance from the mid-1990's involved a jet engine that was incorrectly installed due to errors in technical documentation, and which subsequently fell off at an overseas location. A more recent incident involved push rod bolts that were installed incorrectly. FAA research also identified that maintenance personnel feel that procedures were often inefficient or difficult to perform as described in technical manuals. FAA research also identified that the aviation technical writing community is largely unfamiliar with evaluative techniques (task analysis, cognitive walk through) that can be employed to enhance the quality of technical documentation.

Research was done to identify techniques for improving the process of developing and updating aviation technical manuals. The research was conducted under a cooperative agreement with Wichita State University National Institute for Aviation Research (NIAR).

Working with the aircraft manufacturers (Raytheon, Bombardier, Cessna, and Boeing), the research team conducted experiments with the engineers and technical writers to identify the most effective techniques for developing and validating maintenance procedures for technical manuals.

Based on the research results, an Evaluation Toolbox for Aviation Technical Writers (<http://www.niar.twsu.edu/humanfactors/toolbox/default.htm>) was developed. The on-line toolbox contains concepts, evaluation methods, tools, templates, and references to educate and assist technical writers in developing better technical documentation.

In June 2005, a workshop sponsored by the FAA, the NIAR, and the aircraft manufacturers, was held at the Cessna Conference Center, Wichita, Kansas, to disseminate the research results. About 50 technical writers from the aircraft manufacturers, and representatives from the FAA, NTSB, Boeing, as well as directors of technical publication from Cessna, Bombardier, and Raytheon, participated in the workshop.

The local general aviation manufacturers are working with the Kansas Technology Enterprise Corporation (KTEC), a private/public partnership established by the state of Kansas to promote technology-based economic development, to develop a training program for technical writers based on the research results. The research results will also be used by the FAA to develop an Advisory Circular.

9.2.8 BEST PRACTICES FOR TOOL CALIBRATION

Michael Vu, Federal Aviation Administration, ATO-P, R&D

With technological advances in aircraft design and manufacturing, airplanes are becoming increasingly sophisticated and complex machines. The safe and efficient operation of modern airplanes depends on a proper maintenance program, which requires the use of many precision tools. As mandated in Parts 43.13 (a) and 145.47 (b) of the Title 14 Code of Federal Regulations, the FAA requires aircraft repair station personnel to inspect and calibrate tools to ensure their reliable and accurate performance. A repair station typically develops and uses an internal program to perform and manage the calibration of tools. However, no single standard exists within the aviation community to provide uniform guidance for the development of an effective tool calibration program.

Under a cooperative agreement with the Wichita State University National Institute for Aviation Research, the research team developed calibration “best practices” that could help to establish an effective tool calibration program. Based on a literature review and an analysis of about 10,000 records of the FAA Program Tracking and Reporting System, the researchers identified and developed possible solutions to address major areas of concern. These areas include calibration due date, missing tags and stickers, lack of control, personnel errors, missing records, and traceability. The researchers also shadowed FAA inspectors visiting repair stations to gain field experience and assess the practicality of the proposed solutions.

In May 2006, the research team proposed a calibration management structure that incorporates guidance for best practices in areas such as environmental controls, calibration frequencies and intervals, calibration labeling, personnel and training standards, effective tracking and control, calibration subcontracting, the handling and storage of calibration instruments, calibration certificates, documentation, measurement traceability, and internal audits. The team developed two new checklists to help FAA inspectors in monitoring compliance with the tool calibration requirement. To provide the FAA with guidance on how to approve calibration of foreign-made tools, the research team recommended a path in which a source country’s eligibility can be determined through its association with international accreditation bodies. The FAA plans to use these research results to develop advisory circulars applicable to the tool calibration program.

9.2.9 EVALUATING REMOTE ON-GROUND ICE DETECTION SYSTEMS

James T. Riley, Federal Aviation Administration, ATO-P, R&D

Undetected ice remaining after the deicing process can cause dangerous lift loss during takeoff. This is a critical issue for all aircraft, but especially for hard wing regional jets. In 2006, FAA Flight Safety researchers, scientists in the FAA Human Factors programs, and personnel at the Transport Canada Transportation Development Center teamed to determine the effectiveness of two prototype remote on-ground ice detection systems (ROGIDS). Using a special camera, ROGIDS captures and interprets the infrared reflections given off by ice on critical aircraft surfaces. In preparation for future regulatory approval of a commercial version of ROGIDS, researchers first determined how well deicing personnel detected ice by traditional visual and tactile methods. Those results provided the baseline to evaluate the ability of the two ROGIDS prototypes to detect ice on an aircraft wing.

The ice samples used were beneath a residual layer of deicing fluid typical of what would remain on an aircraft wing after the deicing process is completed. The first study showed that deicing personnel can easily detect very thin ice by touch when the sample is contained in a small area, but they have a much more difficult time seeing clear ice on bare and painted aircraft aluminum surfaces. The study showed that despite the impressive sensitivity of human fingers to ice, the abilities of one ROGIDS prototype were significantly superior to those of experienced deicing personnel (who performed both the visual and the tactile inspections) in detecting ice patches of varying areas and thicknesses scattered on an aircraft wing. The other ROGIDS prototype, which had not had a significant amount of shakedown testing prior to this test, proved to be roughly equivalent to the deicing personnel. As a result of these tests, the FAA and Transport Canada Flight Standards organizations feel ROGIDS has potential to increase the level of safety in icing conditions with further work.

Two reports document these tests: Human Visual and Tactile Ice Detection Capabilities under Aircraft Post Deicing Conditions (DOT/FAA/TC-06/21) and Comparison of Human Ice Detection Capabilities and Ground Ice Detection System Performance under Post Deicing Conditions (DOT/FAA/TC-06/20). Both reports are available online at

http://www.tc.faa.gov/acb300/330_documents.asp. Researchers presented the results of these tests at the SAE Committee G-12 (Ground Deicing) annual meeting in Lisbon, Portugal, on May 24, 2006, and at the Human Factors and Ergonomics Society Conference in San Francisco, October 19 and 20, 2006.

9.2.10 NEW GUIDANCE ON INSTRUMENTATION FOR ICING CERTIFICATION FLIGHTS

James T. Riley, Federal Aviation Administration, ATO-P, R&D

Federal aviation regulations, such as Title 14 Code of Federal Regulations (CFR) 25.1419, "Ice Protection," require flight tests in measured natural or simulated icing conditions for aircraft being certificated for flight in icing conditions. Different aircraft manufacturers have employed different types of instrumentation to measure the relevant icing cloud variables, primarily water content, droplet sizes, and temperature. The available instrumentation ranges from the simple to the complex, from the old to the new, and from the relatively inexpensive to the expensive. Most of the instrumentation comes from the cloud physics research community. The use of this technology requires a certain amount of knowledge and experience to ensure that the probes are properly installed, calibrated, and operated. In addition, all probe types can have subtle systemic errors that may be difficult for the inexperienced operator or data analyst to recognize.

As a result of these complexities, FAA Aircraft Certification Offices (ACO) have either had to rely on the aircraft manufacturers to supply adequate instrumentation and technicians, or they have had to hire experienced contractors to install and operate suitable instrumentation and analyze the icing cloud data.

To provide advice to the ACOs and to help standardize policy and procedures for icing certification projects, research was done to provide technical data on the variety of instrumentation used to analyze and measure the properties of the icing conditions experienced during test flights. The result was the 2006 publication of a set of four technical notes:

- DOT/FAA/AR-TN06/29, "Cloud Sampling Instruments for Icing Flight Tests: (1) Icing Rate Indicators"
- DOT/FAA/AR-TN06/30, "Cloud Sampling Instruments for Icing Flight Tests: (2) Cloud Water Concentration Indicators"
- DOT/FAA/AR-TN06/31, "Cloud Sampling Instruments for Icing Flight Tests: (3) Cloud Droplet Sizers"
- DOT/FAA/AR-TN06/32, "Cloud Sampling Instruments for Icing Flight Tests: (4) Large Drop Sizers"

These reports provide information on the suitability, procedures, and precautions for the most commonly used instruments for measuring icing rate, cloud water concentration, and droplet sizes in natural clouds or airborne tankersprays. They also include advice on the data quality assurance, data processing, and presentation of results. The technical notes are intended to be a ready reference for ACOs, designated engineering representatives, aircraft manufacturers, and other interested parties. They can be found at <http://actlibrary.tc.faa.gov>.

9.2.11 OPERATING AIRCRAFT IN ICE PELLET CONDITIONS

James T. Riley, Federal Aviation Administration, ATO-P, R&D

Under certain atmospheric conditions, precipitation falls on aircraft as pellets of ice. From 1992 to 2004 many air carriers were allowed to operate in ice pellet conditions provided the flight crew did a contamination check of the wings within five minutes of takeoff. For most passenger aircraft, this check was conducted from inside the aircraft, but for freighters, which generally have no cabin windows, it was done from the outside. Operations in the presence of ice pellets were incorporated into the deicing and anti-icing programs of many individual air carriers and were approved annually by the Principal Operations Inspector for those carriers.

Recently, due in part to Agency and industry concerns, the FAA decided to reassess its policy with respect to operation in ice pellet conditions. At the request of Flight Standards Service, the Flight Safety Branch, in cooperation with Transport Canada, conducted relevant runway testing in Canada in March 2006. Using a turbine powered aircraft, they simulated ice pellet contamination in a specific type of anti-icing fluid on the wing. Type IV is the thickened (viscous) anti-icing fluid commonly used by airlines in North America. The aircraft was accelerated to rotation speed, and then stopped. Crushed ice from blenders was used to simulate ice pellets. The ice

mixture was run through sieves to get a size distribution similar to natural pellets. Known quantities were distributed over the wing from modified hand held seed spreaders. The results indicated that, when the aircraft was protected with Type IV anti-icing fluid, the simulated pellets would readily flow off prior to rotation. A review of the research indicated that a 25-minute allowance after anti-icing in light ice pellets afforded a large safety margin, and Flight Standards has since approved that allowance as sufficient to ensure a safe takeoff from most airports.

9.2.12 ASSESSING WIRE SEPARATION AND SEGREGATION ARC DAMAGE

Michael Walz, Federal Aviation Administration, ATO-P, R&D

At the FAA Arc Fault Evaluation Laboratory, researchers have developed a new method for quantifying electrical hazard damage. To develop this method, the research team used arc damage assessment data and separation and segregation of electrical systems data to quantify the damage electrical systems can impose on adjacent electrical and non-electrical systems. Using this new method, they can now determine minimum distances needed between certain electrical bundles to avoid catastrophic damage (loss of functionality of critical systems) and loss of system function. Data from this method will support the development of guidelines on safe separation and segregation distances.

9.3 DURABILITY AND DAMAGE TOLERANCE

9.3.1 THREE-DIMENSIONAL EFFECTS ON FATIGUE CRACK CLOSURE UNDER FULLY-REVERSED LOADING

Robert H. Dodds, Jr., University of Illinois

The increase in crack opening loads (K_{op}) caused by plasticity-induced closure of fatigue cracks plays a key role in estimates of growth rates in structural metals, specifically for thin-sheet materials in common aircraft construction. Under conditions of small-scale yielding, our prior work [1] investigates the existence of a similarity-scaling parameter, $\bar{K} = K_{max} / \sigma_0 \sqrt{B}$, that scales the effects of differing peak load (K_{max}), component thickness (B), and material yield stress (σ_0) on K_{op} / K_{max} across varying materials and loading levels. Here K denotes the average, Mode I stress-intensity factor across the crack front. The work summarized in [2] explores the applicability of this scaling parameter to specimens-components under fully-reversed (*i.e.* $R = -1$) cyclic fatigue loading. The solution for a single value of \bar{K} maybe “unnormalized” to represent a remarkable range of practical conditions. Figure 9.3-1 illustrates the computational model for a “thin” cracked component. The research supports the following conclusions:

- (1) Under SSY conditions with zero T -stress and constant-amplitude, cyclic $R = -1$ loading, the magnitude of K_{op} / K_{max} at each location along the crack front remains unchanged when K_{max} , thickness (*i.e.*, crack-front length), and material yield stress all vary to maintain a fixed value of $\bar{K} = K_{max} / \sigma_0 \sqrt{B}$. This scaling parameter defines a versatile quantifier of opening load behavior across various specimens (see Figure 9.3-2).
- (2) At low levels of normalized remote stress ($\sigma_{R-max} / \sigma_0 < 0.03$), specimens-components with stress ratios of both $R = 0$ and $R = -1$ subjected to constant-amplitude, cyclic loading (and zero T -stress) exhibit similar crack opening loads at the same value of $\bar{K} = K_{max} / \sigma_0 \sqrt{B}$.
- (3) At higher loads for $R = -1$, the entire crack front responds almost uniformly with small differences between the centerplane and outside surface, and with small opening load levels. In contrast, the $R = 0$ case at higher load levels shows a continued, larger difference in opening loads between the centerplane and outside surface, with the larger opening loads moving to the centerplane location (see Figure 9.3-3).

REFERENCES:

- [1] RoyChowdhury S, Dodds Jr RH. Three-dimensional model for overload effects on fatigue crack closure in the small-scale yielding regime. *Fatigue Fract Engng Mater Struct* 2005;28:891–907.
- [2] Carlyle A, Dodds, Jr RH. Three-dimensional effects on fatigue crack closure under fully reversed loading. *Engng Fract Mech* 2007;74:457–466.

9.3.2 FURTHER DEVELOPMENT OF THE NASGRO SOFTWARE FOR FRACTURE MECHANICS AND FATIGUE CRACK GROWTH ANALYSIS

Craig McClung, Joseph Cardinal and Brian Gardner, Southwest Research Institute

Joachim Beek and Royce Forman, NASA Johnson Space Center

Venkataraman Shivakumar, Randall Christian, Yajun Guo and Leonard Williams, Jacobs ESCG

The NASGRO® software for fracture mechanics and fatigue crack growth analysis continued to be actively developed and widely used during 2005 and 2006.

NASGRO Version 4.2 was released for general distribution in January 2005. New stress intensity factor (SIF) solutions (see Figure 9.3-4) included univariant weight function (WF) solutions for center and edge through cracks and a second-generation bivariant WF solution for a corner crack. Cyclic shakedown capabilities were added to calculate stress relaxation and redistribution due to local yielding for commonly used WF crack cases. Load history

input was enhanced to include temperature as an optional parameter. Crack growth rate properties can now be stored as a function of temperature, and interpolation is used to calculate crack growth rates on each cycle at intermediate temperatures. New load spectrum visualization capabilities included exceedance diagrams, histograms, and spectrum statistics. Residual strength diagrams based on fracture and/or net section yield were added for all through-crack models.

NASGRO Version 5.0 was released for general distribution in August 2006. New SIF solutions (see again Figure 9.3-4) included a bivariant WF solution for a corner crack at an offset hole, a univariant WF solution for an offset surface crack at an offset hole, and the standard ESE(T) specimen. New interpolation schemes were added for one-dimensional data table solutions. New spectrum editing features included clipping, truncation, randomization, and enhanced cycle counting, as well as an advanced editing scheme (based on crack closure theory) that removes non-damaging cycles from a complex history. A spectrum generation feature was added to identify cycles in arbitrary stress-time histories. An additional interpolation scheme based on the Walker model was added for tabular da/dN data. A redesigned GUI was introduced for the NASBEM boundary element module.

The Alpha development version of NASGRO 5.1 was released for evaluation in November 2006, with production release targeted for summer 2007. New SIF solutions (see again Figure 9.3-4) included a displacement-controlled through edge crack, a univariant WF solution for a through edge crack in a variable thickness plate, a bivariant WF solution for an offset surface crack in a plate, and enhancements of several existing solutions. New or enhanced net section yield solutions were added for 43 crack cases. The most commonly used univariant WF solutions now accept direct input of static residual stress fields and employ enhanced point-spacing algorithms for all stress fields. Residual strength diagram capabilities were added for all corner, surface, and embedded cracks and one-dimensional data tables.

NASGRO has been jointly developed by NASA and Southwest Research Institute since 2001, with substantial financial support from NASA, the NASGRO Consortium, and the Federal Aviation Administration (FAA). The NASGRO Consortium was in its second three-year cycle during 2005-2006, and the international participants included Airbus, Boeing, Bombardier Aerospace, Embraer, Hamilton Sundstrand, Honeywell Aerospace, Israel Aerospace Industries, Lockheed Martin, Mitsubishi Heavy Industries, Northrop Grumman, Siemens Power Generation, Sikorsky, and Volvo Aero. NASGRO is the standard fracture control software for all NASA Centers and is also used extensively by NASA contractors, the European Space Agency (ESA) and ESA contractors, and FAA Designated Engineering Representatives certified for damage tolerance analysis. In addition to Consortium members and other site licenses, over sixty single-seat commercial NASGRO licenses were issued in 2005-2006.

Further information about NASGRO is available at www.nasgro.swri.org.

9.3.3 VALIDATION OF STRESS INTENSITY FACTORS

Scott A. Fawaz and Daniel W. Hill, Center for Aircraft Structural Life Extension (CASTLE), United States Air Force Academy and Borje Andersson, Swedish Defense Research Agency

Population of the world's largest database of stress intensity factor (K) solutions began in 2002 with the calculation of 5.6 million K solutions for diametrically opposed unsymmetric corner cracks at a straight shank hole in a finite width sheet subject to remote tension, remote bending, and bearing loading. Previous work to validate these K solutions was in the form of fatigue life predictions and crack shape development. The current work builds on the previous validation efforts with the addition of comparing the calculated K solutions with K solutions obtained from carefully controlled laboratory experiments. The latter are obtained via fatigue striation measurements at high magnification, up to 40,000X, using a scanning electron microscope and crack growth rate data, in terms of da/dN vs. ΔK at the same test condition. An additional eight million K solutions have been calculated and added to the database for diametrically opposed unsymmetric corner cracks at a 100° countersunk hole in a finite width sheet subject to remote tension, remote bending, and bearing loading. The validation for this latter set of K solutions is limited to corner cracks that do not intersect the countersunk edge of the fastener hole. Furthermore, due to the complexity of pin loaded holes and the sensitivity of the crack growth life, K solution, to the boundary and loading conditions of the hole; the validation effort only considers remote tension and remote bending. The results show the numerical K solutions are within 20% of the experimentally derived K 's at discrete locations along the crack front. The relatively large error is due to the discontinuous crack extension process of the crack front. Moreover, the entire crack front

does not instantaneously extend uniformly in a self similar fashion. The crack extends stepwise over discrete portions of the crack front. Possibly averaging the striation spacing over a specified arc length of the crack front would ameliorate the discontinuous nature of crack propagation resulting in better correlation between the numerical and experimental results. As a result of the current work, the best assessment of the quality of calculated K solutions is not from comparison to K solutions derived from striation spacing measurements but from fatigue life and crack shape predictions as was done previously. (See Figures 9.3-5 and 9.3-6)

9.3.4 RESIDUAL STRENGTH FINITE ELEMENT ANALYSIS OF C-130 CENTER WING BOX

Matthew J. Hammond, Center for Aircraft Structural Life Extension (CASTLE), United States Air Force Academy

The purpose of this program is to develop a robust 3D Finite Element Model (FEM) of the C-130 Center Wing Box for residual strength determination. Data from multiple sources, including analytical loads models, operational loads and stresses from flight data [1], damage state assessments of high-time airframes from teardown programs [2], and maintenance and repair records can all act as inputs to the model. Such analysis will allow for Safety of Flight (SOF) determinations given critical cracking scenarios. The FEM will also permit modeling of specific damage states by tail number for condition-based assessments. This will greatly enhance the capability, reliability, and confidence in both scenario-specific and fleet-wide residual strength assessments.

This program will rely on the largest structural FEM ever created ($\approx 10^8$ DOF), along with a break-through “splitting method” [3] to solve nearly 10,000 different cracking scenarios. (See Figure 9.3-7)

REFERENCES:

- [1] Greer J, et al, “HC-130H Center Wing Box System Monitoring Update,” Proceedings of the 2007 FAA/DoD/NASA Joint Conference on Aging Aircraft, Palm Springs, CA, April 2007.
- [2] G.A. Shoales, et al, “C-130 Center Wing Box Structural Teardown Analysis Final Report,” USAFA-TR-2006-11, USAF Academy, Co, December 2006.
- [3] Babüska I, Andersson B, Alpman J, “The Splitting Method for 3D Multiple Damage Analysis”, FFA Technical Note 1998-86, Flygtekniska Försöksanstalten, Stockholm, Dec 1998

9.3.5 NONLINEAR FINITE ELEMENT ANALYSIS OF STIFFENED PANELS, WITH AND WITHOUT DENTS

James M. Greer, Jr., Center for Aircraft Structural Life Extension (CASTLE), United States Air Force Academy

This project was funded by the USAF 327th Tanker Sustainment Group, Oklahoma City Air Logistics Center (327TSG/OC-ALC).

This work supplemented a parallel experimental effort on the effect of dents on transport fuselage structure [1]. The purpose of these finite element (FE) analyses was to expand the analytical envelope covered by the testing program in terms of dent size. Because of its long and successful history in nonlinear FE analysis, the Structural Analysis of General Shells (STAGS) program (version 5.0) was used [2].

Two types of fuselage panels were modeled under this effort: (1) an end-compression 16 X 20-inch panel, and (2) a 20 X 20 inch panel loaded in shear. A typical stiffened-skin panel model is shown in Figure 9.3-8.

The (geometrically) nonlinear analyses took panel deformation well into the post-buckling regime. Panel buckling occurred at very low loads early in the analyses. In these thin-skinned panels, buckling occurred at very small end displacements as well: on the order of 0.001 inches of end displacement for the end-compression panels and 0.010 inches of edge displacement for the shear panels. The post-buckled behavior is captured by these runs, and shows the effect of dents on the panels' static response prior to panel collapse, which was found to be negligible for the cases studied. There are local stress increases due to the dents, and the effect of those stresses on fatigue behavior is addressed in the earlier referenced report. Post-collapse behavior (i.e., ultimate failure of the panel) was not captured by these analyses.

A means of incorporating dent geometry into STAGS was developed specifically for this program (Figure 9.3-9). This was done by using STAGS' "user-written subroutine" option for shell geometry. A subroutine was written such that smooth dents of a variety of diameters and depths could be easily made.

The method allows for placing single dents in the panel, as well as groups of five dents. The nonlinear finite element analyses (FEA) in this report verify the experimental results: dents in the bays between stiffeners, where the underlying structure is not damaged, do not significantly change the post-buckled behavior of the fuselage skin panels. The results of this effort are reported in Reference [3].

REFERENCES:

- [1] C. B. Guijt, "The Effect of Dents on KC-135 Fuselage Structure: Final Report," Technical Report USAFA-TR-2005-08, U.S. Air Force Academy, Center for Aircraft Structural Life Extension (CAStLE), Aug. 2005.
- [2] C. C. Rankin, F. A. Brogan, W. A. Loden, and H. D. Cabiness, "STAGS User Manual, Version 5.0," Lockheed Martin Missiles & Space Co., Inc., Advanced Technology Center; O/L9-21; B/204, 3251 Hanover Street; Palo Alto, CA; 94304-1191, January 2005.
- [3] Greer, Jr., James M., "Nonlinear Finite Element Analysis of Stiffened Panels, with and without Dents," Technical Report USAFA-TR-2006-01, U.S. Air Force Academy, Center for Aircraft Structural Life Extension (CAStLE), 13 Jan 06.

9.3.6 COMMERCIALIZATION OF METALLIC MATERIALS PROPERTIES DEVELOPMENT AND STANDARDIZATION (MMPDS)

John Bakuckas, Federal Aviation Administration, ATO-P, R&D

The Metallic Materials Properties Development and Standardization (MMPDS) is an effort led by the Federal Aviation Administration (FAA) to continue the Handbook process entitled "Metallic Materials and Elements for Aerospace Vehicle Structures," (MIL-HDBK-5). The Handbook is recognized worldwide as the most reliable source for verified design allowables needed for metallic materials, fasteners, and joints used in the design and maintenance of aircraft, missiles, and space vehicles. Consistent and reliable methods are used to collect, analyze, and present statistically based aircraft and aerospace material and fastener properties.

The objective of the MMPDS is to maintain and improve the standardized process for establishing statistically based allowables that comply with the regulations, which is consistent with the MIL-HDBK-5 heritage by obtaining more equitable and sustainable funding sources. This includes support from government agencies in the Government Steering Group (GSG), from industry stakeholders in the Industry Steering Group (ISG) and from profits selling the Handbook and derivative products.

Towards this goal, the first commercial version of the MMPDS-02 Handbook was distributed in August 2005. There has been a substantial upgrade with approvals from the 3rd through the 6th MMPDS General Coordination Meetings. This includes 12 new alloys and over 300 pages edited or added. Copies of the MMPDS-02 Handbook will be available in bound five volume set either in hard copy or on a CD-Rom:

- Volume 1 - Introduction and Guidelines (Chapters 1 and 9)
- Volume 2 - Steel and Magnesium Alloys (Chapters 2 and 4)
- Volume 3a - 2000-6000 Series Aluminum Alloys (First part of Chapter 3)
- Volume 3b - 7000 Series and Cast Aluminum Alloys (Second part of Chapter 3)
- Volume 4 - Titanium and Heat-Resistant Alloys (Chapters 5 and 6)
- Volume 5 - Miscellaneous Alloys & Structural Joints (Chapters 7 and 8)

Members of the GSG and ISG are entitled to free copies of the Handbook commensurate with the level of funding.

As the MMPDS secretariat, Battelle Memorial Institute, a not-for-profit organization, was granted an exclusive license, subject to annual renewal, from the FAA to reproduce and distribute the MMPDS-02 handbook and related products. (Figure 9.3-10)

9.3.7 FATIGUE CRACK GROWTH METHODS FOR ROTORCRAFT APPLICATIONS

Dy Le, Federal Aviation Administration, ATO-P, R&D

Researchers at the FAA, NASA, and Mississippi State University are working to adapt fixed-wing aircraft damage tolerance technologies and techniques for rotorcraft applications. The phenomenon of fatigue crack growth is a major area of concern in this work. The stress that can be tolerated before small cracks begin to grow has been determined for many materials used in fixed-wing aircraft and researchers want to determine tolerable stress levels for materials used in rotorcraft.

Currently, the standard crack growth region is defined in American Standard Test Methods (ASTM) E-647. Using this standard, researchers computed and analyzed a substantial body of rotorcraft fatigue crack growth data and identified some problems with the standard test method. As a result, researchers are finalizing a new experimental method to replace or supplement ASTM E-647. The researchers have presented their funding to the ASTM committee. Additional details about the FAA fatigue-crack-growth research can be at: http://aar400.tc.faa.gov/Programs/agingaircraft/rotorcraft/RCDT_FCG_Background.htm.

9.3.8 INTEGRATED ELECTRONICS STRUCTURAL DURABILITY ANALYSIS TOOL

Mostafa Rassain, Jung-Chuan Lee and David W. Twigg, The Boeing Company - Seattle

The electronic components such as chassis, and printed wiring boards (PWB) are subjected to low cycle fatigue under thermal cycling and high cycle fatigue due to vibration. Traditionally the analysis is divided in three phases, i.e., part level, board level, and chassis level. The chassis level analysis is first performed. Next is the detailed board analysis with the board/chassis connections treated as board boundary conditions. The vibration environment is obtained from chassis level analysis through transfer function along the board/ chassis interfaces.

In this paper, Boeing's automated tool will be presented which is used to analyze part, board and chassis in an integrated hierarchical order. The tool integrates parts into board and generates mesh for each board/part component. Chassis and boards are then merged into an assembly FEM. The model is then passed on to a vibro-acoustic analysis tool again developed by Boeing to evaluate loading conditions such as base excitation, pressure load, and acoustic. The resulting root-mean-square (RMS) stresses are then used for chassis fatigue analysis with the RMS-displacement for solder joint fatigue analysis.

This analytic process eliminates error on frequencies and mode shape by not having to smear parts over the board. Since it is an integrated analysis, no board level analysis is required. Therefore, it eliminates a need to perform vibration analysis of a box separately in order to calculate transfer functions that do not necessarily represent the coupling actions when applied at the board/ chassis interface following the tradition approach.

Using the preload capability within the tool, one is able to evaluate avionics interconnect structure in hot temperature while exposed to vibration environment. It identifies failure mode in interconnect structure and predict time to failure. These capabilities have been validated on the F-22 program and were successfully applied to various.

The use of such computer-based analysis tools during early design stage and layout has reduced cost and provided more affordable products by reducing design cycle time and test and design iterations while improving performance and life expectancy. The durability analysis process (Figure 9.3-11) can use AP210 translator of Standard for the Exchange of Product model data (STEP) to define printed wiring assembly parts, geometry and material.

Thermal and structural finite element methods are integrated using automatic mesh generation to perform thermal, structural, acoustic and durability analyses. This analytic process is used to evaluate the chip-level interconnect

durability using cumulative damage index as a metric based on Miner's rule. The analysis accounts for detail geometry and material nonlinearity such as solder as a function of temperature and time.

Figure 9.3-12 shows typical analysis results of such process to qualify candidate commercial off-the-shelf (COTS) SKY multiprocessor modules survive F-15 aircraft thermo-mechanical environment. The validations of the fatigue and damage prediction tools for a wide range of technologies (e.g. surface mount, ball grid array) were performed under Accelerated Commercially Manufacturing Electronics contract with Wright Patterson AFRL under a 4-year contract in circa 1999-2002.

9.4 REPAIR AND LIFE ENHANCEMENT

9.4.1 FATIGUE PERFORMANCE OF NEW ALUMINUM-LITHIUM ALLOYS WITH COLD EXPANDED HOLES

Cindie Giummarra, Alcoa Technical Center

Aluminum-lithium (Al-Li) alloys are increasingly being selected for use on the next generation of aircraft, such as the A380 and 787, due to their lower density, good strength and toughness combination and excellent fatigue crack growth performance under spectrum loading. However, it is important to ensure that these new aluminum alloys are also compatible with the standard and latest aircraft manufacturing and maintenance processes. One such process, which has been used on metallic aircraft for many years, is cold working of fastener holes via split-sleeve expansion for fatigue life enhancement. Split-sleeve cold-hole expansion (SSCx) involves pulling a mandrel and sleeve through a fastener hole. The mandrel and sleeve have a larger combined diameter than the hole, resulting in yielding of material when they are pulled through. After the mandrel is removed, a region of compressive residual stress is left around the hole which alleviates the propensity for fatigue cracks to grow [1, 2]. This process is often applied on an aircraft in fatigue critical locations during manufacture and/or maintenance [3].

Due to the lower ductility of lithium-containing alloys compared to the incumbent alloys, and concerns with the cold-hole expansion capabilities of previous generation Al-Li alloys, it is crucial to prove that this recent series of Al-Li alloys can be successfully cold-hole expanded using standard processes and conditions with beneficial results. This study examined the split sleeve cold hole expansion (SSCx) capabilities of selected new aluminum-lithium plate and extrusion alloys and the resulting effect on fatigue life [4]. The results showed that all the Al-Li alloys tested in the L-LT plane could be SSCx under severe but realistic conditions without cracking. Specimens taken from the L-ST plane had a higher probability of cracking, but the propensity for cracking was reduced by preferentially orienting the split in the sleeve (Table 9.4-1).

The open hole fatigue results showed that all the Al-Li alloys tested obtained significant improvements in fatigue life due to the application of SSCx (Figure 9.4-1). The fatigue life of the Al-Li alloys after SSCx was equal to, or in most cases, greater than alloy 2024-T351. Greater improvement in fatigue life was seen as a function of the yield strength due to the higher elastic constraint of the material after SSCx. This resulted in higher levels of compressive residual stresses, which acted to reduce crack propagation and thus increase the fatigue life.

REFERENCES:

- [1] Cook R. (1995), In: *Estimation, Enhancement and Control of Aircraft Fatigue Performance*, Proceedings of the 18th ICAF Symposium, p.971, Grandage J.M. and Jost G.S. (Eds.), Melbourne.
- [2] Holdway, P., Cook, R., and Bowen A.W. (1994), *Proceedings of the Fourth International Conference on Residual Stresses*, p.1046, Baltimore.
- [3] Ried, L (1993), In: *Durability and Structural Integrity of Airframes*, Proceedings of the 17th ICAF Symposium, vol. II, p. 1121, Blom A.F. (ed.), Stockholm.
- [4] Giummarra, C., (2007), In: *Durability and Damage Tolerance of Aircraft Structures: Metals vs. Composites*, Proceedings of the 24th ICAF Symposium (in review).

9.4.2 LONG-TERM PERFORMANCE OF BONDED COMPOSITE REPAIRS TO METALLIC AIRCRAFT STRUCTURE

J.J. Mazza, C.B. Guijt, D. Kelly, N. Jacobs, J.M. Greer, A. Gaskin and L.W. Butkus, United States Air Force

This project is funded by the USAF 646th Aeronautical Systems Squadron, Wright-Patterson AFB, OH (646th AES).

The installation of adhesively bonded composite patches for repair of damaged metallic structures provides significant advantages over the use of their mechanically fastened counterparts. Bonded joints can transfer structural loads across an entire repair area rather than at discrete fastener locations. The more uniform stress distribution and larger stress-bearing area associated with adhesive bonding coupled with the strength and stiffness tailorability of composite patches allows bonded repairs to be more structurally efficient. Also, elimination of the

need for additional fasteners leads to improved component fatigue life. Other advantages for bonded repairs include their superior ability to stop fatigue cracks, provide a barrier to fuel and other fluids, and avoid fretting and crevice corrosion problems. In addition, bonded repairs can often save weight, time, and money.

Despite the advantages associated with bonded repairs and their use in several highly visible applications [1–2], the technology has seen relatively limited use on United States Air Force (USAF) weapons systems. The infrastructure required to design and apply bonded repairs does not exist throughout the USAF. Although it has been successfully used as a “last resort” to repair several safety-of-flight-critical structures, full benefit of bonded repair technology has not been taken. One reason is the fact bonded repairs are not completely trusted by the USAF Engineering Authority (ASC/EN) when applied to safety-of-flight-critical structure. This places an undue inspection burden when bonded repairs are used.

The low level of confidence in adhesively bonded repairs is due to the current lack of a nondestructive means to assure repair integrity coupled with the inability to quantitatively predict service life. In addition, past adhesive bonding failures exist, particularly for aluminum honeycomb structure. For these reasons, ASC/EN does not allow full credit to be taken for bonded repairs to critical structure. Integrity of such structures must be maintained and the structures must be managed as if the bonded repair has not been installed. For the case of repaired fatigue cracks, inspection intervals are set as if the crack is free to grow uninfluenced by installed bonded repairs. Such repairs can still provide some benefit if they stop or slow crack growth, since repair intervals will not decrease or will decrease less rapidly than they would for the case of unrepaired cracks.

In an effort to boost confidence in bonded repairs and increase the amount of credit that can be taken with their use, a program was conducted to evaluate performance of bonded repairs that had been installed across the C-141 aircraft fleet to address fatigue cracking in lower wing skins. It was hoped the program would promote the idea of permanence for bonded repairs. The effort had ASC/EN backing and support. That organization saw the potential to reduce inspection burdens associated with bonded repairs as the program’s main benefit. This would have potential to increase the use of bonded repairs by making them more economical. It would allow more applications to utilize the advantages offered by such repairs.

In the early 1990s, C-141 aircraft experienced significant fatigue problems in their 7075-T6 aluminum lower wing skins. Fatigue cracks were found emanating from “weep holes” that had been drilled into the skins’ integral stiffening risers at the time of production to maximize fuel usage. A representative C-141 wing plank configuration with typical weep holes is shown in Figure 9.4-2. Most of the weep hole fatigue cracks were removed by enlarging the weep holes which were then cold worked to delay crack re-initiation. Some wing panels were replaced due to widespread cracking. For cases when oversizing holes could not eliminate cracks, adhesively bonded boron/epoxy patches were applied to restore damage tolerance and durability, provided individual cracks were not too close in proximity. The bonded patch approach was seen as the only viable repair option for these cases, and it saved considerable time and money versus wing panel replacement. Due to lack of availability of replacement planks, a significant portion of the C-141 fleet would have been grounded or flown with restrictions for considerable time were it not for the bonded patch repair effort.

Approximately 770 repairs, each with three individual patches for a total of 2300 patches, were applied to over 120 C-141 aircraft. Figure 9.4-3 illustrates the three-patch repair concept that was applied.

The installed bonded patch repairs were designed to stop fatigue cracking for the remainder of the fleet’s service life. However, damage tolerance guidelines for these repairs were to follow the conservative approach favored by ASC/EN. Since the bonded repairs could not be fully trusted to perform as designed for the fleet’s lifetime, credit was not given for applied repairs, and inspection intervals were to be based on the unrepaired structure. The C-141 weep hole repairs flew successfully from 1993 until the last aircraft was retired in 2006.

Bonded Boron Patch Repair Evaluation (BBPRE) Program

With ASC/EN as an advocate, funds were sought and received from the 646th Aeronautical Systems Squadron (646th AESS). Although many potential uses for repairs retrieved from AMARC were envisioned by the team, the primary focus of the evaluation supported by ASC/ENF and funded by the 646th pertained to structural integrity and focused on static residual strength testing of salvaged repairs. It was understood, if all went well, these tests would actually assess the C-141 aircrafts’ metal wing structure rather than the repairs, because repairs that maintained their integrity

in service would not be “weak links” in the tests. In an attempt to evaluate the bonded repairs themselves, a small task was added to assess fatigue performance of retrieved repairs. In addition, the fatigue portion of the effort was used to evaluate software developed under the Composite Repair of Aircraft Structures program (CRAS) to see if it could generate viable alternative designs to those originally conceived by WR-ALC/TI and CTI.

Service-aged durability and residual strength test specimens performed well during the BBPRE program and matched performance of newly repaired, equivalent specimens fabricated and tested as controls. All residual strength test specimens reached Design Ultimate Stress prior to failure, with an average of approximately 150 percent of DUS obtained for the 52 valid tests. A few residual strength specimens showed anomalous indications during testing, as revealed by strain mapping using a stereo-optic system. One of these specimens suffered a patch delamination and the other a disbond of the patch from the metal structure. Both occurred at over 90 percent of DUS. Performance of these two specimens prevented the residual strength tests from being a complete success. However, neither specimen failed at its metal-adhesive interface. It is important to note neither the “failed” specimens nor any other specimens showed signs of degradation that may have occurred during service.

The overall design methodology, materials, and processes used for the bonded boron/epoxy repairs to the C-141 aircraft appear to be robust and worthy of continued use. However, the program once again shows process control and attention to detail are of paramount importance when installing bonded repairs.

Due to the results of this program, it is anticipated ASC/EN will revise its current policy regarding adhesively bonded repairs to safety-of-flight-critical structure and allow some amount of “credit” to be given for such repairs. It is likely, under some ground rules as yet defined, reduced inspection burdens will result. Results of this program have been reported in References [3–7].

REFERENCES:

- [1] W. Schweinberg and J. Fiebig, “Case History: Advanced Composite Repairs of USAF C-141 and C-130 Aircraft,” *Advances in the Bonded Composite Repair of Metallic Aircraft Structure Volume 2*, A. Baker, F. Rose, and R. Jones, eds., Elsevier Science, Amsterdam, 2002, pp. 1009-1033.
- [2] C. Guijt and J. Mazza, “Case History: F-16 Fuel Vent-hole Repairs,” *Advances in the Bonded Composite Repair of Metallic Aircraft Structure Volume 2*, A. Baker, F. Rose, and R. Jones, eds., Elsevier Science, Amsterdam, 2002, pp. 885-895.
- [3] N. Jacobs, “Residual Strength Testing of C-141 Bonded Boron Repair Patch Structure,” Final Report for Contract F33615-03-D-5607 D.O. 0010, August 2006.
- [4] L. Butkus, et. al., “Residual Strength of Bonded Repairs after 10 Years of Service,” *Proceedings of the 2006 Aircraft Structural Integrity Program Conference*, San Antonio, TX, 30 November 2006.
- [5] C. Guijt, “The Effect of In-service Conditions and Aging on the Fatigue Performance of Bonded Composite Repairs,” USAFA-TR-2007-07, Center for Aircraft Structural Life Extension, U.S. Air Force Academy, CO, May 2007.
- [6] Lawrence W. Butkus, Alex Gaskin, James M. Greer, Jr., Cornelis B. Guijt, Nicholas Jacobs, David Kelly, James J. Mazza, J.T. Huang, Surendra Shah, Donald Shelton, “Bonded Boron Patch Repair Evaluation: Final Report,” USAFA-TR-2007-06. Center for Aircraft Structural Life Extension, U.S. Air Force Academy, CO, May 2007.
- [7] James J. Mazza, Larry Butkus, Cornelis B. Guijt, David Kelly, Nick Jacobs, James Greer, Alex Gaskin, “Long-Term Performance of Bonded Composite Repairs to Metallic Aircraft Structure,” *Proceedings of the 2007 DoD, NASA, FAA Joint Conference on Aging Aircraft*, Palm Springs, CA, April 2007.

9.4.3 NEGLIGIBLE DAMAGE LIMITS FOR DENTS IN FUSELAGE STRUCTURE

Justin Rausch, United States Air Force Academy

Fuselage dents in large transport aircraft have been shown to produce a significant amount of maintenance workload, see Figure 9.4-4. Many of these repairs are believed to be unnecessary in terms of structural performance. This research project focused on the study of the effects of dents on aircraft structural performance, with the goal of determining if the negligible damage limitations for dents in aircraft fuselage skin can be expanded, reducing the amount of dent related maintenance.

A previous research project conducted by the Center for Aircraft Structural Life Extension provided data which proved dents outside the effective width of the stiffened panel do not negatively impact the static stability of the structure. This project also concluded that under cyclic loading dents in these panels do reduce fatigue life, but not below the life expectancy of the airframe.

The current repair guidelines typically have a minimum distance requirement from structure that no dent may reside inside. Dents inside the effective width were believed to cause a reduction in panel stability. Compression testing conducted with dents inside the effective width, Figure 9.4-5, did not result in lower static stability as compared to the undamaged specimens. This research indicated that the distance requirement may be alleviated or eliminated by permitting dents inside the effective width for reasons of static stability.

This current research project also addressed additional fatigue concerns not covered in the previous work such as behavior of multiple dents in close proximity to each other and fatigue life of dented and dented/reformed 7075 and 7079 aluminum alloy skin panels. Present work in combination with the 2024 investigated in the previous work covers most ageing aircraft fuselages. Fatigue testing revealed that both 7075 and 7079 did take more of a reduction in residual life compared to 2024 in fatigue, however still has sufficient residual life to not require repair. Multiple dents in fatigue also showed a decrease in residual life, yet still not below that of the expected airframe life.

This research demonstrates that a significant amount of resources can be saved by only making repairs in situations where the damage actually impacts structural performance. By elimination or relaxation of the proximity requirement for damage near structure, and allowing multiple dents, a significant amount of maintenance burden can be saved while increasing operational status.

9.4.4 FINITE ELEMENT ANALYSIS OF THE INFLUENCE OF EDGE GEOMETRY ON SHOT PEENING PROCESS

Jifeng Xu, The Boeing Company - Washington and William J. Koch, The Boeing Company - Seattle

Abstract Shot Peening involves bombarding the surface of a metal part with small spherical media called shot. It creates a uniform layer of compressive residual stress at surfaces and considerably increases in part life. This study is devoted to an evaluation of the edge (corner) effects in shot peening process. Geometry variations in metal parts such as edges or corners cause variance in the residual stress profile induced by shot peening. This paper presents the finite element modeling and scheme that we use to simulate shot peening process by both single impact and multiple impacts for part geometries with different edge radii. The results achieved show that, after the same shot peening process, a part with a relatively larger edge radius possesses satisfactory residual stress profile which could equal or exceed that expected for a part with a smaller edge radius. The results may enable the automated edge preprocess step for shot peening with easily-machined large radius to reduce cost and improve productivity.

CE Database subject headings: Finite element method; Residual stress; Yield stress; Stress analysis; Impact loads; Aluminum; Edge effect.

Introduction

It is well known that fatigue failures of structures in service almost always initiate from a focal point on the surface, which creates a high stress concentration and may also be exposed to a harsh environment. These focal points include fillets, holes, keyways, laps, seams, scratches, tool marks, and other structural variations. Their creation

usually involves edge or radial treatments by a manufacturing process. Therefore, it is important to understand how the edge variations affect the treatment effectiveness and, hence, the fatigue performance.

Although polishing and chemical treatment of a work-piece may improve its resistance to failure initiation, the improvement usually is not enough to significantly increase load carrying capability and performance reliability. Since it is well known that failures or cracks will not initiate or propagate in a compressively stressed zone, one of the most effective methods of improving fatigue strength is through the introduction of high compressive residual stresses into the material surface, especially around the focal points. Shot peening is a low-cost, simple surface treatment, which is widely used throughout industry. In general, shot-peened work-pieces exhibit significantly increased resistance to fatigue and stress corrosion cracking and, therefore, increased service life [see Rios et al. (1999), Namjoshi et al. (2002), and Miller (1993)].

Shot peening is a cold working process performed at room temperature in which the surface of a work-piece is repeatedly impacted by small spherical shots with sufficient kinetic energy to create local plastic flow and permanent deformation within the surface zone. Once the shots rebound from the surface, residual stresses caused by the plastic flow remain in the work-piece. The plastic indentation causes expansion of the surface. The elastically stressed sub-surface tends to recover its original dimensions, but material continuity does not allow that to happen. Hence, a compressive residual-stress field in the surface layer is formed. Due to equilibrium, the stress profile through the thickness of the work-piece varies as follows. It begins with compressive stress at the surface followed by tensile stresses at some depth below the surface. The compressive residual stress, may be several times greater than the tensile stress beneath, and is highly effective in preventing premature failure under conditions of cyclic loading. It is especially effective in reducing the deleterious stress-concentration effects of notches, fillets, pits, and other surface geometric anomalies. Since shot peening can be used for a wide variety of structural components irrespective of shape and dimensions, it is a process widely used in the aerospace and automobile industry to improve fatigue life of components such as axles, springs, gears, and shafting etc. [see Shaw et al. (2003) and Baughman (1981)].

Mechanical shot peening involves a collision between the shot and the work-piece, and results in elasto-plastic flow in the work-piece. Process parameters affecting the shot peening effectiveness include, but are not limited to, shot flow rate, shot velocity, shot size and impact angle [see Schwarzer (2003), Robertson (1997), and Iida (1984)]. The material properties are also a factor, which affect the extent of indentation, dimple radius, and the resulting residual stress profile [see Rouhaud and Deslaef (2002)]. In addition, geometry variations such as chamfered or rounded edges cause variance in the residual stress profile. Many studies on shot peening effects have been conducted both analytically and experimentally to optimize peening parameters. However, a basic study of the effect of edge geometry on the shot peening process has not hitherto been reported in the literature. The purpose of this study is to evaluate how the shot peening process is affected by geometric variations around the edges or corners of a work-piece.

Through our research, we employed finite element impact modeling to investigate shot peening effectiveness with the variations of edge geometries. Particular attention was devoted to determining a trend with respect to plasticity and residual stresses in the peened work-piece.

This paper is divided into five sections. After this introduction, Section 2 describes the general finite element model used to simulate the shot peening process. Section 3 and 4 discuss the models for both single impact and multiple impacts and their corresponding results, respectively. In section 5, concluding remarks are presented.

Finite element modeling

The effect of shot peening process is mainly determined by the resulting profile of the induced residual stress. The compressive stress distribution versus depth is of primary concern, and a uniform stress profile across the work-piece surface is desired. The shot peening process is largely repeatable in macro-scale, meaning that identical peening parameters with same material specifications will produce similar residual stress profile. Therefore, by impacting the surface of the work-piece repeatedly, the “coverage” which is a percentile indicator of the impacted surface area, can approach 100%. A residual stress profile varying through the depth and nearly uniform across the surface can be achieved.

Residual stresses induced by a surface-to-surface impact such as shot peening are developed by the intense plastic deformation in the surface region with two overlaid factors, Hertzian pressure and plastic stretching. The former is responsible for compressive residual stresses with a subsurface peak, and the latter for residual stresses with a maximum on the surface [see Kobayashi et al. (1998)]. Some early studies of contact-impact problems were mainly based on static or quasi-static assumptions. However, in the shot peening process, the work-piece is impacted with very high velocity. There are transient and dynamic effects, which are numerically more complicated and can affect the degree of plastic flow in the work-piece. For example, the force imparted on a work-piece is, in part dependant on the modulus of the work-piece, because the modulus determines the rate of deceleration of the shot. Similarly, the stiffness of a work-piece will determine the degree of compliance, and will modulate the degree of plastic flow due to the impact. Hence if nonlinear dynamic characteristics of shot peening are concerned, the computation of stress state in the materials requires the use of advanced numerical techniques. With recent advances in computer power, nonlinear finite element method is suitable for numerical analysis of shot peening, and some studies have been reported on such applications in Al-Obaid (1990), Levers and Prior (1998), Schiffner and Helling (1999), and Meguid (2002).

Physical tests on shot peening are expensive and time consuming, especially for precise measurement of the in-depth stress profile. Our present work is focused on using finite element method to predict the magnitude and distribution of residual stress and plastic deformation associated with edge geometries in shot peening process. Such analysis will allow us to acquire and examine peening results without conducting costly physical tests, and can be easily repeated for different parameters. We chose to use the finite element software LS-DYNA to carry out the numerical simulation because of its reliability in solving contact problems and versatility in element and material libraries. Some subroutines were also developed to help complete the finite element model and evaluate the results in the post-processing phase.

Among many numerical analyses performed to investigate the fundamental mechanism and characteristics of fatigue improvement by shot peening, the general approach has been to consider small rigid spherical shots impacting on the flat surface of a work-piece. Such modeling works even when there is minor curvature developed in the work-piece because the big difference in dimension between shots and the work-piece. However, when a radius or chamfered edge area of a work-piece is peened, the curvature of the work-piece must be considered because the local mechanical response within the surface zone will be strongly affected by the curvature.

The general parameters used to predict the effect of edge geometries upon the induced residual stress profile and the plastic deformation are described as follows.

Geometry. The aluminum work-piece is a three-dimensional infinite block with one edge chamfered or rounded. Three edge geometries are studied in detail. Two of them with circular edge surfaces are shown in Figure 9.4-6. The radii for the edge circular configuration are $7.62\text{E-}4$ m (0.03 inch) and $3.81\text{E-}3$ m (0.15 inch), respectively. The work-piece is fully constrained on the $x = 0$ and $z = 0$ planes. Since for numerical analysis only a small part of the work-piece is subject to plastic deformation, the work-piece is modeled as a finite block with $5.08\text{E-}3$ m (0.2 inch) along both x and z directions and $2.54\text{E-}3$ m (0.1 inch) along y direction, surrounded by absorbing boundaries on the un-shadowed surfaces. The absorbing boundaries, simulating the presence of the remaining part of the work-piece, are used to minimize the reflection of wave energy back into the model. The area around the radial edge on the shadowed surface is subject to shot peening. The finite element mesh is generated using *TrueGrid*. The mesh density is graded in both x and z directions to reduce the scale of the computational model and to guarantee the finest mesh around the impact area for computing accuracy. The appropriate mesh size is determined by a number of preliminary simulations of a single shot. The steel shot is spherical with $4.064\text{E-}4$ m (0.016 inch) in radius and also is discretized with a finite element mesh. The elements are solid hexahedron elements with eight integration points and hourglass stabilization. The finite element mesh is shown in Figures 9.4-6.

Material. The work-piece is a typical aerospace aluminum alloy 7050-T7451. Since strain hardening is common in metals, it is included in our model to determine the possible plastic deformation. The stress-strain response of the material is characterized as piecewise linear plasticity. Such material model can simulate the whole range of metal behavior from linear elastic to elastic-perfectly plastic by varying the parameters. The effective plastic strains versus corresponding yield stresses, for the work-piece with the compressive yield stress 441.264 MPa (6.40E-4 PSI) and compressive shape factor 19.0, are shown in Table 9.4-2. Other relevant properties of the work-piece are: Poisson's ratio $\nu = 0.33$, Young's modulus $E = 7.102\text{E}4$ MPa (1.03E7 PSI), and density $\rho = 2.823\text{E}3$ kg/m³ (0.102 lb/in³). The

shot material is hard steel with the compressive yield stress 572.26 MPa (8.3E4 PSI), Poisson's ratio $\nu = 0.27$, Young's modulus $E = 2.041E5$ MPa (2.96E7 PSI), and density $\rho = 7.916E3$ kg/m³ (0.286 lb/in³).

Contact. During the contact the kinetic energy possessed by a shot is converted into elasto-plastic energy. The plastic flow and frictional effect contribute to the dissipation. The master-slave contact algorithm is used with the constraint that work-piece and the impacting shot do not penetrate each other. A Coulomb friction coefficient of 0.2 is used in the model. The initial impact speed of the shot is 22.25 m/s (875 inch/s). Once the shot rebounds, no further plastic deformation can occur.

In this study, the shot are directed normal or nearly normal to the work-piece surface around the edges. The nearly normal impingement will impart the optimum of the kinetic energy possessed by the shot to the work-piece and produce the most desirable magnitude of compressive stress on the surface [see Ebenau et al. (1987)]. We focus on normal impingements in this paper. However, we admit that the influence of inclined impact angles is often encountered in practice. Also, surface extrusion folds can occur due to very small impact angles around edges. These aspects of inclined impact angles will be focused on in a future study.

Using the parameters detailed above, two models were set up using the finite element code LS-DYNA. In the first case we consider a single shot and the second case we consider successive multiple shot intended for full coverage. The definition of peening coverage adopted here is the fraction of the area covered by indentation dimples. The center of the indentation dimple lies at the center of the edge area for single shot model, and the dimple centers for multiple impact model lie within the black-lined area, as shown in Figure 9.4-6.

The results revealing the shot peening quality are presented. As we know, the residual stress by shot peening is effective in stopping the growth of micro-cracks and closing or arresting fatigue cracks if they are within the depth of the compressive stresses [see Batista et al. (2000), Song and Wen (1999), and Stefanescu et al. (2004)]. So the quality of shot peening, manifested by the fatigue strength of the work-piece, depends on many attributes relevant to the plastically deformed surface layer. These attributes include the magnitude of surface residual stress, the magnitude and the depth of maximum compressive residual stress, and the depth of plastic deformation. A specially developed method is used to evaluate these attributes using the stress profile simulated by the above finite element models. And the results will be presented in the following two sections.

Single impact modeling and analysis

Since the most detailed approach is to model the individual impact of a shot against the surface of a work-piece, shot peening under a single shot has been the subject of many studies, such as in Iida (1984), Kobayashi et al. (1998), Edberg et al. (1995), and Frija et al. (2006). Single impact model may be used for sensitivity study to verify the finite element mesh density, to validate contact algorithm and material modeling, and to examine the effect of some relevant parameters on local stress field.

The explicit time integration scheme was employed in the simulation because of its computational efficiency without iterative calculations in each time step. Another advantage with the explicit method is that the accumulative errors in plastic regions with material non-linearity can be restrained. The explicit method is conditionally stable with a critical incremental time step that is given in terms of the highest eigenvalue of the model. In geometry, this time step depends on the size of the smallest finite element. Very small elements were used around the contact area for computational accuracy. For single shot modeling, the total integration time was about 37.5 μ s, and each time step was around 0.0033 μ s.

In simulation results, the six-component stress state tensor is expressed in the original global (x, y, z) coordinate system. Since the principal residual stresses in planes parallel to the surface are of the most importance to the beneficial effects of shot peening to fatigue life improvement, it is desirable to devote our attention to these stresses. A local coordinate system (u, v, w) with directions very close to the principal ones, as shown in Figure 9.4-6 (b), is established for points of interests around the edges. This local system indicates circumferential, axial and radial directions respectively. Three stress components ($\sigma_{uu}, \sigma_{vv}, \sigma_{ww}$) are evaluated in local systems at the surface and at nominal subsurface depths spaced at very small increments. The stresses σ_{uu} and σ_{vv} are close to the principal stresses in each sub-layer parallel to the surface, and hence represent bounds upon the possible planar residual

stresses for any orientation at that sub-layer. Selected results for stress state ($\sigma_{uu}, \sigma_{vv}, \sigma_{ww}$) are shown in Figure 9.4-7, 9.4-8 and 9.4-9.

Figure 9.4-7 shows a mid-plane cross section of axial residual stress σ_{vv} and the effective plastic strain ε^p . Apparently the maximum axial compressive stress occurred in the subsurface layer. Also, it is easy to see that the resulting surrounding ridge of raised material changes the axial residual stress σ_{vv} from compression to tension along the circumferential direction. Therefore, the surface axial residual stress field σ_{vv} arising from an individual shot is greater in extent than the physical size of the impact dimple due to surrounding region in tension. These phenomena also happen in the axial direction, shown in Figure 9.4-8, for circumferential residual stress σ_{uu} . The tension area with these hoop stress components with respect to the dimple circle can be suppressed by successive impacts and meanwhile will reduce the extent of compressive stress induced by subsequent impacts. Moreover, with incomplete coverage, a segment line with tensile stress component in certain direction could be formed by a certain pattern of shot. It will lead to undesired fatigue performance around such area, even surface extrusion or fold-over at extreme case.

The profile of plastic deformation directly determines the extent of the hardened layer and is closely related to the residual compressive stress. The effective plastic strain ε^p due to a single shot is illustrated in Figure 9.4-7. It also reflects the fact that the size of the impact dimple is smaller than that of the induced stress field.

Along the axial line through the impact center, the stress state ($\sigma_{uu}, \sigma_{vv}, \sigma_{ww}$) on the surface was examined and the results for edge radii 7.62E-4 m (0.03 inch) and 3.81E-3 m (0.15 inch) are shown in Figure 9.4-8. The principal stress σ_{vv} in axial direction maintains its compressive state along the line. The same statement applies for stress component σ_{uu} in circumferential direction along a circumferential line through the impact center. These steady compressive stress components normal to the dimple circle are of more importance to improve the fatigue strength.

Prevention of crack initiation and arrest of early propagation in the surface layer are paramount for prolonging the fatigue life of a work-piece, especially, an aerospace component subject to low applied stress but high cycles [19, 20, 21]. The comparison of the surface residual stresses between the cases of edge radii 7.62E-4 m (0.03 inch) and 3.81E-3 m (0.15 inch) is shown in Figure 9.4-8. The trends of each stress component for both cases are similar. The case of edge radius 3.81E-3 m (0.15 inch) has greater magnitude in axial stress and circumferential stress around the surface area close to the impact center, and smaller value of maximum tensile circumferential stress at locations away from the center. Although the residual axial stress by a single shot for edge radius 3.81E-3 m (0.15 inch) does not show favorable values in both compressive and tensile areas comparing to the case of edge radius 7.62E-4 m (0.03 inch), but its overall value is one order of magnitude less than both circumferential and axial ones. Hence, the radial stress will contribute less in improving fatigue life. So it can be affirmed by the comparison that the work-piece with edge radius 3.81E-3 m (0.15 inch), peened by a single shot at edge area, shows potential of greater improvement in fatigue life.

For reliable prediction of fatigue strength of the peened area, it is essential to evaluate the compressive stress distribution in subsurface layers. The residual stress profile at sampled nodes through the depth is shown in Figure 9.4-9 for both cases of radii 7.62e-4 m (0.03 inch) and 3.85E-3 m (0.15 inch). The differences are reflected most in near surface layers. On the surface the magnitudes of both the compressive stresses σ_{uu} and σ_{vv} for edge radius 3.85E-3 m (0.15 inch) are noticeably larger than those for edge radius 7.62e-4 m (0.03 inch). Therefore, fatigue crack initiation at the surface is more preventive with the larger edge radius of 3.85E-3 m (0.15 inch). With higher surface compressive stress, it is also more likely that the crack source will be pushed under the material surface. This is important because the surface of the part is prone to scratches, damage, chemicals, and moisture. All of these will reduce the fatigue life of a part. The compressive layer neutralizes the scratches and other crack starters. The case with larger edge radius 3.85E-3 m (0.15 inch) has slightly greater depth of the compressive stress and less magnitude of the maximum tensile stress. All these characteristics demonstrate the potential of greater resistance to fatigue failures for the case of larger edge radius 3.85E-3 m (0.15 inch).

The only unfavorable characteristic for larger edge radius is that the slightly smaller maximum compressive residual stress occurs at shallower depth. But this characteristic is progressively affected by the successive multiple shots, and moreover, it may not play a major role in determining the better case for fatigue strength between edge radii, since the work piece is subjected to frequent cycle stress, stress reversal, and torsional stresses, and it usually fails through a surface fracture.

Nevertheless, the above analysis is based on a simple single impact model with a very simplistic view. The single impact model was devoted to verify the elasto-plastic finite element model with contact algorithm for shot peening simulation and to obtain the basic understanding of the edge effects on shot peening. To simulate the practical process of shot peening, multiple impact modeling should be employed.

Multiple impact modeling and analysis

While many researchers studied the single impact for first-order approximation evaluations, few studies have been reported on shot peening by multiple impacts. Single impact model is appropriate and efficient for sensitivity study, local plasticity effect, and indentation estimation, as shown in the previous section. However, for certain application such as metal forming, it is obvious that the residual stress by single impact model is not up to the practical specification and of limited practical use [see Kopp and Ball (1987)]. The same applies for any other real shot peening applications in manufacturing. The residual stress field due to multiple shots is the resultant sum of all the fields by repeated and progressive impacts with complicated plastic flow in the material. It is not feasible to extrapolate results from the single impact model to a practical shot peening process with multiple impacts, and in fact it is beyond any theoretical analysis to predict the residual stress field by multiple shots. Hence again we resort to finite element method to set up multiple impact models to study the result of progressive impacts on edge geometries.

The coverage rate of multiple impacts in shot peening is an important control parameter to the resultant residual stress profile [see Meguid and Klair (1984)]. In practice, the compressive residual stress by shot peening at each spot is superposed progressively by residual stresses induced by surrounding shots. Usually, full coverage is recommended for best fatigue life improvement. However, a better understanding of partial coverage shot-peening would benefit from modeling multiple impacts on edges.

The finite element model for multiple impacts is similar to that for the single impact study. The finite element mesh for the work-piece is identical. All of the shots are also modeled in the same way as spherical solids discretized with eight-node brick elements. The inter-shot configuration is arranged in such a way that the minimum distance between centers of shots with nearly same arrival time is farther than twice of the indentation dimple radius. The in-line configuration is arranged so that the difference of arrival time between successive shots is longer than the contact duration. The judgment for in-line configuration lies in the fact that the transit time of induced stress wave by a single shot is much shorter than the contact residency. With such configurations, we can assume that no shots will interfere with each other mechanically. Although there is some geometric overlap and interference of the shot geometry, the contact surfaces are only effective between the work piece and each individual shot. With such layout we also assume all shots do not collide after rebound. Such configurations make the finite element model more feasible and more efficient in simulating the progressive effects of multiple impacts, with increased coverage rate and reduced computing time.

The coverage areas around the edge geometry for both cases of radii $7.62\text{E-}4$ m (0.15 inch) and $3.85\text{E-}3$ m (0.03 inch), with dots representing the impact locations, are illustrated in Figure 9.4-10. The uniform 45-degree shot angles around the edges are also shown in Figure 9.4-10.

By impacting the whole surface of the work-piece repeatedly and progressively, all shots produce a residual stress distribution, which varies in depth but is assumed to be nearly uniform in the plane directions. Hence, the plastic deformation layers along the plane directions are also nearly uniform with the non-zero effective plastic strains. The depth of plastic deformation was measured normal to the surface at the intersection of geometry mid-planes. They are around $8.382\text{E-}4$ m (0.033 inch) and $1.346\text{E-}3$ m (0.053 inch) for both cases of radii $7.62\text{E-}4$ m (0.03 inch) and $3.85\text{E-}3$ m (0.15 inch), respectively. These results demonstrate the effectiveness of the shot peening process around the edges and show better fatigue life improvement for the case of the larger radius.

As for the principal stresses $[\sigma_{uu}, \sigma_{vv}, \sigma_{ww}]$ along the axial line through the impact center, the values are [-203.12, -201.26, 31.65] and [-160.99, -163.47, -4.83] in the unit of MPa ([-29.46, -29.19, 4.59] and [-23.35, -23.71, -0.70] in the unit of ksi) for both cases of radii 7.62e-4 m (0.03 inch) and 3.85E-3 m (0.15 inch), respectively. The compressive stresses in plane directions are comparable between both cases with the same magnitude. The case of radius 7.62e-4 m (0.03 inch) possesses greater compressive stresses in plane directions, but the depth of compressive stresses is less than that for the case of radius 3.85E-3 m (0.15 inch).

It should be noted that for the case of radius 7.62e-4 m (0.03 inch), the radial stress is tensile which is not desirable for fatigue performance. This result is consistent with the single shot case shown in Figure 9.4-9 with radial stress close to zero for the case of radius 7.62e-4 m (0.03 inch). With radial tensile stresses, the work piece with edge radius 7.62e-4 m (0.03 inch) is more likely to develop fold-over or extrusion around edge corners during shot peening. This observation agrees with experimental results in Keenan (2003)].

In the multiple impact models, surface residual stress was nearly independent of peening parameters [see Rios et al. (1995) and Torres and Voorwald (2002)], and hence it should be altered most by subsequent overlapping shot, which induce greater plasticity. The resulting difference in our multiple-shot simulation is mainly due to the geometric differences, i.e., the different edge radii.

It is very complex to determine the better case for fatigue strength between different radii of edges because it may depend on many different conditions we have not considered here. It is still possible, from our simulation results, to conclude that the shot peened work-piece with larger edge radii will perform, at least as well, in fatigue performance as smaller edge radii.

Conclusions

Through this work the proposed finite element model is validated to capture the main features of the residual stress profile in the impacted material, especially around the edge area, and can be used as an effective tool for further study of the edge effects of shot peening with respect to other parameters.

This work was limited to simulating and quantifying the influence of the edge radii upon the residual stress field induced by shot peening. We used finite element modeling to investigate several cases. The resulting residual stress profiles are presented. These results highlighted the capability of the shot peening process to induce compressive residual stress around edge geometries. The creation of such compressive stress is the result of the surrounding material's resistance against the plastic deformation caused by the shots. It turns out that the residual stress profiles around edge area in the work-piece are indeed sensitive to the edge radii. In general, a shot-peened part with sharp edges has reduced fatigue properties relative to the flat portion of the same part. As the radius of the edge is increased, it approaches the geometry of a flat part. The likely mechanism which is responsible for fatigue life reduction involves the "free edge" of the part which does not provide resistance against plastic deformation as discussed earlier. Since the plastic deformation is not resisted residual stress is not as effective shot that are fully surrounded by elastic material boundaries. Understanding this effect is important in determining a practical solution..

We found that the shot-peened work-piece with larger edge radius gains better fatigue strength around edge geometry. Usually edges with large radii can be machined more easily with lower cost than edges with small radii. The ability to impact edges with large radii in a manner that results in a desired stress profile will help in designing or improving the manufacturing process to conduct effective shot peening on such easily machined edges to reduce cost.

In manufacturing, the shot peening process is a stable and repeatable process amenable to automation. However before shot peening, the work-piece usually needs to be preprocessed for smoothing edges or corners to prevent fold-over during shot peening. The preprocess step is usually performed with hand-held tools and has risk for ergonomic related injuries. The preprocessing also may take a substantial amount of time for some large structural components. With work-pieces with larger edge radius, the preprocess step of hand peening can be automated. This will greatly reduce the manufacturing time and cost.

Acknowledgements

We would like to thank Joseph Keenan for fruitful discussions.

REFERENCES:

- [1] Al-Obaid, Y.F. (1990). "Three dimensional dynamic finite element analysis for shot peening mechanics." *Comp Struct*, 36, 681-689.
- [2] Batista, A., Dias, A., Lebrun, J., Flour, J.L., and Inglebert, G. (2000). "Contact fatigue of automotive gears: evolution and effects of residual stresses introduced by surface treatments." *Fatigue Fract. Eng. Mater. Struct.*, 23, 217-228.
- [3] Baughman, D.L. (1981). "The evolution of centrifugal wheel shot peening in aerospace industry and recent applications." *The First International Conference on Shot Peening*, Paris, France.
- [4] Ebenau, A., Vöhringer, O., and Macherauch, E. (1987). "Influence of the shot peening angle on the condition of near surface layers in materials." *The Third International Conference on Shot Peening*, Garmisch Partenkirchen, Germany.
- [5] Edberg, J., Lindgren, L., and Ken-ichiro, M. (1995). "Shot peening simulated by two different finite element formulations." *The Fifth International Conference Numerical Methods in Industrial Forming Process*, Ithaca, New York.
- [6] Frija, M., Hassine, T., Fathallah, R., Bouraoui, C., and Dogui, A. (2006). "Finite element modelling of shot peening process: Prediction of the compressive residual stresses, the plastic deformations and the surface integrity." *Mater. Sci. and Eng. A*, 426(1-2), 173-180.
- [7] Iida, K. (1984). "Dent and affected layer produced by shot peening." *The Second International Conference on Shot Peening*, Chicago, USA.
- [8] Keenan, J. (2003). "Aluminum shot peening: preparation of part edges via machining, the triple pass machined edge." *SR 10351*, The Boeing Company.
- [9] Kobayashi, M., Matsui, T., and Murakami, Y. (1998). "Mechanism of creation of compressive residual stress by shot peening." *International J. of Fatigue*, 20, 351-357.
- [10] Kopp, R., and Ball, H.W. (1987). "Recent development in shot peen forming." *The Third International Conference on Shot Peening*, Garmisch Partenkirchen, Germany, 298-307.
- [11] Levers, A., and Prior, A. (1998). "Finite element analysis of shot peening." *J. of Mater. Proc.Technol.*, 80-81, 304-308.
- [12] Meguid, S.A., and Klair, M.S. (1984). "Finite element studies into incomplete coverage in shot peening." *The Second International Conference on Shot Peening*, Chicago, USA.
- [13] Meguid, S.A., Shagal, G., and Stranart, J.C. (2002). "3D FE analysis of peening of strain-rate sensitive materials using multiple impingement model." *International J. Impact. Eng.*, 27, 119-134.
- [14] Miller, K.J. (1993). "Material science perspective of metal fatigue resistance." *Mater. Sci. Technol.*, 9, 453-462.
- [15] Namjoshi, S.A., Jain, V.K., and Mall, S. (2002). "Effects of shot-peening on fretting-fatigue behavior of Ti-6Al-4V." *Transactions of the ASME*, 124, 222-228.
- [16] Rios, E.R. de los, Trooll, M., and Levers, A. (1999). "Life extension-aerospace technology opportunities." The Royal Aeronautical Society Publication, London, 26, 1-8.
- [17] Rios, E.R. de los, Walley, A., Milan, M.T., and Hammersley, G. (1995). "Fatigue crack initiation and propagation on shot-peened surfaces in A316 stainless steel." *International J. of Fatigue*, 17, 493-499.
- [18] Robertson, G.T. (1997). "The effects of shot size on the residual stresses resulting from shot peening." *The Shot Peener*, 11(3), 46-48.
- [19] Rodopoulos, C.A., Curtis, S.A., Rios, E.R. de los, and SolisRomero, J. (2004). "Optimisation of the fatigue resistance of 2024-T351 aluminium alloys by controlled shot peening-methodology, results and analysis." *International J. of Fatigue*, 26, 849-856.
- [20] Rouhaud, E., and Deslaef, D. (2002). "Influence of shots' material on shot peening, a finite element model." *Materials Science Forum*, 404-407, 153-158.
- [21] Schiffner, K., and Helling, C.D. (1999). "Simulation of residual stresses by shot peening." *Comp. Struct.*, 72, 29-40.
- [22] Schwarzer, J., Schulze, V., and Vöhringer, O. (2003). "Evaluation of the influence of shot peening parameters on residual stress profiles using finite element simulation." *Materials Science Forum*, 426-432(5), 3951-3956.

- [23] Shaw, B.A., Aylott, C., O'hara, P., and Brimble, K. (2003). "The role of residual stress on the fatigue strength of high performance gearing." *International J. of Fatigue*, 25, 1279-1283.
- [24] Song, P. and Wen, C. (1999). "Crack closure and crack growth behaviour in shot peened fatigued specimen." *Eng. Fract. Mech.*, 63, 295-304.
- [25] Stefanescu, D., Santisteban, J.R., Edwards, L., and Fitzpatrick, M.E. (2004). "Residual stress measurement and fatigue crack growth prediction after cold expansion of cracked fastener holes." *J. of Aerospace Engineering*, 17(3), 91-97.
- [26] Torres, M.A.S., and Voorwald, H.J.C. (2002). "An evaluation of shot peening, residual stress and stress relaxation on the fatigue life of AISI 4340 steel." *International J. of Fatigue*, 24, 877-886.

9.4.5 A SIMPLIFIED MODELING APPROACH FOR PREDICTING GLOBAL DISTORTION CAUSED BY THE INSTALLATION OF INTERFERENCE FIT BUSHINGS

Richard D. Widdle, Jr. and Lee C. Firth, The Boeing Company - Seattle

One technique for improving the fatigue life of fastener holes in a built-up structure is to use interference fit bushings. Installation of these bushings produces residual compressive stress around the hole that improves the fatigue life. It also causes residual strains and therefore distortion of the part. The distortion is both in-plane growth of the part and out-of-plane deflection, or cupping. The resulting distortions can cause difficulty in downstream assembly. For small parts with several bushings, it is possible to explicitly model the installation process using a finite element approach and predict the distortion. However, for a large part with many bushings, it is not practical to build a model with a detailed finite element representation of each bushing installation. This paper presents a simplified approach to predicting the distortion of large shell-like parts caused by the installation of many interference fit bushings. The simplified approach consists of representing the bushings, in a shell-based finite element model of a large part, with equivalent springs. The properties of the elements that make up the equivalent springs were estimated from experiments on small rectangular plates. Additionally, to help minimize the number of experiments, detailed models of the test plates were constructed to simulate the actual installation process. Equivalent spring properties were estimated based on these results as well. The simplified modeling approach was validated by using experimental data from several large structures.

9.5 COMPOSITES

9.5.1 COMPOSITES AFFORDABILITY INITIATIVE

John D. Russell, Air Force Research Laboratory - Materials and Manufacturing Directorate

INTRODUCTION

In the mid 1990's, the Air Force Research Laboratory (AFRL) recognized that despite the potential of advanced composites to drastically reduce aircraft structural weights compared to conventional metal structures, the aircraft industry was reluctant to implement them in new aircraft. Although composites were used on the F-15, F-16, and F-18 in small percentages, data showed that composite applications had reached a plateau. For example, despite early projections of the F-22 airframe being 50% composite by weight, it settled back to 25% [1]. As a result, AFRL launched the Composites Affordability Initiative (CAI) to address the perceived risks and barriers. What resulted was a team of the AFRL Materials and Manufacturing Directorate and Air Vehicles Directorate, the Office of Naval Research-ManTech, Bell Helicopter Textron, The Boeing Company, Lockheed Martin Corporation, and Northrop Grumman Corporation. Ultimately, a \$152M, 11 year effort was performed to attack the problem.

What Needed to be Done?

The CAI Team found that the key to affordability in composite structures was to reduce assembly costs. State-of-the-art aircraft structures have thousands of parts and hundreds of thousands of fasteners (Figure 9.5-1). In addition, drilling holes and installing fasteners has been and still is a major source of labor and rework in aircraft structures. If the number of fasteners is reduced substantially, structural assembly costs and cycle time could be drastically reduced. The CIA team pursued part integration and structural assembly through bonding parts together to achieve this goal. As a result, CAI's objective was to "establish the confidence to fly large integrated and bonded structures". The technical program to meet this objective was structured to ensure that Department of Defense (DoD) structural integrity goals were met (see Figure 9.5-2). This required a multidisciplinary approach: maturation of materials and processes, an understanding of the structural behavior of bonded joints, quality assurance and non destructive evaluation to ensure bonded joints remain bonded throughout an aircraft's service life, and the buy-off of DoD aircraft certification authorities.

The CAI business strategy was intended to maximize leveraging of knowledge and funding as well as improve transition of game changing technologies. CAI was a collaborative effort among all parties, each sharing data equally for core technology efforts and delaying data release on specific technology applications (transition demonstrations). The industry partners agreed to a 50% cost share with the government which increased the leveraging and also created an internal company incentive to realize an acceptable ROI on the investment by using the CAI technologies in their products. Technology transition demonstration projects ("T"-programs) were also a key feature of CAI. These T-programs focused the development of large integrated and bonded structures technology tailored to specific needs for several DoD weapon systems. Demonstrations were performed for several aircraft, including the X-32 (Boeing JSF prototype), F-35, X-45, and C-17. A key feature of these T programs was that the integrated product teams (IPTs) were staffed with people from the DoD laboratories, industry development personnel, DoD program office personnel, and industry program personnel. Having representatives from each type of organization greatly improved the lines of communication and ensured the technology being delivered met the needs of the customer.

TECHNICAL ACHIEVEMENTS

The goal of CAI was to "establish the confidence to fly large integrated and bonded structures". The primary technology pursued for integrated structures was Vacuum Assisted Resin Transfer Molding (VARTM), and bonding was enabled by the pi-joint bonded primary structure design and robust manufacturing processes. These technologies, along with the supporting tools and methods to make certification possible are described in the following sections.

Vacuum Assisted Resin Transfer Molding:

For integrated structures, a non autoclave process for making large yacht hulls was transitioned to the aerospace industry. VARTM is a process that uses a lower than atmospheric pressure (typically full vacuum) to pull a liquid resin into a fiber bed. It was made famous in the boatbuilding industry with the advent of the SCRIMP process. There are two key advantages of VARTM over conventional autoclave curing. First is that an autoclave is not

needed as is the case for conventional aerospace composite parts, resulting in reduced capital equipment costs. Furthermore, removing the need for the autoclave provides industry with a much larger supplier base for part fabrication. Second is that the typical VARTM resins cure at a low enough temperature to enable the use of inexpensive tooling such as medium density fiberboard rather than the typical invar tooling used for 177C (350F) curing autoclave materials. This again reduces system development costs.

While the aerospace industry dabbled in VARTM over the years, CAI has demonstrated its viability as a valid production method for aerospace parts up to 5.4 m³ (160 ft³). As shown in Figure 9.5-3, several parts were demonstrated including an X-32 like one piece cockpit tub (upper left), a braided compact inlet duct with bonded frames (upper right), a C-17 like fuselage skin with integral stiffeners (lower left), and a C-17 nose landing gear door (lower right). CAI's VARTM efforts resulted in fiber volumes and per ply thickness comparable to typical autoclave cured aerospace composite parts. In addition, the process worked with several resins, including EX1510, SI-ZG-5A, and VRM-34. Further use of the VARTM process would be enabled through the development of toughened resins with properties similar to 977-3 resin.

Overall, VARTM has enabled reduced part counts (up to 80%), reduced fastener counts (up to 100%), and lower part fabrication costs as compared to conventional structures (30% to 50%). CAI has demonstrated the VARTM process to be versatile in the parts it can create, achieving acceptable quality and validated its repeatability. VARTM is a production ready process for the aerospace industry.

Adhesively bonded structures

While bonded primary structural joints are currently in service on DoD aircraft including the F-18 and Global Hawk, there continues to be an unease in the DoD airframe certification community with regards to bonded structures. That community has a legitimate concern based on past research programs to broaden the use of bonded structures. The inability to discriminate between a good bond and a "kissing" bond (intimate contact between adhesive and structure without adhesion) has been the key roadblock to further use of bonded structures. Despite this unease, bonded structures have tremendous potential for aircraft structures. If designed correctly, bonded aircraft structures have greatly reduced part count and fastener count and also greatly reduced structural assembly times. The CAI attacked each barrier to increase the confidence to fly bonded primary structures.

Pi Joint: The first area to be addressed was design of the bonded joint. CAI's bonded structures work centered on the "pi" joint (Figure 9.5-4.), this stiffener, shaped like the Greek letter π , can be co-cured or co-bonded to the skin. The pi joint has several advantages. First, it provides structural redundancy. The pi joint acts as two independent bondlines, and the joint is stronger than a double lap shear joint. When used with EA 9394 adhesive, the pi joint takes advantage of the inherent properties of the material. EA 9394 has excellent shear properties and performs better in shear than in tension loaded bonds. It also paves the way for much reduced assembly times by providing a determinate assembly feature. Tension loaded bonded structures typically have the adhesive spread over the skins and/or spar/rib caps prior to assembly. This leads to adhesive out time issues. They also may require several verifilm cycles to ensure the correct tolerances to get the adhesive thickness required by the designer. Conversely, out time is minimal with the pi joint. It takes much less time to apply the adhesive into the clevis of the pi and much less surface area is exposed to the air before bonding takes place.

CAI spent considerable energy in analyzing and verifying the design and manufacture of the pi joint. Testing has shown that the joint is very robust and has predictable performance. A key finding from the CAI pi joint studies is that the room temperature paste bonded pi joint has three to five times more strength than the co-cure joint of the pi stiffener to the skin. Thus, the pi joint will not be the weak link in a primary structural application. It is tolerant of several defects including: thick bondlines; a canted blade; a blade skewed to one side of the clevis; and typical manufacturing defects such as voids and peel plies that were not removed prior to bonding. This robustness was proved by a series of successful tests ranging from coupons to full scale airframe components (examples in Table 9.5-1).

The X-45 A wing carry through and X-45 C wing (Figure 9.5-5) were structurally tested to design limit load, design ultimate load, and finally to failure. Both articles failed just above the predicted design ultimate load. These structural and ballistic tests show that bonded structures can meet structural requirements for military aircraft. In addition, these structural demonstrations showed that assembly times are drastically reduced. By filling the pi joints

with adhesive rather than mating, drilling, deburring, remating, and installing fasteners, assembly times can be reduced from 50 to 80% depending on the article, translating to a cost savings of 20 to 50%.

Enabling tools for bonding

Besides the validation of robust designs and manufacturing processes, several key supporting tools and technologies had to be matured and validated to make the application of bonded primary structures a reality. More accurate analysis tools which took into account peel as well as shear stresses in a bonded joint, tools to evaluate damage progression, non-destructive inspection for the production and maintenance of bonded primary structures and finally an acceptable certification approach.

Analysis Tools: Conventional analysis methods for bonded joints were found to be limited in their capabilities and accuracy. Conventional analysis methods for bonded joints, such as the widely used A4EI code, are limited in their capabilities and accuracy. A4EI, for instance, is only applicable to adhesive failures in shear-loaded joints and does not account for peel stresses or for potential adherend failures. To date, the only alternative to these limitations has been to develop detailed finite element models of a joint. This approach is time consuming and requires great skill and care by the analyst to ensure stresses and strains in critical locations of the joint are properly quantified. Small errors in modeling can lead to substantial errors in joint performance prediction.

To alleviate these problems, the CAI team implemented improvements to the StressCheck® P-version finite element software from ESRD Inc, including the incorporation of a strain invariant failure theory. The StressCheck® tool handbook function was used to expertly model typical joints, thereby developing reusable joint models including: single lap shear, double lap shear; scarfed lap shear; and step lap joints for in-plane loading; as well as a 'Pi' and back-to-back angle joints for out-of-plane loading. These handbooks are parameterized so that similar joints in the future can be modeled by simply updating geometric parameters of the existing model. Stress Check will then automatically remesh the model, calculate results, check for convergence problems in the new joint configuration, and even post-process the results.

3 Durability and Damage Tolerance Analysis Methods: Users are also concerned about how the damage would progress in order to understand the full impact of damage and the durability of the structural design. Software based on a novel implementation of the Virtual Crack Closure Technique (VCCT) was developed under CAI and was being applied to the evaluation of delaminations and disbonds in composite structure after the on-set of initial failure. VCCT plays an important role by providing unprecedented capability for the design of aerospace structures involving composites. Boeing has filed a patent application for this interface fracture analysis software and ABAQUS, Inc., will market an enhanced version of the technology commercially. "This technology has been of great interest to us for some time and I am pleased to see it becoming a part of the ABAQUS software," commented Ronald Krueger, Senior Staff Scientist for the National Institute of Aerospace [2].

Quality Assurance: One major hurdle inhibiting the application of bonded primary structures has been the lack of a non-destructive technique to assess the strength of a bonded joint. Boeing, a CAI team member, led the quality assurance technology effort and has developed (patent pending) a laser bond inspection technique.

High peak-power, short-pulse-length laser excitation generates stress waves that can be used to discriminate between kissing, weak and strong bonds in graphite-epoxy composite-to-composite bonded structures. The technique is able to discriminate between variations in surface preparation techniques, levels of surface contamination and/or changes in paste adhesive mixing. In over 3000 laser stress wave experiments this approach has been found to be repeatable and reliable in the detection of weak versus strong bonded joints. Such an approach offers a potentially cost effective method to be certain of a minimum predetermined load carrying capability of a bonded joint after manufacture or in-service. A production floor laser bond inspection device is being developed and optimized in two Small Business Innovative Research programs with LSP Technologies sponsored by AFRL/ML.

Certification: The CAI team worked with certification authorities from the Air Force, Navy and FAA to understand and eliminate the barriers to advanced bonded structures. The CAI team prepared certification plans for 3 structures, each with increasing levels of innovation. The plans started with a secondarily bonded rib to a skin/stringer interface. Next up was a vertical tail featuring 3-D pi performs and z-pinning. The final plan featured a bonded wing that carried fuel with 3-D pi performs and z-pinning. These plans included the use of CAI developed analysis tools and their validation, CAI developed process controls for bonding and guidelines for advanced processes as

well as advanced bondline inspection tools. These tools and technologies along with a sound certification plan of analysis supported by test provided the certification authorities with enough confidence that they believe the methods were sound enough to certify an actual structure. This is a major breakthrough to realizing the cost, cycle time and durability benefits of advanced bonded structures

TECHNOLOGY TRANSITION

CAI tools and technologies have transitioned across the industrial base. AFRL is currently aware of 22 companies/organizations benefiting from CAI derived technologies. Technologies include VARTM, pi-joints, laser bond inspection, StressCheck® and crack propagation analysis tools, and certification plans. Bonded structures are flying on the F-35 AA-1. StressCheck® and crack propagation analysis tools have become standard industry practices and are being used to design and analyze DoD and commercial aircraft. The C-17 landing gear door (Figure 9.5-3) will be fabricated by a first tier supplier for future C-17's and as a preferred spare. This article only covers a portion of the technologies developed under CAI. Other tools include an improved cost model for composites being sold by Galorath. This cost model is being used by over 10 organizations worldwide. A process maturation database capturing the entire CAI database with a complete pedigree of processing data, environmental exposures, etc. is hosted on the AMMTIAC, NAMIS website (<https://ames.alionscience.com/CAI/>). An exhaustive set of guidelines has been prepared to provide potential users with clear understanding for advanced materials, designs, analysis tools, process controls, fabrication and assembly processes, quality assurance and repair. All of the CAI technologies, reports and data are open to the DoD and DoD contractors.

SUMMARY

The Composites Affordability Initiative was a huge technical success. CAI matured technologies for large integrated and bonded composite structures across the fixed and rotary wing industrial base. Technology advancements were accelerated and structural performance and cost effectiveness exceeded the current state-of-the-art. Technology applications are increasing and are anticipated to continue to expand.

REFERENCES:

- [1] <http://www.globalsecurity.org/military/systems/aircraft/f-22-mp.htm>. Accessed July 5, 2006.
- [2] ABAQUS Press Release, ABAQUS Selected by Boeing to Commercialize Composite Structure Design Technology, 14 April 2004

9.5.2 PERFORMANCE OF AN IMPROVED COMPOSITE JOINING CONCEPT UNDER FATIGUE

Xinyuan Tan and Erian Armanios, Georgia Institute of Technology

Three composite joint configurations, namely the Straight Laminate (SL), the Single Lap and the Single Nested Overlap (SNO) joints, depicted in Figure 9.5-6, are investigated to ascertain the improvement of the SNO joint over the single lap joint under quasi-static and cyclic loading. The SNO joint is a co-cured composite joint design proposed previously while the SL represents a perfect joint and serves as an upper bound for static strength and fatigue life comparisons. S-N curves are generated based on constant amplitude tension-tension cyclic loading at a frequency of 5 Hz and stress ratio (R) of 0.1 for quasi-isotropic graphite/epoxy (IM7/8551-7) joints. The maximum fatigue load is varied between an average of 70-90% UTS for SL, 20-80% UTS for single lap joints and 40-95% UTS for SNO joints. Fatigue run-out is defined at 1×10^6 cycles. The fatigue strength improvement of SNO joint is ascertained quantitatively through two indicators. The S-N curve comparison for the three joint configurations is provided in Figure 9.5-7. The static strength of SNO over single lap joints compares at approximately 4% while the corresponding improvement in the fatigue strength is approximately 21%. The SNO joints have a higher fatigue to static strength ratio than the single lap joints (38.4% vs. 23.1%), demonstrating the efficiency of the SNO joint under cyclic loading. Three quasi-static Acoustic Emission (AE) count peaks were identified during monotonic loading before eventually reaching a maximum at ultimate failure. The cumulative AE count peaks are used as a collective measurement of the significant damage event incurred under specific loading and subsequently correlated to the fatigue performance of each of these three joint configurations.

ACKNOWLEDGEMENTS

This work is sponsored by the National Rotorcraft Technology Center through the Georgia Institute of Technology Rotorcraft Center of Excellence.

9.5.3 CHARACTERIZATION OF FATIGUE DAMAGE IN COMPOSITE SANDWICH HULL MATERIALS AT LOW TEMPERATURES

Samirkumar M. Soni, Ronald F. Gibson and Emmanuel O. Ayorinde, Wayne State University

Introduction

Ships navigating in the Polar Regions are generally subjected to fatigue loading conditions at temperatures below the freezing point, which leads to changes in the mechanical behavior of ship hull materials by comparison with room temperature (RT) behavior. In recent years, foam core composite sandwich structures have become viable candidates for use in ship hulls. Thus, it is very important to characterize the fatigue behavior of foam core composite sandwich beams at low temperatures. This paper summarizes the results of experimental and numerical studies on the fatigue behavior of foam core composite sandwich (CS) beams at room temperature and low temperatures (down to -60 0C) for their potential applicability in the hull materials of ships navigating in the Polar Regions.

Experiments

Static 4-point bending tests were performed on the CS beams with Rohacell (PMI) foam core and unidirectional carbon/epoxy skin material at 22 0C, 0 0C, -30 0C and at -60 0C respectively inside the environmental chamber of an EnduraTec servo-pneumatic testing machine (Figure 9.5-8) in order to establish a baseline on their static behavior at different temperatures. Based on the results from the static tests, load-controlled 4-point fatigue bending tests in accordance with ASTM C393-62 [1] were performed at 2 Hz frequency and 0.1 loading ratio (min. load/max. load per cycle) in the same set up to simulate sea wave effects at different temperatures (RT, 0 0C and -60 0C) and load levels ranging from 0.7-0.9 of static ultimate load. A digital camera was used to follow the crack propagation path during the fatigue tests.

Results and Conclusions

The clear effects of low temperatures on the flexural static behavior of the CS beams are seen from the increases in stiffness, strength and elastic limit, and decreases in the displacement to failure with reductions in temperature as shown in Figure 9.5-9. The principal failure mode was core shear under static loading conditions at each temperature.

As in previous studies [2-5] at room temperature, core shear was also found to be the dominant failure mode under fatigue loading conditions at different temperatures. Thus, there was no effect of low temperature on the failure mode of CS beams, but at -60 0C catastrophic brittle type core shear failure occurred without any visual crack formation during the useful fatigue life. Significant increase (two times at 0 0C and more than 100 times at -60 0C) in the useful fatigue life was observed at low temperatures with respect to RT. Figure 9.5-10 showing the SN data for carbonfiber/Rohacell (PMI) foam core (CF/RC) sandwich beams gives a clear indication of the effect of low temperature on fatigue life. Two approaches were used to investigate stiffness reductions during fatigue testing; one used the changes in the absolute mean displacement vs. number of cycles (Figure 9.5-11) and another used the changes in the slope of the hysteresis loop with increasing numbers of cycles. The two approaches showed good agreement with each other. It was clear that there were negligible stiffness reductions at -60 0C throughout most of the useful fatigue life, with corresponding significant increases in the fatigue life, but there were significant and early stiffness reductions under fatigue conditions at RT. FE models of the CS beams showed the effects of skin stiffness on the crack initiation location under fatigue loading conditions.

Acknowledgements

The authors gratefully acknowledge the financial support of the U. S. Office of Naval Research (ONR) throughout this research program. In particular, we are indebted to Dr. Kelly Cooper and Dr. Yapa Rajapakse of ONR for their encouragement and support.

REFERENCES:

- [1] "Annual Book of the ASTM Standards". C 393-62: Standard Method of Flexure Test of Flat Sandwich Constructions, American Society for Testing and Materials, Philadelphia, PA. Vol. 15. No. 03, pp 23-24, 1998.
- [2] Kulkarni N., Mahfuz H., Melanie S. and Carlson L. "Fatigue failure mechanism and crack growth in foam core sandwich composites under flexural loading", Journal of Reinforced Plastics and Composites, Vol. 23, No. 1, pp 83-94, 2004.

- [3] Kanny K. and Mahfuz H. "Flexural fatigue characteristics of sandwich structures at different loading frequencies". *Composite Structures*, Vol. 67, No. 6, pp 403-410, 2005.
- [4] Burman M. and Zenkert D. "Fatigue of foam core sandwich beams – 1: undamaged specimens", *International Journal of Fatigue*, Vol. 19 No. 7, pp 551-561, 1997.
- [5] Sharma N., Gibson R. and Ayorinde E. "Fatigue of Foam and Honeycomb Core Composite Sandwich Structures: A Tutorial", *Journal of Sandwich Structures and Materials*, Vol. 8, No. 4, pp 263-319, 2006.

9.5.4 ENVIRONMENTAL AND AGING EFFECTS ON COMPOSITE STRUCTURES

Curtis Davies, Federal Aviation Administration, ATO-P, R&D

Because more composite materials are being used on aircraft structures, the FAA is evaluating environmental and loading effects on aging composite structures. Researchers are studying a composite stabilizer after 18 years of service. In August 1982, Boeing manufactured and certified five shipsets of 737-200 graphite/epoxy stabilizer as part of the NASA Aircraft Energy Efficiency (ACEE) program. Three shipsets have been retired, and two are still in service. This past year, FAA-funded researchers at Wichita State University's National Institute of Aviation Research (NIAR), a member of the Joint Advanced Materials and Structures (JAMS) Center of Excellence, performed an evaluation of one of the retired structures.

Researchers from NIAR, the FAA Airworthiness Assurance Nondestructive Inspection Validation Center, located at Sandia National Laboratories, and Boeing assessed the results of a number of standard and novel nondestructive inspection (NDI) methods performed on the stabilizer prior to teardown. These inspections included thermography, RapidScan, laser ultrasonics, pulse-echo ultrasonics, and photogrammetry. The research team compared the accuracy of the different inspection methods in detecting flaws, such as delaminations, disbonds, impact damage, moisture ingress, or corrosion of the aluminum lightning protection scheme.

After tearing down the stabilizer, researchers found it in good condition, with only a few corroded fasteners. Then they compared the results of the teardown with the NDI data obtained prior to the structure's disassembly. After that, researchers performed a complete destructive evaluation, including physical and mechanical testing, to confirm the structural condition of the stabilizer. This sequenced investigation resulted in better understanding the effects of aging on the composite structure and identified changes in the material properties over the service life. Ultimately, they found the structure had not degraded in its 18 years of service.

9.5.5 TRAINING MAINTENANCE AND REPAIR PERSONNEL FOR COMPOSITE STRUCTURES

Curtis Davies, Federal Aviation Administration, ATO-P, R&D

Working with Edmonds Community College, a member of the Joint Advanced Materials and Structures Center of Excellence, the FAA is developing a course to teach the maintenance and repair of composite aircraft structures. The FAA's latest developments in composite maintenance research will be incorporated into the course. The SAE Commercial Aircraft Composite Repair Committee (CACRC), which is chartered to establish airline industry consensus on standards regarding composite materials maintenance and repair, is also involved in course development and will provide continuing support through its Training Task Group. The course will blend distance (web-based) learning on composite maintenance and repair knowledge with work in regional laboratories, where students will receive hands-on training. A composite specialist from industry will teach the course and advise laboratory instructors.

In FY 2006, researchers held two workshops with industry to develop course standards. At these workshops, Airbus and Boeing, major aerospace original equipment manufacturers (OEMs), provided detailed internal reviews of the course content. The FAA gained industry consensus on items that must be addressed in composite maintenance training.

9.5.6 FLAME RETARDANT EPOXY RESINS CONTAINING PHOSPHORUS FOR AIRCRAFT STRUCTURAL APPLICATIONS

Richard E. Lyon, Federal Aviation Administration, ATO-P, R&D

The use of composite structures in both commercial and general aviation aircraft has been increasing primarily because of the advantages composites offer over metal (e.g. lower weight, better fatigue performance, no corrosion, better design flexibility, etc.). The new Airbus 380 is expected to have about 22% of the structural weight in composites and about 50% of the structural weight of the new Boeing 787 is proposed to be composites, including for the first time a composite fuselage and wings in a large commercial airliner. Currently no fire resistance requirements exist for exterior polymer composite structures on airplanes. However, the aircraft manufacturer will be required to demonstrate that polymer structural composites provide equivalent safety to the current material system (aluminum alloy). The primary hazards during aircraft fires are heat, smoke, and toxic gas. In a severe aircraft fire, life-threatening levels of these hazards are produced by cabin flashover, the time to which is largely governed by the rate of heat release of the materials in the fire.

Phosphorus is a flame retardant for epoxy resins that is known to impart fire retardation by condensed phase and gas phase mechanisms. In the condensed phase, phosphorus catalyzes formation of a carbonaceous char that protects the underlying material from heat and acts a barrier to the release of fuel gases from the surface. When acting in the condensed phase as a char catalyst, phosphorus retards the spread of fire with minimal release of toxic gases. In the gas phase phosphorus acts as a flame poison with PO species participating in a kinetic mechanism that is analogous to that of halogens in flames. Gas phase activity is indicated by one or more of the following as a consequence of incomplete combustion: low heats of flaming combustion, high levels of visible smoke, and high yields of carbon monoxide. Phosphorus has been incorporated into polymeric materials as an additive and as part of the polymeric chain. Additives are normally more economical to use but tend to leach out and have a negative impact on processing characteristics and mechanical properties. Epoxy resins and curing agents that contain phosphorus as part of the chemical structure are more expensive but the phosphorus is permanently incorporated into the polymer and the effect on physical and mechanical properties is minimal. The intent of this work was to identify an epoxy resin and/or curing agent containing phosphorus that could be incorporated into existing aerospace epoxy formulations at low levels to provide fire resistant structural composites with little or no compromise in processing, handling, and mechanical properties.

Epoxy resins and their curing agents (aromatic diamines) containing phosphorus were synthesized by the NASA Langley Research Center, Hampton, VA. The phosphorus-containing epoxy formulations (resin + curing agent) were characterized by thermogravimetric analysis, propane torch test, elemental analysis, microscale combustion calorimetry, and fire calorimetry. Figure 9.5-12 shows results for flammability (heat release capacity) of epoxy formulations versus the weight percent phosphorus incorporated into the polymer as either a phosphorus-containing curing agent (diamine) or epoxy resin. A three-fold reduction in flammability is observed for the phosphate epoxies (Epoxy 6 and 8).

Flaming combustion efficiency, used as a global measure of gas phase activity, did not indicate that phosphorus had any significant effect on flame chemistry for the compounds studied. Instead, flammability reduction was attributed to the promotion of charring by the phosphorus. Phosphorus appears to act in the condensed phase as a catalyst for char formation, i.e., phosphorus promotes char but is not consumed in the chemical reactions that form char. Catalytic activity is indicated by: 1) the several-fold increase in char mass per unit mass of incorporated phosphorus; 2) lowering of the temperature and activation energy for thermal decomposition; and 3) saturation of charring at higher P loadings, typically greater than 3%. The activity of phosphorus as a char catalyst is on the same order as the oxidation state of phosphorus in the diamine or epoxide, i.e., organophosphate (PO_4) > organophosphate (PO_3) \approx organophosphonate (RPO_3) > organophosphine oxide (R_3PO). This hierarchy of activity could indicate that the catalyst for char formation is a phosphorus oxide or phosphorus acid. The fracture toughness and compressive strength of several cured formulations showed no detrimental effect due to phosphorus content. The chemistry and properties of these new epoxy formulations are discussed.

9.6 LOADS

9.6.1 HC-130H CENTER WING BOX MONITORING PROGRAM

James M. Greer, Jr. and Gregory A. Shoales, Center for Aircraft Structural Life Extension (CAStLE), United States Air Force Academy

The first year of this program (2005-06), which included design and installation of the system, as well as one year of data collection, were funded by the USAF 646th Aeronautical Systems Squadron, Aeronautical Systems Center. Current program funding is from the U.S. Coast Guard.

Effective structural fleet management using the damage tolerance approach depends upon accurate knowledge of the progression of damage during the service life of the aircraft. Durability and damage tolerance assessment (DADTA) methods, models, and tools are dependent upon accurate knowledge of material behavior, loads, stresses and geometry effects. Data from full-scale ground and flight tests, which are usually collected during aircraft development, provide key inputs for these purposes. However, over time, uncertainties introduced or revealed by new modeling and testing methods, aircraft modifications, and changes to missions and usage lead to uncertainties in damage predictions. For good reason, these uncertainties lead fleet managers to opt for conservatism in life prediction. But this may have the unintended consequence of restricting or retiring airframes prematurely.

In-flight data collection is one means of reducing this uncertainty, which may extend the useful lives of aircraft or anticipate safety-of-flight issues. Such data can be used to validate and/or update DADTA models and lead to more accurately assessments of remaining structural life.

In 2003, the C-130 center wing box (CWB) was identified as an excellent candidate for an in-depth assessment of the effects of corrosion and fatigue on a 7000 series aluminum aircraft structure. The assessment plan included the teardown of a retired CWB, the development of structural damage management software tools, and the collection of representative flight data for the purposes of updating and validating finite element tools. The U.S. Coast Guard, with a small fleet of C-130s (some of which were nearing the end of their service lives) expressed an interest in participating in the flight data collection effort, leading to their involvement in this effort.

After extensive planning and coordination efforts, in the summer of 2005 a U.S. Coast Guard HC-130H aircraft (Figure 9.6-1) was instrumented for the purposes of monitoring the loading and environmental conditions affecting the CWB. The primary instrumentation consists of accelerometers (two channels, N_z) and strain gages (43 channels, uniaxial and rosette). Sensors for cabin and pressure altitude, temperature, and humidity were also installed. Other aircraft parameters, such as true airspeed, weight-on-wheels, ramp door position, and flap position are also collected by the monitoring system. Collecting aircraft parameters facilitates matching loads and environmental information to different phases of flight, flight conditions, and aircraft configurations.

In its first year of operation, the system collected 535 hours of flight data during operational missions from its duty station, U.S. Coast Guard Air Station Kodiak, Alaska. Missions included a mix of ferry, training, sea surveillance, resupply, and search and rescue. Of primary interest in the data collection effort is the severity of the operational environment. The data collected by this effort is being used to assess and update (if necessary) models for life prediction. As of December 2006, the test aircraft is now based at U.S. Coast Guard Air Station Clearwater, Florida, so additional severity information from another operational location is now becoming available.

The HC-130H flight data acquisition system consists of the following items:

- The ACRA KAM-500 Data Acquisition Unit (DAU)
- Five rosette strain gages
- Twenty-eight uniaxial strain gages
- Eleven Resistance Temperature Devices (RTD)
- The Vaisala PTU200 pressure, temperature, and humidity transducer and remote probe
- The Coleman SV8 GPS receiver with the Raven BT-2DGPS antenna signal splitter
- Two Kistler DC single-axis accelerometers
- Two Honeywell Precision Pressure Transducers (PPTs)

- A Flap Position Sensor (FPS) for counting revolutions of the flap torque tube
- A mounting pallet that contains the KAM-500, GPS, PTU200, and one of the Honeywell pressure sensors

Data are recorded on a Compact Flash (CF) card located inside DAU and accessible via an external slot. The CF card is removed and replaced approximately every three weeks and sent to the CAStLE research center for processing. At CAStLE, the data are converted to engineering units, then transferred to Lockheed servers for additional analyses.

The recorded parameters and their sample rates are shown in Table 9.6-1. "Record Rate" indicates the frequency at which data are written to the CF card.

Analysis of the Kodiak-based results indicate that flight severities, as measured by N_z , are somewhat lower than anticipated. This is probably not representative of the USCG fleet, however, as Kodiak's cold-water environment, lack of flight training missions, higher crew qualification standards, and recent USCG guidance regarding avoiding certain more severe flight regimes could all be contributing to these results.

Currently, the aircraft is operating from Clearwater, FL, and it is quite possible that a different flight severity will be observed there. Conclusions as to whether severity factors should be adjusted will be considered after collecting data from Clearwater for at least one year.

9.6.2 HELICOPTER COMPONENT FATIGUE LIFE WITH USAGE MONITOR

Suresh Moon and Nam Phan

The American Helicopter Society (AHS) Fatigue and Damage Tolerance Subcommittees conducted a round robin in 2006 on the reliability of usage monitored based component retirement. The author's approach to compute reliability for the AHS round robin 2006 problem is presented in reference 1. Usage and loads have distinct Weibull distributions for each regime with associated Weibull parameter values, which results in different loads and percentage usage for the regimes in the spectrum. To simulate a problem to three variables (usage, loads, and strength), one incremental PDF (ΔP_i) is required to represent the loads from all regimes, another PDF (ΔP_j) to represent the percent usage from all regimes, and a third PDF (ΔP_k) to represent strength. To achieve these objectives, the load and usage distribution variable range above the 50th percentile and the component strength range below the 50th percentile were divided into segments. The Weibull parameters and the upper and lower bounds of each segment were utilized to compute the Weibull Cumulative Probability Distribution (CPD). CPD's thus evaluated were employed to obtain equal incremental PDF (ΔP_i) for usage in all regimes, another incremental PDF (ΔP_j) for loads in different regimes, and a third incremental PDF (ΔP_k) for strength, Figure 9.6-2. The failure probability was computed using the following expression and associated fatigue life was evaluated using Miner's cumulative damage theory.

$$\Delta P_{ijk}(u,l,s) = \Delta P_i(u) \cdot \Delta P_j(l) \cdot \Delta P_k(s)$$

Figure 9.6-3 shows the variation of reliability computed using this approach at constant usage severity of 95th percentile, 50th percentile, and 5th percentile. As expected, reliability decreases with an increase in component life. At six nines reliability, component life increases with a decrease in usage severity from 95th percentile to 5th percentile. The methodology proposed is based on mathematical probability theory and produces consistent results.

9.6.3 HELICOPTER ROTATING COMPONENT FATIGUE TRACKING USING ENERGY HARVESTING WIRELESS SENSORS

S. Moon, N. Phan, S. Arms, C. Townsend, D. Churchill, M. Augustin, D. Yeary and P. Darden

Loads on helicopter rotating components cannot be measured without an elaborate and costly instrumentation package involving slip rings. Therefore, individual condition based component replacement (CBCR) is difficult. To overcome this limitation, an energy harvesting wireless sensors for load recording system is being developed. The piezoelectric elements were unidirectionally aligned, 250-micron PZT fibers embedded in a resin matrix and epoxy

bonded to the surface of test pitch link specimens. To test and record operational pitch link loads, a conventional full strain gauge bridge was bonded to the pitch link using high resistance (4500 ohm) bonded foil strain gauges. During the cyclic loading, the PZT element converted the applied strain energy into electrical output, Figure 9.6-4. This output was connected to an energy harvesting and storage circuit consisting of a rectifier and storage capacitor and the charge was used to power wireless sensor node. For flight test, Figure 9.6-5, the energy harvesting wireless pitch link was installed on a Bell Model 412 experimental rotorcraft and successfully flight tested at the Bell facilities in Fort Worth Texas during February of 2007. The test included ground and in-flight EMI evaluations, Rotor Track and Balance verification, and data collection during a scripted flight, Figure 9.6-6. The wireless sensor node is embedded with peak-valley algorithm for data compression and fatigue damage computation using rain-flow counting and Miner's rule. The system is envisioned with the base station including a remote cellular telephone interface that allows access to the recording system and stored data. Cellular communication is available and will transfer data without fleet maintenance personnel intervention.

9.6.4 STUDY OF SIDE LOAD FACTORS DURING AIRCRAFT GROUND OPERATIONS

Tom DeFiore, Federal Aviation Administration, ATO-P, R&D

The FAA conducted a study of ground operations using airplane data recorded by Digital Flight Data Recorders (DFDR) to assess the suitability of the 0.5G limit lateral load for 14 CFR 25.495 and in particular for use as a limit load for the Airbus 380 airplane. The results of this study are documented in Technical Report DOT/FAA/AR-05/7, "Study of Side Load Factors During Ground Operations" containing data to supporting a special condition for a lateral load of 0.42G for the A380 airplane. The data presented in the report provides the user with data comparing the side load factors encountered during ground operations for airplane models B-747-400, B-767-200, B-737-400, CRJ-100 and A320 in actual operational usage.

Lateral acceleration certification criteria from Title 14 Code of Federal Regulations (CFR) for commercial aircraft operations are based primarily on the following two ground events that are considered to be the most critical to the aircraft structure: (1) the touchdown (14 CFR 25.485) and (2) ground turning (14 CFR 24.495).

The research findings can be summarized as follows. There is a significant difference in the touchdown lateral acceleration between widebody airplanes and narrow body airplanes. Figure 9.6-7 (from DOT/FAA/AR-05/7) clearly shows that the B-767 and B-747 lateral acceleration distributions are much higher than that of the narrowbody airplanes.

In addition, there is a significant difference in the ground turn lateral accelerations among airplanes with different weights. There is a marked decrease in lateral acceleration distribution for increasingly heavy airplane models.

As shown in Figure 9.6-8, (from DOT/FAA/AR-05/7) the highest recorded lateral acceleration during a ground turns of 11,000 flights of B-747 airplane usage was approximately 0.16G. The data from this figure was presented to the Aviation Rulemaking Advisory Committee which recommended a special condition to 14 CFR 25.495 to reduce the ground turning requirement from 0.5G to 0.42G.

The data in these two figures show that, in general, the size (and weight) of the aircraft does appear to be a significant factor affecting, not only when high lateral acceleration values occur, but also the magnitude of the lateral accelerations. Smaller airplane models such as the CRJ-100 and B-737 tend to incur most of their higher lateral acceleration values while turning, likely due to higher speed and gear layout. Heavier airplanes are prone to encounter lower values of lateral acceleration while taxiing and tend to have their highest lateral accelerations occur during the touchdown event and subsequent rollout.

9.6.5 LOADS DATA FOR THE BOEING 777

Tom DeFiore, Federal Aviation Administration, ATO-P, R&D

FAA researchers have collected the operational loads history of the Boeing 777-200 in DOT/FAA/AR-06/11, "Statistical Loads Data for the B-777/200 Aircraft in Commercial Operations" (<http://tc.faa.gov/its/worldpac/techrpt/ar06-11.pdf>). This report provides analysis of Boeing 777-200ER aircraft operational usage data

from 10,047 flights, representing 67,000 flight hours of a single international airline operator. It also contains statistical information on aircraft usage, ground and flight loads occurrences, and the operational usage of certain systems, as well as statistics on aircraft weights, flight distances, altitudes, speeds, and flight attitudes. Ground loads data include statistics on vertical, lateral and longitudinal load factors along with ground speed and aircraft weight during different ground operational phases. Flight loads data include statistical information on gust and maneuver load factors, derived gust velocities, and ground-air-ground cycles. Systems operational data include statistics on flap usage and engine fan speed.

9.6.6 STRUCTURAL LOADS ON FIRE-FIGHTING AIRCRAFT

Tom DeFiore, Federal Aviation Administration, ATO-P, R&D

Recognizing that U.S. Forest Service air tanker aircraft carry heavier loads than those anticipated in their original design and certification, the FAA initiated a loads monitoring research program to characterize the structural loads environment on these aircraft. In cooperation with the U.S. Forest Service, FAA researchers installed multi-channel load recorders on a P-2 and P-3 airplane used in fire-fighting operations. The research team collected data from approximately 400 flights during the 2005 firefighting season and expect to collect data on another 400 flights during 2006. The operators provided the data to the FAA-funded researchers at Wichita State University for analysis.

The team found that, contrary to the common assumption, the highest wing loads do not occur during the retardant drop, but while fully loaded and cruising to the drop zone. Because they need to get to the fire scene quickly, the pilots of these aircraft generally do not alter their route to avoid turbulence, a major stress factor on wing loading. During firefighting operations, the pilot drops retardant approximately 4,600 seconds into the flight. The associated wing strain at the time of the drop is considerable less than that experienced during the outbound flight cruise. Actually, there is only one peak load during the drop, while there can be multiple higher loads prior to the drop.

Based on these findings, it is recommended that the U.S. Forest Service develop a structural health monitoring program and undertake an engineering analysis to ensure the structural safety of firefighting aircraft. Also, it is recommended that these aircraft undergo a fatigue and damage tolerance assessment of critical structural areas. The FAA published its research results in DOT/FAA/AR-05/35, "Consolidation and Analysis of Loading Data in Firefighting Operations: Analysis of Existing Data and Definition of Preliminary Air tanker and Lead Aircraft Spectra" (<http://155.178.136.203/eosweb/opac/index.asp>).

9.7 STRUCTURAL TEARDOWN ASSESSMENTS

9.7.1 T-37 STRUCTURAL TEARDOWN ANALYSIS PROGRAM

Gregory A. Shoales, United States Air Force Academy

The USAF Academy's Center for Aircraft Structural Life Extension (USAF/CAStLE) initiated a program for the Ogden Air Logistics Center, 506th Aircraft Sustainment Squadron T-37 System Program Office (506 ACSS/GFMT) to conduct a teardown analysis program. Specifically, the Program Office required an investigation which would document any evidence of fatigue, stress-corrosion cracking, corrosion, and any other damage/defects in specified key structural elements which might result in loss of an aircraft during normal operation.

The first phase of the program began execution in January 2006. This phase targeted a complete inspection and analysis of four T-37B ship sets of wing structure. Two ship sets included entire wings previously removed from aircraft and in storage at Hill Air Force Base (AFB). Two additional ship sets in storage at Columbus AFB included portions of the fuselage carry through structure. These wings in these ship sets had the outboard half of the wing removed and were therefore not included in the analysis. The structure from all four ship sets were disassembled and had coatings removed in preparation for nondestructive inspection (NDI). NDI was accomplished by the Air Force Research Lab, Materials Integrity Branch (AFRL/MLSA) in Dayton, Ohio. The final ship set completed NDI was inspections in April 2007. Upon completion of NDI, all parts with NDI indications along with inspections reports were transferred back to CAStLE for evaluation of these findings. Evaluation of NDI inspections in the first ship set was completed by May 2007. Documented stress corrosion cracking and exfoliation findings during this program, Figure 9.7-1, supported development and fielding of a new fleet inspection requirement. Additionally, fatigue crack findings were evaluated by the T-37B chief engineer for fleet management implications. Phase I of this program is scheduled to be complete by September 2007. A final report of this program phase along with all data will be published as a USAF Academy technical report and delivered to the T-37B fleet manager.

The Phase II program began execution in January 2007 with the delivery of two entire T-37B airframes to CAStLE as shown in Figure 9.7-2. This program was more focused in its intent. Rather than analyzing every structural element of entire aircraft components, the Phase II program had the goal of analyzing all T-37B fatigue critical locations. This program had the further goal of providing validation data for the new fleet inspection which was developed during the Phase I program and cited above. By May of 2007 all program components had been extracted from the teardown aircraft and disassembled from the surrounding structure. NDI inspections commenced in April 2007 and the first fractographic evaluations report was completed that same month. Phase II of this program is scheduled to be complete by December 2007. A final report of this program phase along with all data will be published as an additional USAF Academy technical report and delivered to the T-37B fleet manager. All data from both programs will be archived in a searchable database and similarly provided to the T-37B fleet management.

9.7.2 C-130 CENTER WING BOX STRUCTURAL TEARDOWN ANALYSIS PROGRAM

Gregory A. Shoales, Sandeep R. Shah, Justin W. Rausch, Molly R. Walters, Saravanan R. Arunachalam and Matthew J. Hammond, United States Air Force Academy

Aircraft structural fleet management by the damage tolerance method depends upon accurate knowledge of the progression of damage during the service life of the aircraft. The only way to determine the true damage state is by destructive analysis. Since such analysis is impractical in operational aircraft, fleet managers rely on predictive models. These models are dependent upon accurate modeling of material behavior, loads, stresses and geometry effects. Damage predictions are monitored at regular intervals during the aircraft life cycle by various non destructive inspections. Any uncertainty in the model or the inspection data leads to corresponding uncertainty in the actual condition of a given aircraft. Fleet managers can reduce risk to safety by choosing the conservative side of uncertainty. However, such conservatism can increase the risk to aircraft availability. Performing a structural teardown analysis program of one or more aircraft with known service history provides precise damage data resulting from a given usage. These data can then be used to further validate damage models and reduce uncertainty in the damage condition assessment of the remaining fleet.

This work represents a complete summary of just such a structural teardown analysis. Specifically, the center wing box (CWB) was analyzed from a C-130E aircraft with more than 46,000 equivalent baseline hours. This particular usage level is significant since, by current fleet management standards, it had surpassed the retirement usage level by more than 1,000 hours. This teardown program examined fatigue critical locations (FCLs) as well as the entire lower wing structure, upper spar caps, and rainbow fittings. The subject structural elements were evaluated by a variety of operational and emerging NDI techniques both prior to and during the teardown process in order provide correlation to true damage found by failure analysis. In general, poor correlation was noted between NDI indications and actual crack findings. Comparisons are presented between damage findings in FCLs versus non-FCLs.

The data from all damage characterized in this teardown program is presented in terms of location, damage type and physical dimensions. The results of all NDI indication evaluations are shown by finding category in the figure below. Additionally, for crack findings, crack nucleation site location and crack mechanism details are presented. Finally, possible reasons for the poor correlation between NDI indications and true crack findings are presented. This work provides an important input to understanding the actual condition of the C-130 center wing. Having such understanding can lead to less conservatism in fleet management while still retaining required safety. Furthermore, the correlation between NDI indications and actual crack findings can help fleet managers better use the data obtained from NDI inspections when making structural management decisions.

This work characterized the existing state of damage for all key structural elements of the subject aircraft providing invaluable condition assessment data for C-130 fleet managers. Comparison of damage indications from a developmental NDI technique with actual damage characterization demonstrated the unsuitability of this technique for fielding before resources were committed. Finally, the archived data from this effort will serve as validation for new high fidelity finite element models currently under development.

This work was funded entirely by the 646th Aeronautical Systems Squadron (AESS), Wright-Patterson AFB, Ohio and was published as USAF Academy Technical Report, USAFA TR-2006-11. All NDI inspection and evaluation finding data has been archived in a searchable data as USAF Academy Technical Report, USAFA TR-2007-03. (Figure 9.7-3)

9.7.3 USAF HANDBOOK FOR STRUCTURAL TEARDOWN ANALYSIS PROGRAM

Gregory A. Shoales and Lt Col Scott A. Fawaz, United States Air Force Academy

The USAF Academy's Center for Aircraft Structural Life Extension (USAFA/CAStLE) initiated a program to document best practices for planning and executing aerospace structural teardown analysis programs. This document will be published initially as a USAF Technical Report by the end of 2007 and ultimately transitioned to a United States Air Force (USAF) handbook or military specification. This USAF document may then serve as a reference for USAF fleet managers seeking to obtain fleet condition data such as that required by MIL-STD-1530C.

The Handbook chapters will be organized by tasks which are typical to such programs. These typical tasks included:

- Establishing teardown program goals and objectives
- Teardown program subject selection
- Vendor selection and qualification
- Component disassembly
- Nondestructive inspection (NDI)
- Prioritization of indications
- Metallographic and fractographic evaluation of indications
- Analysis of data
- Small sample size statistics
- Archival database design
- Reporting

This handbook shall also capture the available lessons learned from current ongoing and previously completed aircraft structural teardown programs. Such lessons learned have been accumulated from analysis of teardown program final reports obtained by CAStLE engineers, interviews with teardown program engineers and discussions with USAF fleet managers. The Air Force Research Lab, Materials Integrity Branch (AFRL/MLSA) serves as both

consultant and reviewing agency during all phases of handbook development. Additionally, the data required for the sections which document NDI best practices to included selection and qualification of NDI vendors will be provided by AFRL/MLSA.

9.7.4 ASSESSING THE AIRWORTHINESS OF COMMERCIAL AIRCRAFT

John Bakuckas, Federal Aviation Administration, ATO-P, R&D

Airframe teardown inspections and extended fatigue testing are effective means to help determine the continued airworthiness of high-time operational aircraft – particularly those approaching their design service goal (DSG). Essential information and data needed to evaluate the kinds of airframe structures that are susceptible to widespread fatigue damage (WFD) are obtained from teardown inspections. While the expertise and knowledge base required to conduct teardown inspections are well established by the large commercial airframe original equipment manufacturers and military sectors, the broader aviation community lacks well-documented guidelines and data.

In a joint effort by the FAA and Delta Air Lines, researchers conducted a teardown inspection and extended fatigue testing of a fuselage obtained from a retired Boeing 727 revenue-service passenger airplane near its DSG. They removed eleven large fuselage sections, selected as representative of structure susceptible to developing WFD. Focusing on the lap joints, the research team used both conventional and emerging nondestructive inspection (NDI) methods before and after removing the fuselage sections from the airplane.

Using a destructive evaluation procedure developed for the study, the team performed fractographic examinations on each of the seven panels to characterize its state of multiple-site damage. They then used this confirmed information to assess the capability of 20 NDI methods to predict the presence of small hidden cracks. Later, the researchers used the FAA Full-Scale Aircraft Structural Test Evaluation and Research Facility to conduct extended fatigue testing on two of the panels, while continuously assessing damage of those panels through both conventional and emerging NDI methods.

The project collected and analyzed an extensive amount of data, which is documented in a five-volume report. The team developed a companion engineering database that contains the processed data collected from fractography, nondestructive inspections, and full scale testing of the crown skin panels. This database can be used to evaluate the sensitivity and effectiveness of standard and emerging NDI methodologies to detect small cracks hidden in assembled structures. It also provides for the efficient transfer of information to engineering organizations for the future calibration and validation of predictive methodologies for structural fatigue. Data from this project will continue to provide guidelines for future programs that help to ensure the continued airworthiness of the aging commercial fleet.

9.7.5 CRACKING IN ACROBATIC AIRCRAFT FLEET

Michael Shiao, Federal Aviation Administration, ATO-P, R&D

To understand the fatigue and corrosion problems of aging acrobatic aircraft better, FAA-funded researchers at the National Institute for Aviation Research conducted a tear down inspection of a T-34A N141SW that had previously been involved in an accident. In their destructive evaluation, the researchers looked particularly for signs of cracks and corrosion in the right wing front carry-through lower spar, horizontal and vertical stabilizer attachment points, right wing rear spar lower cap wing station 66, and right wing rear spar lower bathtub fitting.

The researchers opened the cracks found on the aircraft and analyzed them to determine their responsible failure mode. They also inspected the surrounding structure microscopically for additional defects. During the destructive evaluation, the research teams found a total of 25 cracks on the right wing front carry-through lower spar, ten cracks on the horizontal and vertical stabilizer attachment points, two cracks on the right wing rear spar lower cap, and one crack on the right wing rear spar lower bathtub fitting. In the carry-through structure, overload caused three cracks, ranging in size from 0.15 to 5.28 inches. Sixteen cracks had fatigue origins with fatigue lengths ranging from 0.05 to 0.53 inch. These sixteen cracks then extended due to overload conditions. The cause of failure could not be determined in the other six cracks, which ranged in length from 0.10 to 1.17 inches.

The researchers found four cracks, resulting from overload, on the vertical stabilizer bulkhead; these cracks ranged from 0.28 to 1.4 inches. They also found six cracks, caused by overload, on the horizontal stabilizer bulkhead; these ranged in length from 0.13 to 1.13 inches. Two 1.187-inchlong cracks also appeared on the right wing rear spar at WS 66. Extensive metal smearing on the fracture faces made the cause of failure for these cracks difficult to determine. In addition, another crack, measuring 3.29 inches, was found on the right wing rear spar lower bathtub fitting. The failure mode of this crack could not be determined.

Due to the recent history of fatigue cracking and failure on T-34A aircraft, this research will aid the FAA in understanding and addressing T-34A concerns, and will help determine the condition of a high-time acrobatic category aircraft. A complete report of the teardown evaluation can be found at www.tc.faa.gov/its/worldpac/techrpt/artn05-57.pdf

9.8 NONDESTRUCTIVE EVALUATION/INSPECTION (NDE/I)

9.8.1 CRACK DETECTION UNDER RAISED HEAD FASTENERS IN HIGH CYCLE FATIGUE JOINTS

Dave Galella, Federal Aviation Administration, ATO-P, R&D

Increasing niche applications, growing international markets, and the emergence of advanced rotorcraft technology are expected to greatly increase the population of helicopters over the next decade. As the helicopter industry adopts the damage tolerance philosophy, the appropriate application of nondestructive inspection (NDI) equipment will play a critical role in managing safety. Fatigue failures in flight critical structure have necessitated a number of in-field inspections based on damage tolerance analysis (DTA). The FAA Airworthiness Assurance Nondestructive Inspection Validation Center (AANC) at Sandia National Labs recently collaborated with Bell Helicopter and others in the rotorcraft industry to evaluate NDI capabilities to detection of small cracks that are still under the heads of button head fasteners. The FAA and rotorcraft industry identified this as an important near-term need because cracks in high cycle fatigue joints, such as those found in the tail boom and transmission assembly regions, can quickly grow from small initiation lengths to critical lengths in a relatively few number of flight hours.

A series of panels (see Figure 9.8-1) were designed to isolate and study the effects of different rivet scenarios on eddy current signals. The parameters studied include loose, tight, alodine and anodized rivets, rivet coating removed parallel and perpendicular to cracks, and crack direction. Insights into the effect of rivet type and installation parameters on the eddy current signals (conductivity across the rivet site) were also studied (see Figure 9.8-2). The goal was to determine how the eddy current signal variations, which were determined to be realistic in field tests on rotorcraft, affected the POD levels measured in the lab.

Remote field eddy current (RFEC) and linear array ultrasonics both demonstrated increased sensitivity. Smaller cracks, further under the rivet heads, were consistently found with these two methods. Specifically, the RFEC technique was successfully used to detect angled, first and second layer cracks hidden beneath raised head fasteners in rotorcraft joints. Linear array ultrasonics, as applied by the USUT 2300 equipment, also showed consistent crack detection well under the rivet head.

An overall summary of NDI performance is included here:

- First layer angled crack detection of 90 percent POD was between 0.050 and 0.060 inches.
- Second layer angled crack detection of 90 percent POD was between 0.080 and 0.100 inches.
- Bolt hole inspection (with fastener removed) had a 90 percent POD of 0.030 inches.
- Rivet conductivity affects (due to coating variations and fretting) increases noise floor and raises the 90 percent POD levels by 0.010 to 0.015 inches in crack length.
- False calls which were between 2 and 3 percent were reduced with improved reference standards
- Importance of training and feedback was demonstrated as significant improvements in POD and false calls were seen when the experiment was repeated by the same inspector.

This effort will now move on to technology transfer activities to move these inspection methods into routine use in rotorcraft maintenance depots. Such will aid the rapid integration of these improved NDI methods in a cost-effective manner.

9.8.2 DEVELOPMENT OF NONDESTRUCTIVE INSPECTION METHODS FOR REPAIRS OF COMPOSITE AIRCRAFT STRUCTURES

Paul Swindell, Federal Aviation Administration, ATO-P, R&D

Composite use is growing in commercial large transport aircraft as evidenced by the planned production of the Boeing 787 and the production of the Airbus 380 aircraft; both contain more composite materials than previous aircraft built by those manufacturers. Appealing characteristics of composites are that they offer lighter weight and equivalent strength to the metals that they replace. However, by the nature of their fabrication, composites offer new challenges to the nondestructive inspection (NDI) community. Traditional inspection problems involving

corrosion and cracks around fasteners in metal structures are being replaced with the need to detect disbonds, delaminations, impact damage, adhesive porosity, and the quality of a repair. Inspection of composites often requires scanning large areas for subsurface damage. This can be time consuming and may require intricate mapping of the surface when damage is detected. The most common NDI method used to inspect composites is ultrasonic testing (UT). Ultrasonic inspections using C-scans are more frequently being used because they can provide a three-dimensional image of the damaged area which can be color coded to ease mapping and interpretation of the inspected area.

Composite sandwich panels with honeycomb cores are widely used in aircraft as secondary structures and control surfaces. Examples of these include rudder skin panels, spoilers, flaps, engine cowlings, landing gear doors, and body fairings. When a honeycomb structure is crushed or damaged, the damaged area may be removed and repaired with patches of similar layers of material bonded in place at an airline composite shop. Repairs are occasionally performed on-aircraft and cured without the benefit of an autoclave which may introduce more porosity than typically found in undamaged structure. A primary maintenance concern is how to determine if these repairs are structurally sound.

Funded as part of the FAA Airworthiness Assurance Center of Excellence (AACE), Iowa State University has undertaken a project that has developed an NDI prototype for assessing composite damage and repairs using air-coupled ultrasonic testing (ACUT). Figure 9.8-3 shows a schematic of the ACUT system.

The system consists of the following: (1) a QMI SONDA 007CSX Airscan pulser/receiver and associated transducers, (2) a Flock-of-Birds magnetic position encoder, (3) a transducer holder and scan yoke, and (4) a laptop computer and software. The QMI air-coupled UT system comes with piezoceramic transducers with 120 and 400kHz frequencies to provide for the through transmission capability. The transducer position information needed to produce C-scan images is obtained from the Flock of Birds (FOB) magnetic position encoder. The FOB is a motion and position tracker that uses a pulsed magnetic field to acquire positional data of a receiving sensor with respect to a stationary transmitter. The receiving sensor is attached to the yoke which holds the transducer. The laptop and software receive data from the FOB and amplitude data from the QMI system to develop the C-scan image. The resolution of the image pixel sizes can be selected among 1.0, 0.5, 0.25 and 0.125 inch sizes, which allows an inspector to scan large areas quickly and then refocus on smaller areas when damage is detected. Figure 9.8-4 shows an example image from an ACUT scan of a repaired honeycomb panel.

Over the course of the project, the prototype ACUT system was field tested and modified numerous times to incorporate the valuable input provided by the host facilities. A field test of the FOB-based air coupled UT scanner at the Army Aviation Support Facility in Boone, Iowa demonstrated the advantage of instantaneously being able to change scanning resolution. Another test at Northwest Airlines demonstrated the concept of the generic scanner breadboard and confirmed the validity of the approach. ACUT was also used to map the extent of damage to rotors on a Blackhawk (UH-60) helicopter at the Iowa Army National Guard Unit.

Blind performance tests were also conducted on a set of 42 honeycomb panels containing engineered flaws at the FAA Airworthiness Assurance NDI Validation Center (AANC). Figure 9.8-5 shows the probability of detection (POD) curves of the ACUT on carbon and fiberglass honeycomb panels with skin thickness of 3, 6, and 9 plies.

This research marks the first time that a non-contacting, non-contaminating air-coupled ultrasonic inspection technique was taken out of the laboratory and made into a practical tool in the field. Efforts are underway to license the technology and transfer its use into the commercial sector. Immediate plans in this regard will focus the use of the ACUT on inspecting the new carbon wing spar of the Cirrus aircraft.

9.8.3 UPDATING DEFAULT PROBABILITY OF DETECTION CURVES FOR ULTRASONIC INSPECTION OF HARD-ALPHA INCLUSIONS IN TITANIUM BILLET

Cu Nguyen, Federal Aviation Administration, ATO-P, R&D

The United Flight 227 accident in Sioux City, Iowa, in 1988 led to the incorporation of damage tolerance principles into the design and life-cycle management of the rotating components of aircraft jet engines. A key parameter in

establishing damage tolerance is a quantification of the ability of inspections to remove flawed components from service based on the probability of detection (POD).

Traditional means for determining POD are based on empirical measurements made on samples containing known representative defects. However, using this method, it would be cost prohibitive to manufacture the number of samples required for the POD determination of rotating engine components. With these component flaws, mostly hard-alpha inclusions, an alternate approach is to estimate POD based on defects found during the manufacturing process. The FAA used such an approach to produce the 1995 Default POD Curves that appear in AC33.14-1, Damage Tolerance for High Energy Turbine Engine Rotors (ANE-110, 1/8/01). In FY 2006, a FAA research team used a small sample size with the addition of data readily available within the community to derive better estimates of the default POD curves. Besides drawing on alternative sources of data, such as physics-based models of the inspection process, they applied more powerful statistical analyses than had previously been used in estimating POD curves. Drawn from larger data sets that included multi-zone inspection data as well as conventional inspection data, and analyzed more rigorously through physics-based techniques, the new curves are more realistic than those previously available. This ability to quantify current performance and its variability will help shape the development of future damage tolerant design concepts of fracture-critical titanium alloy rotor designs.

9.8.4 VALIDATING NONDESTRUCTIVE INSPECTION TECHNOLOGIES WITH TEARDOWN DATA

David Galella, Federal Aviation Administration, ATO-P, R&D

A collaborative research team had an opportunity evaluate a group of nondestructive inspection methods using data from a destructive evaluation of an in-service aircraft. While performing extensive destructive evaluation and extended fatigue testing of a fuselage structure from a retired transport aircraft, the researchers looked into the effectiveness of twenty NDI technologies that were applied to the aircraft prior to its being dismantled. They focused on the ability to detect cracks emanating from lower row fastener holes in the lower lap joint skins of a Boeing-727 aircraft. The Airworthiness Assurance Working Group had previously identified these longitudinal lap joints as susceptible to widespread fatigue damage, and the vulnerability of these parts is also the subject of Airworthiness Directives (AD) 99-04-22 and 2002-07-09.

Researchers from the FAA, Delta Airlines, and the FAA's Airworthiness Assurance NDI Validation Center assessed the readiness of conventional and experimental NDI technologies for use at airlines or maintenance, repair, and overhaul (MRO) facilities. The various NDI findings had indicated the test lap joint panels removed from the retired aircraft contained service-induced cracks. Destructive tests later confirmed these findings.

The conventional NDI technologies used in the study included directed visual inspection, external low-frequency eddy-current (LFEC) sliding probe, and internal medium-frequency eddy-current (MFEC) methods. All of these are called out in the Boeing NDI manuals. The emerging methods, designed to inspect the inner skins from the exterior fuselage surface, included a variety of advanced eddy current, ultrasonic, and radiography systems. The research team evaluated each technique according to its sensitivity and reliability, ease-of-use, speed, and fieldability.

The study yielded useful results. The internally-applied MFEC methods reliably detected cracks longer than 0.090-inches, better sensitivity than that of any externally-applied NDI technologies. External methods that provided the best sensitivity were the Meandering Winding Magnetometer (MWM), Remote Field Eddy Current (RFEC), Giant Magnetoresistive Sensor (GMR), digital radiography, and Rivet- Check. The LFEC sliding probe, Array Eddy Current, the Magneto Optical Imager (MOI), and Turbo-MOI Methods proved the fastest methods to deploy. Emerging methods determined to be ready for immediate implementation at airline or MRO facilities included the MOI, Turbo-MOI, and MAUS. All of these technologies are currently in use, but not on a widespread basis. The technologies deemed promising for implementation at an airline or MRO facility in the near future included MWM, RFEC, GMR, digital radiography, RivetCheck, and a high frequency ultrasonic array.

Results from this study will aid in the acceptance and adoption of these emerging technologies as alternate means to inspect for cracks in aircraft fuselage substructures without the need to tear the aircraft down.

9.9 RISK ASSESSMENTS

9.9.1 RISK QUANTIFIED STRUCTURAL ASSESSMENT

Eric Tuegel, Air Force Research Laboratory - Air Vehicles Directorate

The new aerospace systems desired by the USAF to enable revolutionary capabilities, such as air-breathing hypersonic flight, will operate under new and poorly understood conditions that render traditional airframe design and certification practices obsolete. The operating conditions for these new systems, as well as the new materials from which they will be made, will have vastly different variability characteristics than those for which the current safety factors were determined. The operational environments of systems such as a reusable space vehicle or an air-breathing hypersonic vehicle cannot be easily created for a full airframe ground test.

Under the current paradigm, the factor of safety for these revolutionary aerospace systems will evolve slowly over time as experience with these new vehicles is developed. When accidents occur, the safety factor for the next generation system will be increased. If no accidents occur, the safety factor will be decreased to save weight and improve performance. This adaptive process is slow and costly. It will be made more so by the small numbers in which these vehicles will be purchased. Clearly there is a benefit to the USAF to develop a new paradigm for ensuring structural integrity that is able to more rapidly accommodate new loadings, new materials, and new systems.

The Air Vehicles Directorate of the US Air Force Research Lab is investigating a risk-based structural design, assessment and certification for airframes similar in concept to the processes used to design and certify nuclear power plants and off-shore oil platforms. The design of an aerospace system seeks to maximize system effectiveness in terms of results versus expenditures of money, manpower, materials, and time. Achieving the maximum system effectiveness is a trade off between structural integrity against performance. The traditional balance that has been reached for conventional aircraft needs to be re-examined for new revolutionary aircraft in terms of the risk to safety, structural integrity, performance, maintenance, etc. This is what Risk-Quantified Structural Assessment (RQSA) proposes to do.

Lacking an large experience base for structure operating in these extreme conditions, RQSA will need high-fidelity, physics-based finite element models of the airframe structure to predict the response of the structure to environmental inputs, the development of damage in structural components, the eventual failure of components, and the effect of component failures on the response of the structure. These predictions will be in the form of probability distributions that will be used in conjunction with various probabilistic methods to estimate the risk to the air vehicle of operating in certain flight regimes at any time during its service life. From these simulations, the risk trade-offs can be examined in order to design the airframe for peak effectiveness.

Across the aerospace industry, there is a universal desire for no surprises in the force that result in “not mission capable” status, in-flight failure or a “hard downing” event. The ability to see ahead of both unplanned and some necessary maintenance events and predict the remaining life accurately with sufficient lead time that appropriate corrective action can be taken via an aircraft health management system is the only way to get close to this utopian ideal, especially in this era of tight budgets. Prediction of remaining life, or prognostics, by its very nature is probabilistic and relies heavily on the quantification of risk. Thus, RQSA also supports the development of the prognostic capabilities of structural health management systems.

9.9.2 FURTHER DEVELOPMENT OF THE DARWIN SOFTWARE FOR PROBABILISTIC DAMAGE TOLERANCE ANALYSIS

R. Craig McClung and Michael P. Enright, Southwest Research Institute

The Federal Aviation Administration (FAA) has been working with the aircraft engine industry to develop an enhanced life management process, based on probabilistic damage tolerance principles, to address the threat of material or manufacturing anomalies in high-energy rotating components. The process is documented in current and planned FAA Advisory Circulars. Funded by a series of grants from the FAA, an integrated team of Southwest Research Institute, GE Aviation, Pratt & Whitney, Honeywell, and Rolls-Royce Corporation has developed

predictive tool capability and supplementary material/anomaly behavior characterization and modeling to support and enhance the process and the advisory material.

The centerpiece of this research effort is the DARWIN (Design Assessment of Reliability with INspection) computer code, which integrates 2D and 3D finite element stress analysis results, fracture mechanics models, material anomaly data, probability of anomaly detection, and inspection schedules to determine the probability-of-fracture of a rotor as a function of operating cycles with and without inspections. DARWIN includes state-of-the-art algorithms for risk assessment and fracture mechanics analysis within a powerful graphical user interface.

Earlier versions of DARWIN addressed the risk of rotor fracture due to titanium hard alpha anomalies or surface damage due to machining at bolt holes in all rotor materials. The latest version, DARWIN 6.0, was released for production use in December 2006. Major new capabilities in this version include an accurate probabilistic treatment of materials with large numbers of inherent anomalies, three-dimensional anomaly modeling, simulation of production inspections, a user-defined crack formation life module linked at execution, a new bivariant stress intensity factor solution for a corner crack at a hole, encryption capability for materials input files, and comprehensive verification checks. DARWIN can now be used for any metallic material, either for inherent material anomalies in any axisymmetric component, or for surface anomalies in any three-dimensional component.

Royalty-free DARWIN licenses are available to all U.S. government agencies. In addition, DARWIN is currently licensed commercially by five aircraft engine companies and two government laboratories in seven different countries.

The second major FAA grant (“Turbine Rotor Material Design—Phase II”) was completed in 2005, and a comprehensive final report is in press. This research is continuing under a new FAA grant entitled “Probabilistic Design for Rotor Integrity,” initiated in 2005, with a focus on surface anomalies in all rotor alloys and inherent material anomalies in nickel-based superalloys.

Further information about DARWIN and related research is available at www.darwin.swri.org.

9.9.3 ELECTRICAL SYSTEMS RISK ANALYSIS TOOL

Michael Walz, Federal Aviation Administration, ATO-P, R&D

FAA sponsored research has led to the development and enhancement of an electrical systems risk analysis tool (RAT). Designed to perform risk analysis of an aircraft electrical wire interconnect system (EWIS), the new software simplifies analysis of hazards that can cause damage to structures and cause fires. The tool can also be used to examine how potential failures in the EWIS could affect the functionality of the connected systems.

The tool combines routing and architecture data with an automated structured safety analysis. It considers common cause failures that can result in the functional loss of systems sharing a common wire bundle. The analysis logic considers all wire failure modes, including arcing faults occurring within a wire bundle and arcing to adjacent wire bundles or structure.

This new tool provides a simplified method of processing large quantities of EWIS design data through a powerful analysis process that will assess virtually all potential EWIS hazards. In addition, it can be updated with fleet data to reflect the latest effect of fault mitigation technology on wiring systems. It will also help to bring about greater consistency in the certification process and be of considerable safety benefit to the aviation community. The tool will provide advanced capabilities to help certification officials analyze EWIS designs.

9.10 ENGINES

9.10.1 RAPID FATIGUE CRACKING IN A WING LIFT STRUT

The original DeHavilland DHC-3 Otter single-engine aircraft was powered by a Pratt & Whitney R1340 Wasp piston engine. The DHC-3 was certificated in 1952 and since then has undergone many modifications. One popular modification replaces the piston engine with a more powerful Pratt & Whitney PT6A turbine. Another popular modification increases the gross weight of the turbine version and it includes reinforcement of the wing lift strut. A fleet of DHC-3 Otters with these modifications experienced cracking in numerous wing struts including new replacement struts. The cracking was not typical and not explainable by the usual fatigue mechanisms.

A major investigation was undertaken that began with a review of the fleet service history and interviews with maintenance crews. The cracking was being reported but the severity of the problem was not recognized. Fracture surfaces were studied using metallography. Wing struts were subject to modal testing. One wing strut was instrumented and calibrated to measure in-flight loads and frequency response. Flight testing was undertaken for various mass configurations and the measured results were extrapolated to design loads. During one flight test a wing strut was excited with a mid-span transverse amplitude that exceeded 1 inch. Direct measurements were augmented with stress and modal analysis using finite element models.

Cracking occurred randomly at four sites on the inboard or outboard ends and either upper or lower surfaces. Cracking always occurred on the rear fairing which is a structurally significant item. Figure 9.10-1 shows one cracking pattern. Through-cracking initiated on a smooth surface away from stress concentrations and proceeded simultaneously in two directions as noted. The crack initiation site and crack propagation are not consistent with axial loading. Figure 9.10-2 shows surface cracking through the Alclad layer – this was typical at all four sites.

The change to a turbine engine altered the propeller blade pass frequency. Pulses from the propeller blade are a major source of excitation of the wing strut. The reinforcement altered the natural frequencies of the strut. Most notable was 2nd bending which became similar to the blade pass frequency during takeoff and climb. The wing strut is simply supported at each end. Under appropriate conditions during climb, the propeller excited strut 2nd bending. Exciting one harmonic excites all harmonics on a simply-supported beam. This caused excitation of the 1st bending mode. The 1st bending mode was then greatly energized by single-degree-of-freedom flutter (due to the streamlined shape). The modal response of the strut resulted in nodal lines at the four possible crack sites. The extreme state of stress along the nodal lines resulted in wide spread fatigue damage (surface cracks) and eventually through-cracking. Time to through-cracking was estimated to be as low as 50 minutes.

This failure is the unintended consequence of several modifications. It is an example of why the FAA introduced ‘Changed Product Rule’ (see FAA Advisory Circular 21.101). Modifications to aircraft with wing struts need to be carefully investigated for potential problems.

9.10.2 ENHANCED LIFE MANAGEMENT PROCESS FOR DAMAGE TOLERANCE OF ENGINE COMPONENTS

Joseph Wilson, Federal Aviation Administration, ATO-P, R&D

The FAA is currently working with industry to enhance the current life management processes for aircraft engines. Based on probabilistic damage tolerance principles, the new process will address the threat of material or manufacturing anomalies in high-energy turbine engine rotating components. One existing process for detecting hard alpha (HA) anomalies in titanium rotors is documented in FAA Advisory Circular (AC) 33.14- 1. Future revisions to AC 33.14 will address other materials and anomaly types. In FY 2006, researchers completed a multi-year research program and published their findings in “Turbine Rotor Material Design—Phase II.” This work addresses data and technology requirements to support and enhance the AC and its implementation.

The team includes researchers from Southwest Research Institute (SwRI), GE Aircraft Engines, Pratt & Whitney, Honeywell, and Rolls-Royce Corporation. Together, they developed the DEFORM™ forging microcode, an enhanced predictive tool capability with supplementary material/ anomaly behavior characterization and modeling.

They used detailed nondestructive evaluation and metallography techniques to validate the tool, as applied to forgings with HA anomalies. They also used the microcode to characterize the conditions associated with cracking of HA anomalies during forging. Studies of representative forging shapes indicated that ingot-to-billet conversion and component forging would, under common processing conditions, create cracks in all HA anomalies.

The researchers conducted additional experiments to understand the fatigue behavior of embedded HA. They performed fatigue tests on coupons machined from seeded forgings and conducted spin pit tests with material from earlier forgings containing HA anomalies. The total fatigue life observed was at least twice as long as the calculated life, based on the assumptions that crack nucleation life was zero and the initial crack size was equal to the core plus diffusion zone size. Analyses using the fracture mechanics module (Flight-Life) in the Design Assessment of Reliability with Inspection (DARWIN ®) code indicated that initial crack sizes more nearly corresponded to core sizes than core plus diffusion zone sizes. As a result of this work, researchers have improved the overall efficiency and accuracy of the DARWIN risk assessment computations. In addition, they developed an infrastructure for software management, code licensing and distribution, and support for users.

9.10.3 UNCONTAINED ENGINE DEBRIS DAMAGE ASSESSMENT MODEL

William Emmerling, Federal Aviation Administration, ATO-P, R&D

Hazards from uncontained engine failures must be mitigated during the design layout of the aircraft systems that will be used in turbine-powered aircraft. Uncontained engine failure events release high-energy fragments that can impact and disable critical systems and reduce the airworthiness of the vehicle. When multiple systems are disabled, the potential for an accident increases. The redundancy and separation of systems, coupled with the thoughtful location of components in the design of an aircraft, can make significant improvement in the vehicle's ability to survive a high-energy event.

In FY 2006, FAA researchers, working with their counterparts at the Naval Air Warfare Center, released an improved version of the Uncontained Engine Debris Damage Assessment Model (UEDDAM). This model is designed to support the certification process and has tailored outputs that match the certification package requirements. Although the model is not yet being used for commercial certification, the U.S. Air Force has been using the model for several years. In a 2004 description of its C5 re-engine program, the USAF reported: "In a unique approach to the problem, we were able to answer both LFT&E (live fire test and evaluation) and safety issues by using the latest Federal Aviation Administration endorsed methodology. The use of the Uncontained Engine Debris Damage Assessment Model (UEDDAM) allowed the program to realize large cost savings while answering vital questions about the safety and vulnerability of the upgraded engines due to cascading damage."

Version 3 of the Uncontained Engine Debris Damage Assessment Model, released in September 2006, incorporates several improvements, including the ability to support analysis of decompression hole-size as a code output. Other significant improvements include the user defined material property inputs that make it possible for manufacturers with proprietary materials to insert their own material data within the code.

9.11 MULTIPLE-SITE DAMAGE (MSD)

9.11.1 DAMAGE CHARACTERIZATION OF A LAP JOINT FROM A COMMERCIAL AIRCRAFT AT DESIGN SERVICE GOAL

John Bakuckas, Federal Aviation Administration, ATO-P, R&D

Comprehensive teardown inspections can provide substantiating data to perform structural evaluations and assessments for continued airworthiness of high-time operational aircraft. The fuselage structure of a retired Boeing 727 aircraft was destructively evaluated to describe the state of damage near the end of its design service goal of 60,000 flight cycles. The focus of the teardown was on the fuselage crown lap joint that had a known history of multiple-site damage (MSD) cracking in the outer row of the lower skin.

A teardown protocol was established to characterize the state of damage; to measure crack sizes, shapes, and distributions; to study crack initiation sources and sites; and to reconstruct crack growth histories through striation counts. A procedure was established to disassemble joints and reveal fracture surfaces using a section of the lap joint with both visual and nondestructive inspection (NDI) crack indications at several fasteners, as shown in Figure 9.11-1. First, 1" square pieces were cut from the joint with the fasteners in the center. These parts were mounted in a stereomicroscope to determine the location of cracks around the fastener and to identify the region around the base of the fastener, Figure 9.11-1a. In regions away from the cracks, two wedge cuts were made through a fastener-hole interface to remove the fastener, Figure 9.11-1b. The samples were soaked in a solution to soften the sealant and pry open the layers, and cracks were located on the faying surface. A slot was machined in the plane of the crack, leaving a 0.05" ligament to the crack tip, Figure 9.11-1c. The samples were cooled using liquid nitrogen, and the ligament was broken using a pair of pliers, exposing the fracture surface of the crack, Figure 9.11-1d.

This procedure was used to characterize the state of damage in the lap joint along a stringer in the crown region, S-4R. In general, the majority of cracks found were in the inner skin of the outer rivet row. There were over 350 cracks in 270 holes in the outer row between frame stations (FS) 460 to 720E, an approximate 30 ft length. Cracks typically ranged in size from 0.01" to 0.2". The maximum size crack found was 0.225 inches. Approximately 38% of the cracks found were less than 0.05". An example of the types of crack information obtained is shown in Figure 9.11-2. The majority of holes had multiple cracks, up to six or seven in some cases, in a starburst pattern around the lower two-thirds region of the hole in the lower skin, Figure 9.11-2a. Many of these cracks had multiple origins at the corner of the hole and the faying surface, which eventually formed a contiguous crack, Figure 9.11-2b. The crack fronts were semi-elliptic and tunneled under the clad layer with the longer side on the faying surface. Examples of fatigue striations are shown in Figure 9.11-2c and the resulting measured crack growth rate in Figure 9.11-2d. The fracture surfaces were free of corrosion and any gross mechanical rubbing damage.

The crack data from this study will be used to: (1) characterize MSD crack initiation, crack linkup, and residual strength; (2) assess the inspection capability of NDI in crack detection; and (3) determine widespread fatigue damage average behavior in the structures removed.

9.11.2 DEVELOPMENT OF MULTIPLE-SITE DAMAGE IN FUSELAGE STRUCTURE

John Bakuckus, Federal Aviation Administration, ATO-P, R&D

Since the 1988 Aloha Airlines accident in which a large portion of the fuselage crown of a Boeing 737 tore apart due, in part, to the linkup of small cracks emanating from multiple rivet holes in a debonded lap joint, much effort has been placed on developing methodologies to assess multiple-site damage (MSD) in aircraft structure. Research efforts sponsored by the Federal Aviation Administration (FAA), National Aeronautics and Space Administration (NASA), and the Department of Defense (DoD) include the development of various analytical tools that address this complex problem at several levels. Both rigorous numerical methods and simplified engineering approaches have been developed to predict crack initiation, growth, linkup, and residual strength.

In an effort to provide experimental data for model validation, the Full-Scale Aircraft Structural Test Evaluation and Research (FASTER) facility was used to investigate MSD initiation and growth in a pristine fuselage lap joint panel. The test panel, representative of a generic narrow-body fuselage, was a stiffened structure containing six frames,

seven stringers, and a four rivet row lap joint. During the fatigue test, damage formation and growth in the lap joint were monitored and recorded in real time using the Rotating Eddy-Current Probe (RECP) system and high-magnification visual methods. Cracks were initially detected in the outer critical rivet row A in the lap joint after 12,600 cycles using RECP. Visually detectable cracks eventually developed in the rivet head of the critical rivet row after 51,500 cycles and then in the lap joint outer skin after 80,500 cycles. The first MSD linkup occurred after 106,217 cycles, forming a lead crack, Figure 9.11-3.

Subsequently, the lead crack grew very rapidly along the outer rivet row eventually forming 16.04" two-bay crack after 107,458 cycles, Figure 9.11-4.

A residual strength test was then conducted to determine the load-carrying capacity of the panel. The panel failed catastrophically when the lead crack extended instantaneously in the lap joint across four skin bays without crack turning or crack flapping. Several frames failed under the lap joint, Figure 9.11-5.

Posttest fractographic examinations were conducted to determine initiation sites and mechanisms and to reconstruct subsurface crack growth behavior from marker band locations in the first visually detected crack. The results from this single crack revealed multiple initiation sites and extensive fretting damage along the faying surface of the skin. A map of the locations of marker bands showed crack-tunneling behavior before the crack penetrated the surface, Figure 9.11-6.

More details can be found in Ahmed, A and Bakuckas, J. G., "Development of Multiple-Site Damage in Fuselage Structure," *DOT/FAA/AR-05/38*, September 2005.

9.12 ADVANCED STRUCTURES

9.12.1 ADVANCES IN TESTING AND ANALYTICAL SIMULATION METHODOLOGIES TO SUPPORT DESIGN AND STRUCTURAL INTEGRITY ASSESSMENT OF LARGE MONOLITHIC PARTS

R.J. Bucci, M.A. James, R.W. Schultz and H. Sklyut, Alcoa Technical Center

Virtually all new aircraft programs face the challenge to deliver dramatic reductions in weight and cost of structure. To achieve this end, designers have drawn attention to expanding the use envelope for large single-piece components to capture benefits of simpler assembly, fewer connections, and buy-to-fly improvements. The appeal of structural unitization has driven manufacturers to consider creative uses of product form (e.g., machined thick plate, extrusions, forgings, castings) and other associated developments (e.g., high-speed machining, welding/joining, etc.) as a means to reaching their structural cost and weight reduction targets.

Residual stress management, however, remains an obstacle to deriving full return from large monolithic component technologies [1]. Specifically, the inability to integrate residual stress and its effects into the data generation and analysis phases of the design process has been a long-standing hurdle to deploying large, single-piece structures. A common problem for many large metallic forms arises from internal stress states that result from prior thermo-mechanical processing steps. After isolation from their host, test coupons frequently retain internal stress states sufficient in magnitude to bias and ultimately corrupt the subsequent test measurement, preventing intrinsic property characterization. Further data corruption can arise from sampling sensitivities to specimen size, type and placement within the spatially varying internal stress state of the host, which in turn explains the large scatter common to many pooled data sets representing three-dimensional product forms. In particular, property data and design curves derived from tests of deep-notched fracture-mechanics-type specimens are especially susceptible to contamination effects of residual stress [1-4]. Within present state-of-the-art, a typical end result is either design uncertainty or undue penalty that in effect impedes or eliminates promising unitized structure options from consideration [1].

Recent Alcoa experimental and analytical work has contributed breakthroughs in both understanding and analytical tools to help overcome current material characterization and design practice limitations arising from residual stress complications [1-5]. The work has and continues to provide impetus for advanced alloy insertion and innovative uses of large monolithic forms in damage-tolerant critical designs. The work also provides a directional basis for fracture toughness and fatigue crack growth test/analysis protocol upgrades, thus enabling "true" material behavior to be partitioned from residual stress effects and preventing data corruption. Multiple examples constituting an emerging body of new and re-analyzed data are presented to validate benefits of the procedural upgrades.

The requisite technology improvements attend to the following requirements:

- pedigree material input; e.g., Figure 9.12-1
 - property data free of residual stress bias, sampling, and/or geometry effects;
 - appreciably reduced testing scatter and repeatable measurements, part-to-part, and location-to-location;
- coupon-to-component transfer; e.g., Figure 9.12-2;
 - hierarchical understanding of the role of host, coupon, and end-part residual stress states over the entire design cycle (from material characterization to end-component design);
- coupon and part crack drive solutions with all forces considered (internal and external);
 - treatment of residual stress impact on crack drive as an independent loading case that is not proportional to external applied loads.

Finally, a vision for virtual design of large monolithic parts (Figure 9.12-3) integrating host process simulation, machining, testing, and end-component performance prediction is presented for the first time with examples given to illustrate opportunities for use in fracture critical component design and manufacturing planning [1-3].

REFERENCES:

- [1] R. J. Bucci, M. A. James, H. Sklyut, M. B. Heinemann, D. L. Ball, and J. K. Donald, "Advances in Testing and Analytical Simulation Methodologies to Support Design and Structural Integrity Assessment of Large

- Monolithic Parts, SAE Paper No. 2006-01-3179, 2006 SAE Aerospace Manufacturing & Automated Fastening Conference, De Congrès Pierre Baudis, Toulouse, France, Sept. 12-14, 2006
- [2] R. J. Bucci, H. Sklyut, L. N. Mueller, M. A. James, D. L. Ball, and J. K. Donald, "Advances in Testing and Analytical Simulation Methodologies to Support Design and Structural Integrity Assessment of Large Monolithic Parts – A New Perspective," *Proceedings ASIP 2005 USAF Structural Integrity Program (ASIP) Conference*, Memphis, TN, Nov. 29-Dec. 1, 2005; also 17th Annual AeroMat Conference & Exposition, Seattle, WA, May 15-18, 2006
- [3] R. J. Bucci, "Advances in Testing and Analytical Simulation to Account for Residual Stress Effects in Design and Integrity Assessment of Large Monolithic Parts," *Proceedings Boeing 7th Industry Wide Unitized Structure Technical Interchange*, Dallas, TX, Nov. 10, 2005; also ASTM E08.04.05/E08.06 Mini-Workshop on Fracture Issues of Integral Structures, ASTM Committee Week, Dallas, TX, Nov. 7, 2005
- [4] M. A. James, R. J. Bucci, J. R. Brockenbrough, R. W. Schultz, H. Sklyut, M. B. Heinemann, and M. Kulak, "Understanding the Residual Stress Effect in Damage Tolerance Evaluation of Integral-Stiffened and Friction Stir Weld Panels," *Proceedings ASIP 2006 USAF Structural Integrity Program Conference*, San Antonio, TX, Nov. 28-30, 2006; also appears in *Proceedings Boeing 8th Industry Wide Unitized Structures Technical Interchange Conference*, San Antonio, Dec. 1, 2006
- [5] D. L. Ball, "A Proposed Analytical Approach for the Incorporation of Residual Stresses in the Design of Large Forged Components," *Proceedings Boeing 7th Industry Wide Unitized Structure Technical Interchange*, Dallas, TX, Nov. 10, 2005; also ASTM E08.04.05/E08.06 Mini-Workshop on Fracture Issues of Integral Structures, ASTM Committee Week, Dallas, TX, Nov. 7, 2005

9.12.2 ADVANCED HYBRID STRUCTURES AND MATERIALS

R.J. Bucci, M. Kulak, M.B. Heinemann, J. Hinrichsen, M.A. James and J. Liu, Alcoa Technical Center

Competitive realities facing the air travel industry have intensified the need for aerostructures that are dramatically more lightweight, offer increased passenger comfort, and create significant cost savings (both acquisition and life cycle). Both primes and component suppliers are acutely aware that these trends signal a need for a paradigm shift in how aircraft materials and structures are designed, used, and built. Airframers have responded with aggressive weight-saving goals for next-generation wing and fuselage structures, which in turn commands increases in operating stress to levels that challenge state-of-the-art metallic structure damage tolerance. Simultaneously, primes and suppliers are investing heavily in areas most apt to produce substantial cost reductions—manufacturing simplification, consolidations of parts, and buy-to-fly improvement technologies. Novel manufacturing approaches, however, introduce new complexities into the design process, particularly in regard to potential deviances from comfortable design margins of the past. To compound the challenge, operators also want aerostructures that last longer and can be sustained affordably through extremely long crack-free lives and freedom from corrosion, both of which help to capture the significant cost savings associated with greatly reduced inspection and repair.

These realities motivated Alcoa to fundamentally shift its aerospace R&D strategy from continuous (incremental) alloy improvements to an integrated, longer term initiative to redefine the performance, cost, and value of materials and components for tomorrow's aircraft [1-5]. Alcoa's goal was to strengthen its supply chain position and become a solution provider capable of meeting the demanding mission requirements of current and future-generation aircraft. This major, new R&D initiative was launched in 2003 as Alcoa's 20/20 vision. It sought to identify, validate, and mature promising transport aircraft wing and fuselage material/concept options that would produce 20% weight and 20% cost reductions for incumbent baseline aircraft (e.g., the B777 or A380) [3-6].

To achieve the extraordinary performance and cost saving gains, Alcoa undertook an approach that combined modern aluminum alloys with other advanced materials and leverages of innovative design, manufacturing, and assembly methodologies to assure minimal disruption of existing aircraft design, construction, and operation methods. Early in the trade-study process, Alcoa identified crack growth and residual strength as the key design drivers sizing most of the lower wing and fuselage crown and side cover panel structure. Consequently, much of the concept development/validation testing in the 20/20 initiative focused on demonstrating the ability to accommodate significant operating stress and/or inspection interval increases while meeting or surpassing all state-of-the-art design requirements for structural damage tolerance.

Early analytical design studies supported by data from lab-scale tests demonstrated that the 20/20 goals are attainable through near term technologies with a 3-5 year deployment range [2-4, 7, 8]. Further proof-of-concept scaling to wider central cracked test panels revealed that impressive life and residual strength improvements could be achieved by selectively placing bonded fiber/metal laminate (FML) straps to offload the skin and slow crack growth [9]. This multi-material approach of selective strap reinforcement represented a low level of hybridization, and several variations on this theme are illustrated in Figure 9.12-4. Ensuing studies confirmed promising results could be achieved by FML strap reinforcement of stiffened lower wing and fuselage cover panels especially when used in conjunction with the new improved property 2xxx/7xxx aluminum alloys and the low density Al-Li alloys [10-16]. Further work demonstrated that selective reinforcement can be used to overcome the historical fast fracture and residual strength deficits linked to integral stiffened skins, an appealing result that supports industry's movement to unitization of structure as a viable low cost manufacturing alternative [13, 16].

Looking forward, Alcoa began to explore new ways of combining metallic and advanced fibrous material combinations, as shown in the reinforced hybrid laminate concepts of Figure 9.12-5. This goal for this new class of hybrid structures was to significantly surpass the original 20/20 weight/cost saving goal by invoking a structural systems approach to capture the enormous synergy potential of combining best attributes of mature material technologies (viz., metals, composites, and FMLs) in highly tailored fashion [12-16].

Bolstered by the confidence from this test data and analysis, Alcoa moved to the next proof-of-concept scale with design, build, and successful testing of large, stiffened panel demonstrators to validate the weight/cost saving benefits of identified promising concepts, e.g., Figure 9.12-6. The large-panel testing simulated the damage tolerance requirement for tension-dominated lower wing and fuselage crown and side cover panels [13, 14, 16]. The primary measured results were crack growth and residual strength (two-bay crack scenario), which typically size many areas of these components for today's transport aircraft. The evaluated concepts entailed advanced alloys, novel design, and innovative manufacturing methods, all carefully selected in response to governing weight and cost drivers. Built-up and integrally stiffened panel variations composed of advanced alloys (including Al-Li), FML internal or external reinforcement, and friction stir welded integral panels were tested. Both reinforced and non-reinforced variants options were evaluated to assess the benefits of fiber placements. The full description and results from these large-panel tests, to be presented at this conference [17], validated Alcoa's premise that optimized combinations of advanced alloys and FML materials offer breakthrough possibilities to maximize structural performance and cost benefits. For example, the wing simulation results in Figure 9.12-7 show impressive improvements in fatigue crack growth performance for the tested fiber reinforced hybrid alternatives. Even at the 25% operating stress increase over today's metallic baseline, lifetimes of the hybrid options remain superior by a wide margin. The ability to operate at substantially higher stress can be used to drive out significant weight. Conversely, hybrid's significant life enhancement potential can be exploited to drive down the inspection/maintenance burden. Finally, the ability to tailor hybrids offers designers many choices for driving down manufacturing cost, several paths of which are highlighted in Figure 9.12-5.

Building on the above successes, Alcoa has expanded its R&D scope to explore the integrated benefit potential of this technology when applied to an entire structure—for example, to the entire wing box, including upper and lower covers, spars, and ribs, Figure 9.12-8, and to the fuselage barrel in Figure 9.12-9. Internal studies have shown that on both a weight and cost basis the optimized metallic intensive hybrid solution is highly competitive against a pure composite solution [17]. Many lessons learned to date have been catalogued to form a basis for discussion on design/use rules governing inspections with the ultimate goal of creating "carefree" structure design principles for highly sustainable, next-generation aircraft [18, 19].

REFERENCES:

- [1] "Advanced Metallic Structure - the Alcoa Vision," J. Liu, M. B. Heinemann, M. Kulak, M. D. Goodyear, R. J. Bucci, 15th Annual AeroMat Conference & Exposition, Seattle, Washington, June 7-10, 2004
- [2] "Lightweight Aluminum Wing Structures (LAWS) – Advanced Structural Technology," M. Kulak, R. J. Bucci, M. B. Heinemann, B. Bodily, D. J. Spinella, NASA Contract No. NNL04AA35C, Phase I Final Report – Vol. 1, July 28, 2004
- [3] "Advanced Metallic Structures – The Alcoa Vision," M. B. Heinemann, R. J. Bucci, M. Kulak, J. Liu, D. J. Spinella, *Proceedings Alcoa Future Aerostructures Symposium*, Defuaski Island South Carolina, Alcoa, Inc., Nov 15-18, 2004

- [4] "Alcoa Aerospace – Optimized Solutions Meeting Mission Requirements," J. Hinrichsen Plenary Address, 16th Annual AeroMat Conference & Exposition, Orlando, Florida, June 6-9, 2005
- [5] "Future Mission Requirements: Advanced Alloys, Hybrid Materials and Innovative Designs," J. Liu, *Proceedings Symposium on the Quest for New Aerostructural Materials and Designs*, Northwestern University, Evanston, IL, October 25-26, 2005
- [6] "Advanced Structures Initiative," R. P. Evert and R. J. Bucci, 05-15-PKM Request for Information, Air Force Research Laboratory, Wright Patterson AFB, Ohio, September 23, 2005
- [7] "FCG Evaluation of New Lower Wing Concepts," M. D. Garratt, R. J. Bucci, and M. Kulak, 15th Annual AeroMat Conference & Exposition, Seattle, Washington, June 7-10, 2004
- [8] "Advanced Metallic Studies for Commercial Fuselage Structure," M. Kulak, B. H. Bodily, M. B. Heinemann, and R. J. Bucci, 15th Annual AeroMat Conference & Exposition, Seattle, Washington, June 7-10, 2004
- [9] "Improving Damage Tolerance of Aircraft Structures through the Use of Selective Reinforcement," M. B. Heinemann, R. J. Bucci, M. D. Garratt and M. Kulak, *Proceedings International Committee on Aeronautical Fatigue (ICAF), Hamburg, Germany, June 6-10, 2005*
- [10] "Validation Testing of Lower Wing concepts for Improved Performance and Cost.... Progress toward the Alcoa Vision," M. Kulak, R.J. Bucci , M. B. Heinemann, and B. H. Bodily, 16th Annual AeroMat Conference & Exposition, Orlando, Florida, June 6-9, 2005
- [11] "Large panel testing of advanced fuselage concepts for improved performance and cost - Progress towards the Alcoa vision," B. H. Bodily, M. Kulak, M. B. Heinemann, R. J. Bucci and J. Scheuring, 16th Annual AeroMat Conference & Exposition, Orlando, Florida, June 6-9, 2005
- [12] "Advanced Metallic & Hybrid Structural Concepts for Future Aircraft, J. Liu, Plenary Address, 17th Annual AeroMat Conference & Exposition, Seattle, WA, May 15-18, 2006
- [13] "Advanced Metallic Lower Wing Stiffened Panel Concepts: Results of Large Panel Validation Test Program," M. Kulak, J. Liu, G. Dixon, W. H. Grassel, R.L. Brazill, M. B. Heinemann, R. J. Bucci, H.R. Zonker and J. Scheuring, 17th Annual AeroMat Conference & Exposition, Seattle, WA, May 15-18, 2006
- [14] "Validation of Advanced Fuselage Concepts Integrating Materials, Design and Manufacturing, M. Kulak, J. Scheuring, B. H. Bodily, R. J. Bucci, G. Dixon, M. Ripepi, J. Newman, 17th Annual AeroMat Conference & Exposition, Seattle, WA, May 15-18, 2006
- [15] "Advanced Aluminum and Hybrid Aerostructures for Future Aircraft," J. Liu, International Conference on Aluminum Alloys, Vancouver, Canada, July 9-13, 2006
- [16] "Advanced Metallic & Hybrid Structural Concepts, ... tailorable solutions to meet the demanding performance/ affordability requirements of tomorrow's aircraft," Luncheon Presentation, R. J. Bucci, *Proceedings ASIP 2006 USAF Structural Integrity Program Conference*, San Antonio, TX, November 28-30, 2006
- [17] "Validation of Advanced Metallic Hybrid Concept with Improved Damage Tolerance Capabilities for Next Generation Lower Wing and Fuselage Applications," M. B. Heinemann, M. Kulak, R. J. Bucci, M. A. James, G. S. Wilson, J. R. Brockenbrough, H. R. Zonker and H. Sklyut, 24th ICAF Symposium, Durability & Damage Tolerance of Aircraft Structures: Metals vs. Composites, Napoli, Italy, May 16-18, 2007
- [18] "Requirements for "Care-Free" Aircraft Structures and Expected Benefits from Hybrid Structures/Materials," J. Hinrichsen, 65th Annual Conference of Society of Allied Weight Engineers, Inc., Valencia, CA, May 20-24, 2006
- [19] "Advanced Metallic & Hybrid Structural Concepts, ... tailorable solutions targeted to demanding use and affordability requirements of tomorrow's aircraft," R. J. Bucci, U.S. Air Force Scientific Advisory Board (SAB) Study on Use and Sustainment of Composites in Aircraft, 2007 SAB Winter Meeting, January 18, 2007

9.13 FIGURES/TABLES



Figure 9.2-1 Eclipse 500 Test Article



Figure 9.2-2 T-38 Trainer



Figure 9.2-3 T-38 Fatigue Test Installation

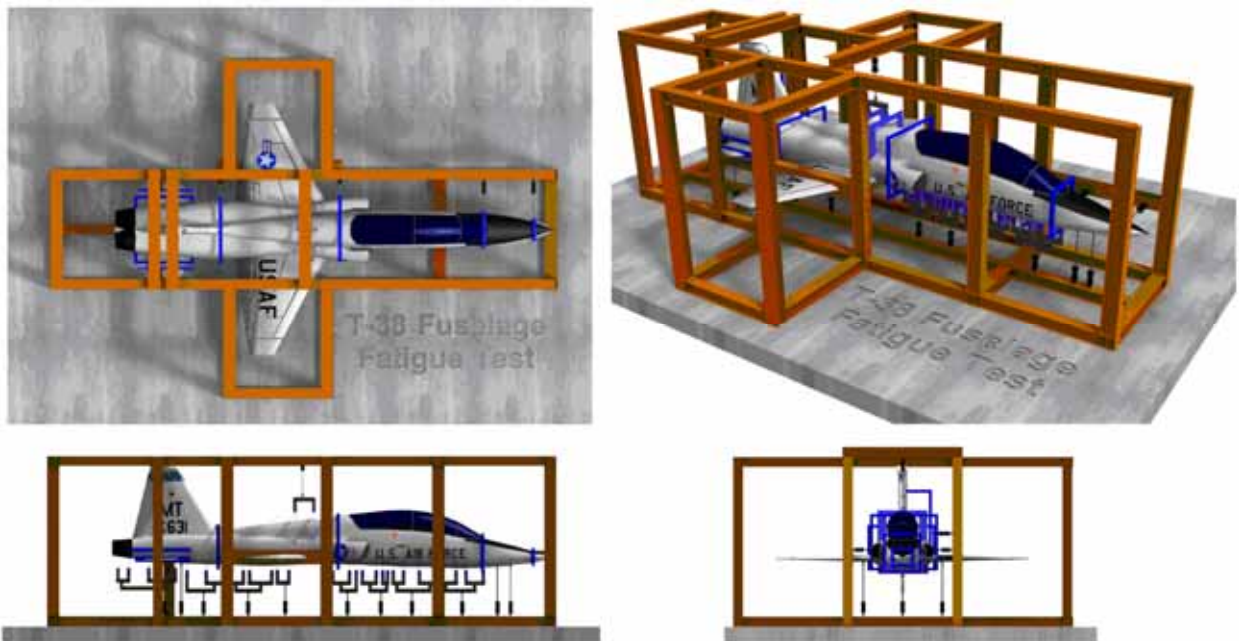


Figure 9.2-4 T-38 Fuselage Fatigue Test Configuration



Figure 9.2-5 Bulkhead Bonded Repair

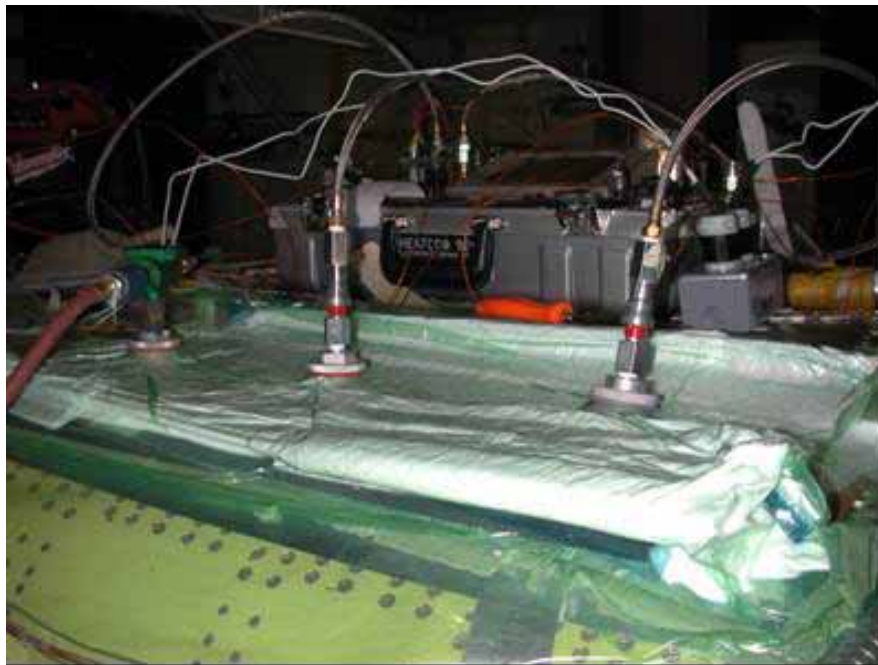


Figure 9.2-6 Boron Repair Co-Curing to Dorsal Longeron

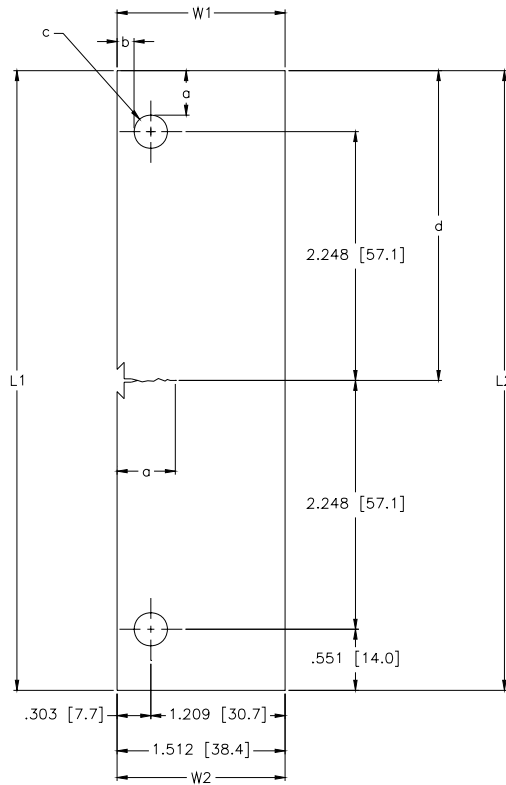


Figure 9.2-7 ESE(T) Specimen Chosen for Thin Sheet Capabilities (Thickness of 0.063 Inches - Dimensions in Inches and Millimeters in Brackets)

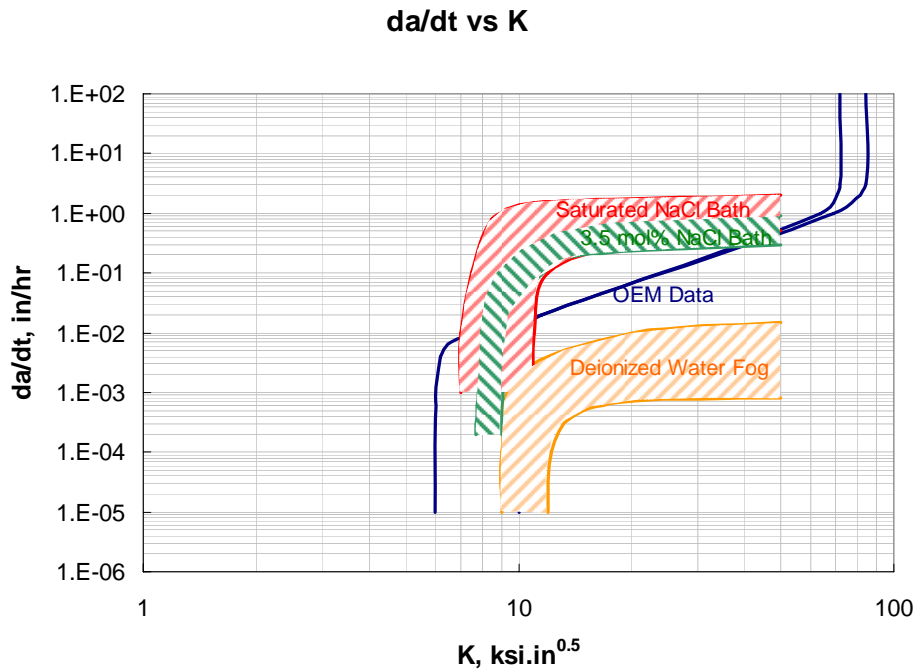


Figure 9.2-8 CAStLE Generated Results in Comparison to Data OEM Has Been Using

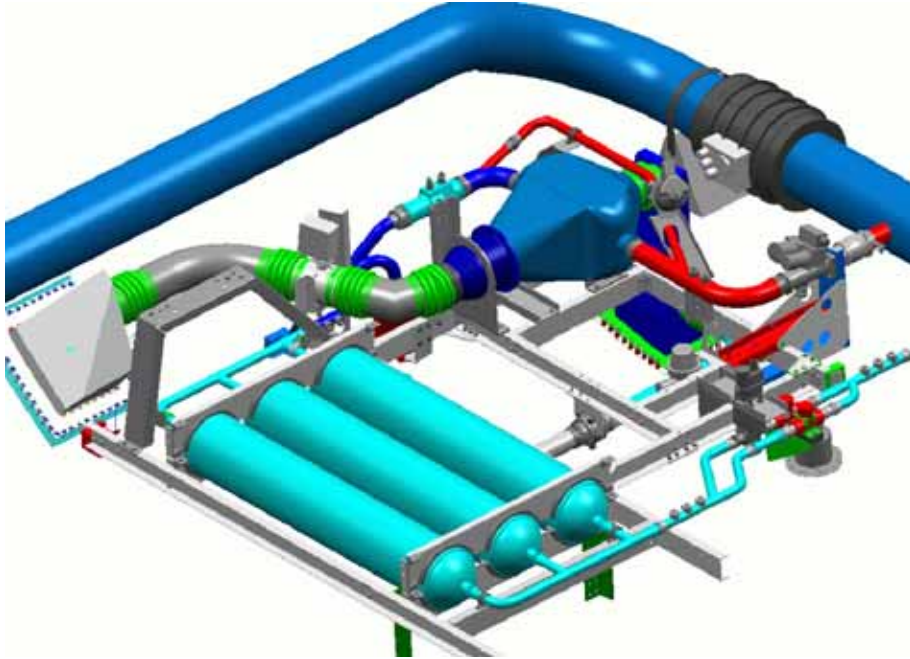


Figure 9.2-9 Prototype Onboard Inert Gas Generation System



Figure 9.2-10 Inerting System Mounted on NASA 747 SCA

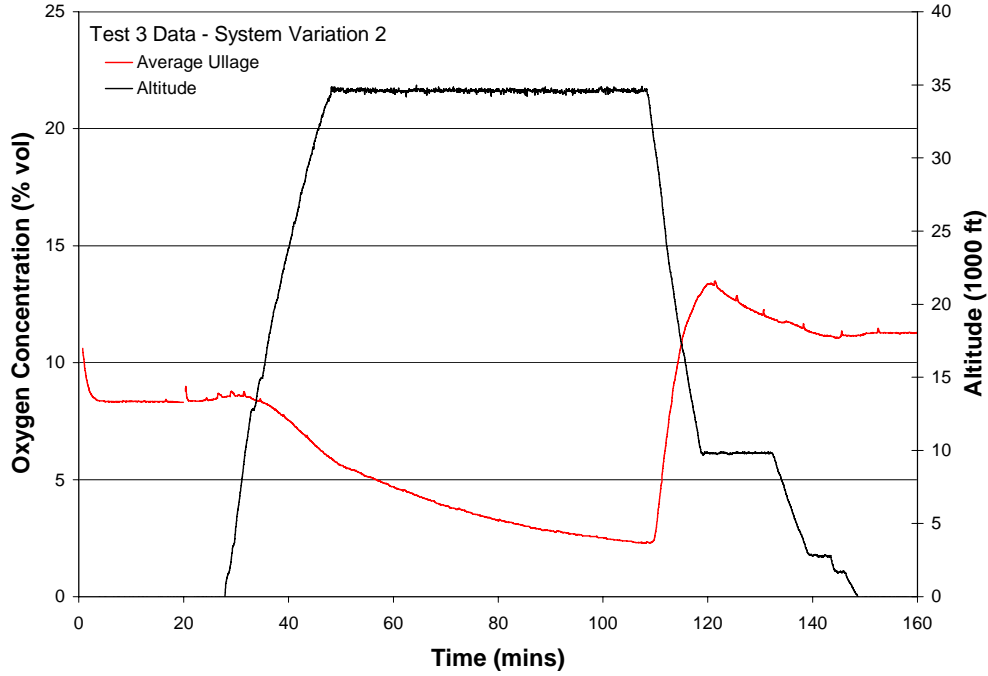


Figure 9.2-11 Average CWT Ullage Oxygen Concentration Measured During SCA Flight Testing

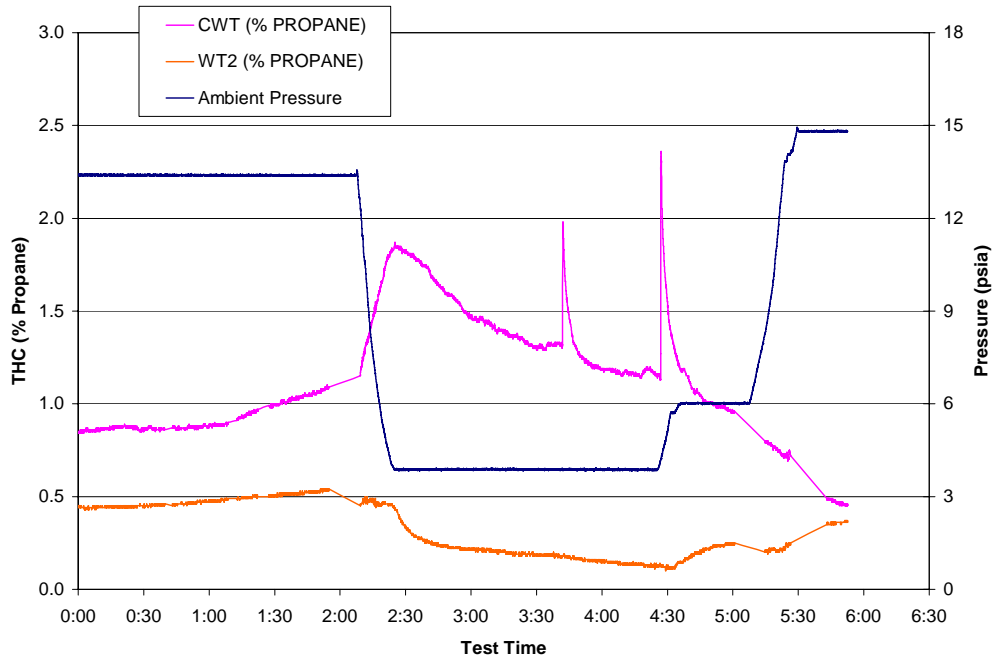


Figure 9.2-12 Flammability in Both the CWT and Wing Tank Measured During SCA Flight Testing

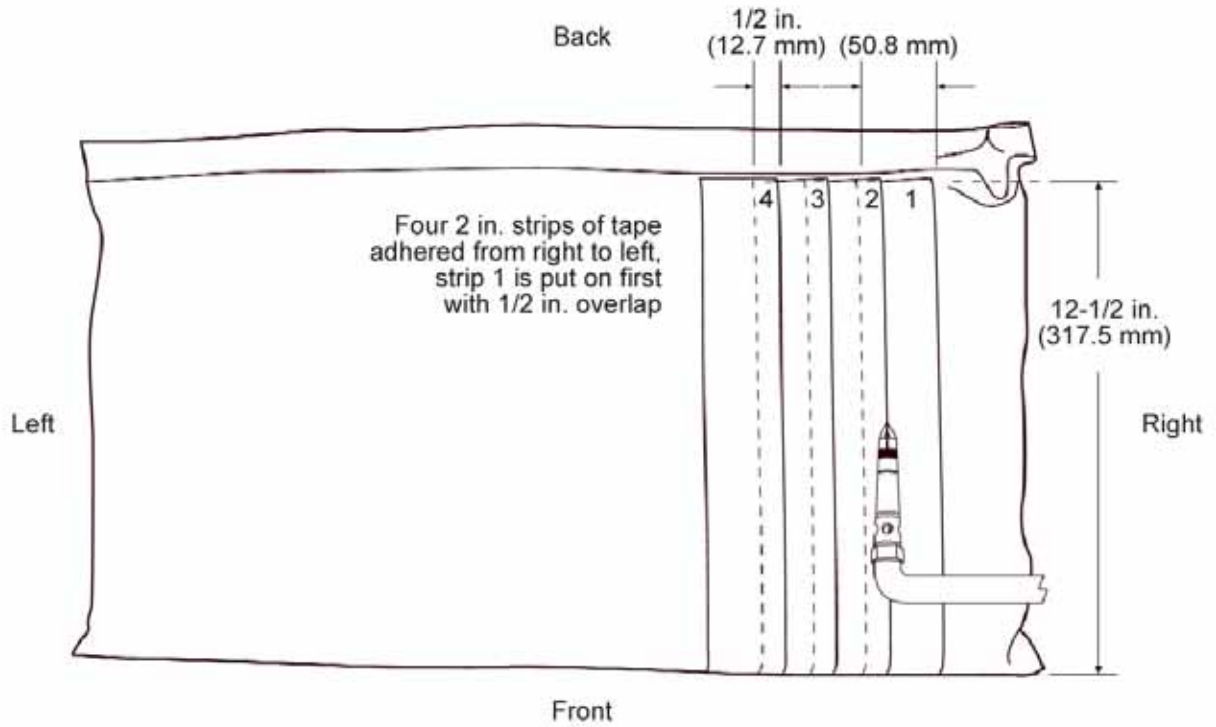


Figure 9.2-13 Method of Testing Tapes in Radiant Panel Test Apparatus

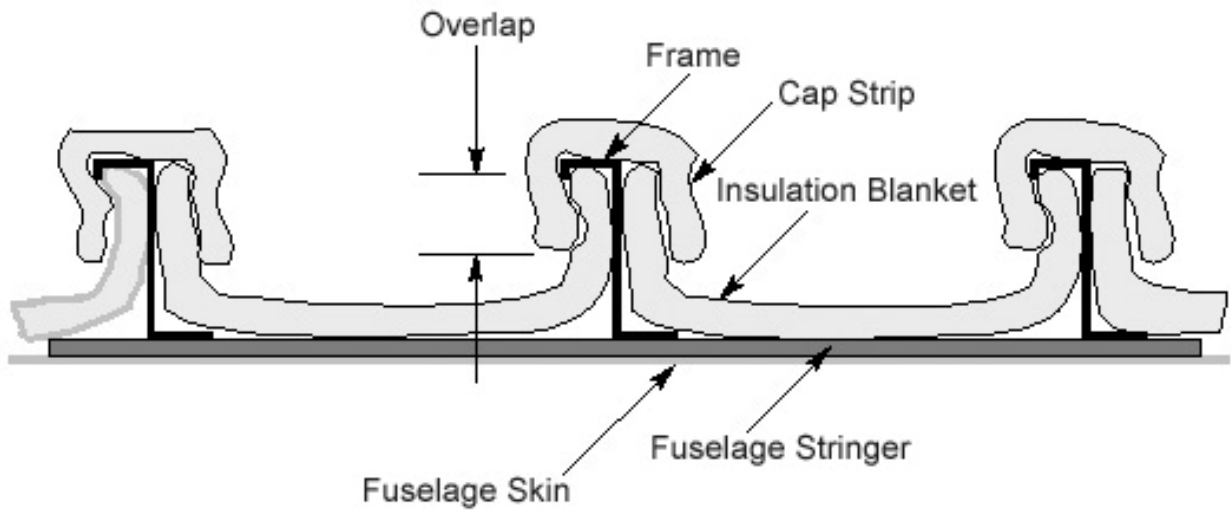


Figure 9.2-14 Description of Blanket Overlap to Ensure Continuous Burnthrough Barrier

Table 9.2-1 60° Flammability Test Results (Average of 3 Tests)

Wire/Cable	Burn Length (inches)	After Flame (seconds)	Drippings
Polyimide	1.5	0	0
PVC/nylon	14.8	121	0
Tefzel™	2	0	0
X-linked Tefzel™	1.8	0	0
PTFE/polyimide/PTFE	1.2	0	0
Spec 2112	2.1	1.7	0
Plenum cable (A)	2.5	0	0
Riser cable (A)	2.5	0	0
Telecommunication cable zero halogen	3.1	60.3	0
Limited combustible, CMP CAT 6	2	0	0
Riser cable, CMR CAT 5E	2.5	0	0
Plenum cable, CAT 5-E	1.8	0	0



Figure 9.2-15 Riser Cable (A) Test Progression

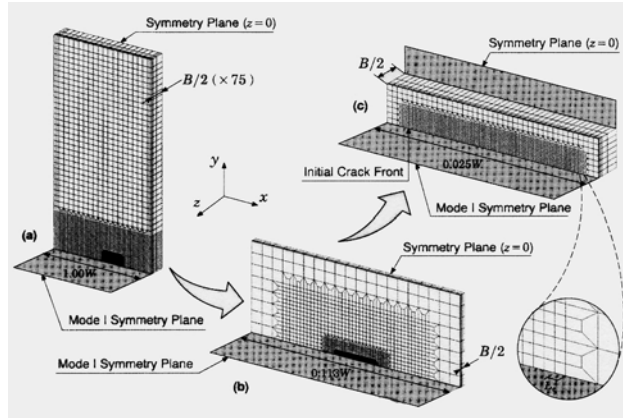


Figure 9.3-1 Computational Model of Cracked Component

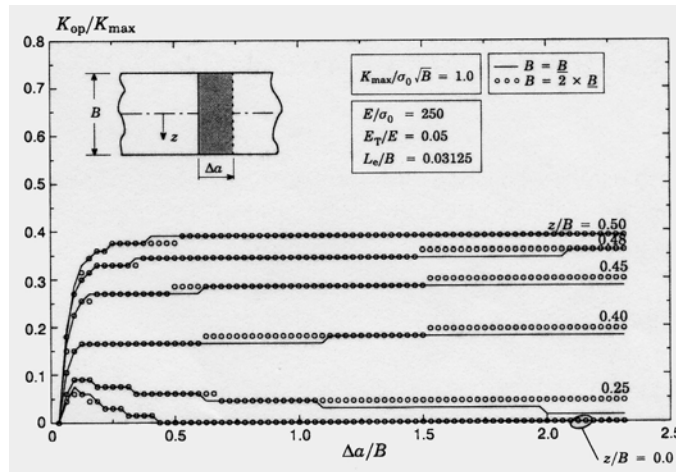


Figure 9.3-2 Similarity Scaling of Normalized Opening Load at Each Crack Front Location, $R = -1$ Loading

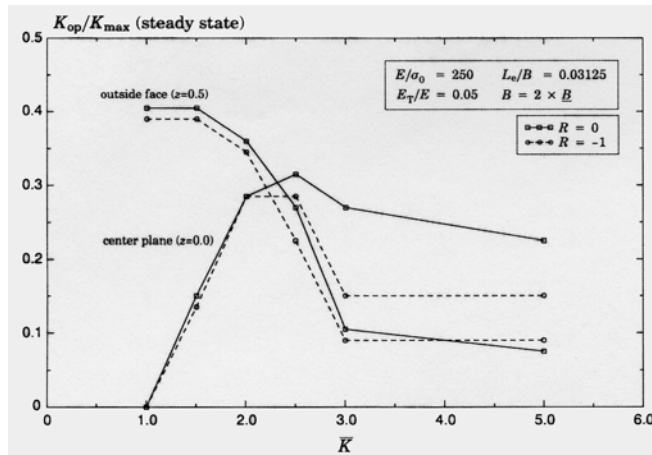


Figure 9.3-3 Comparison of Steady State Opening Load Levels in Identical Specimens Under $R = -1$ and $R = 0$ Loading

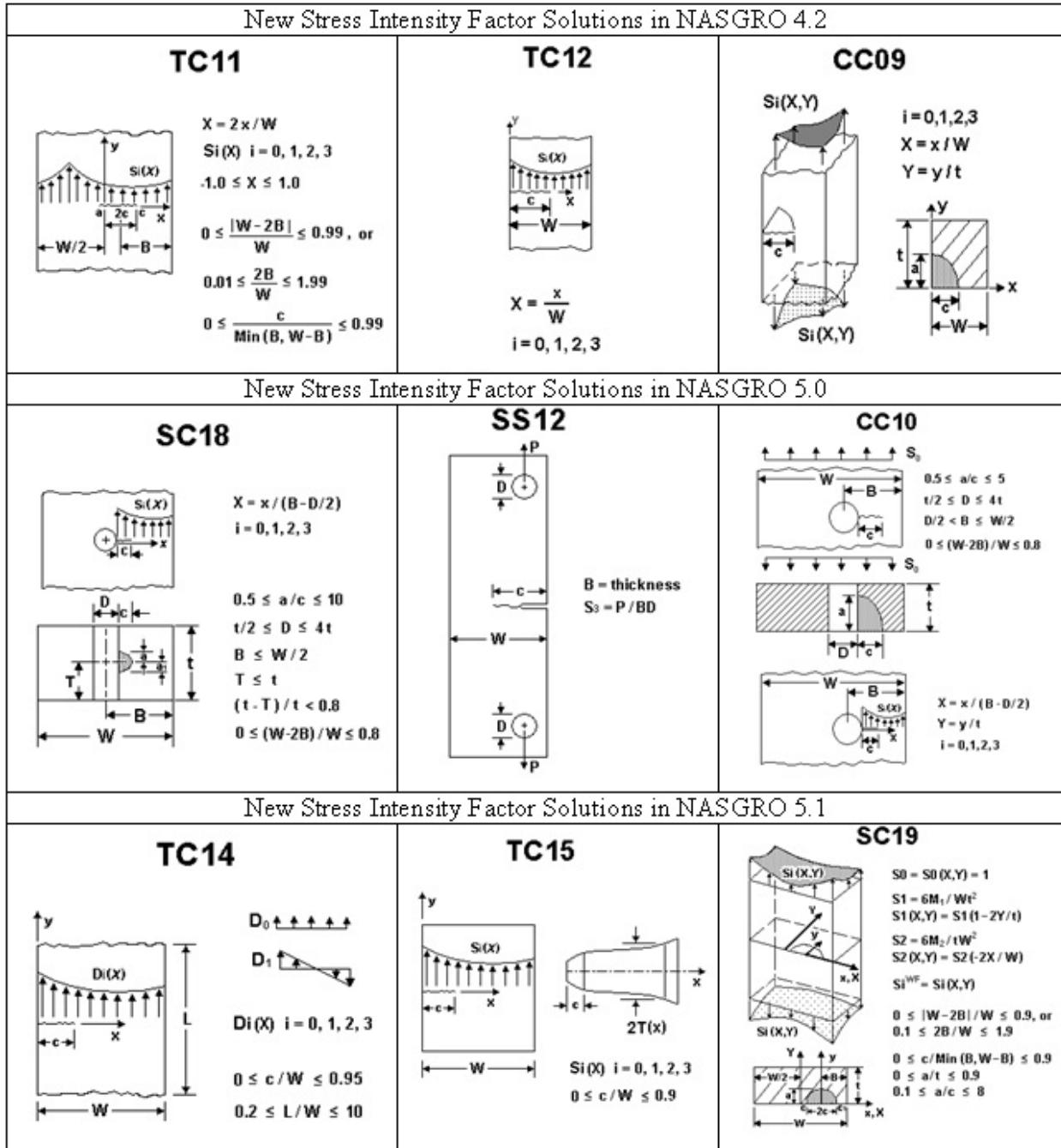


Figure 9.3-4 New Stress Intensity Factor Solutions in NASGRO Versions 4.2, 5.0 and 5.1

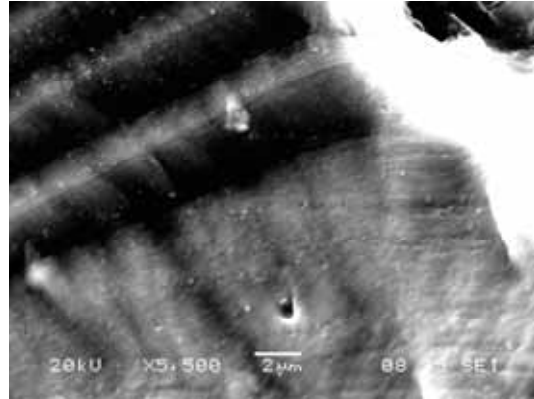


Figure 9.3-5 Micrograph of Marker Bands on Test Specimen 3 at 5,500X

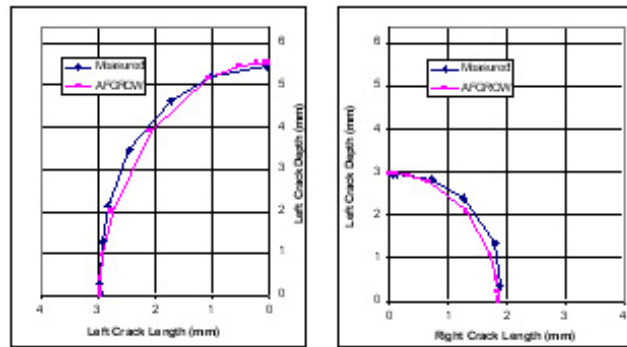


Figure 9.3-6 Left and Right Side Crack Shape Predictions for Test Specimen 3

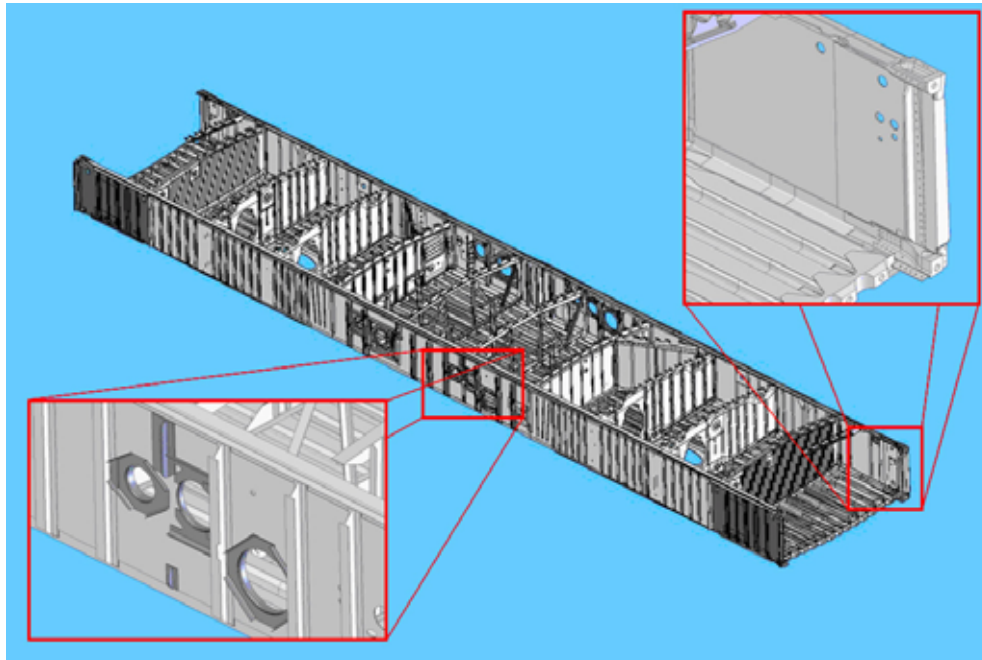


Figure 9.3-7 Cut-a-way View of the C-130 CWB Solid Model With Close-up Views Showing Model Detail

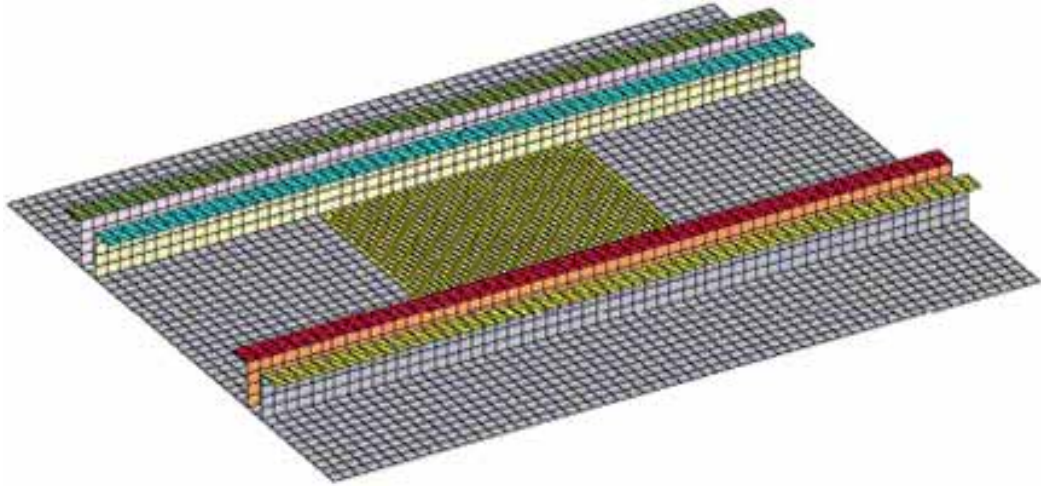


Figure 9.3-8 Typical Fuselage Panel Model

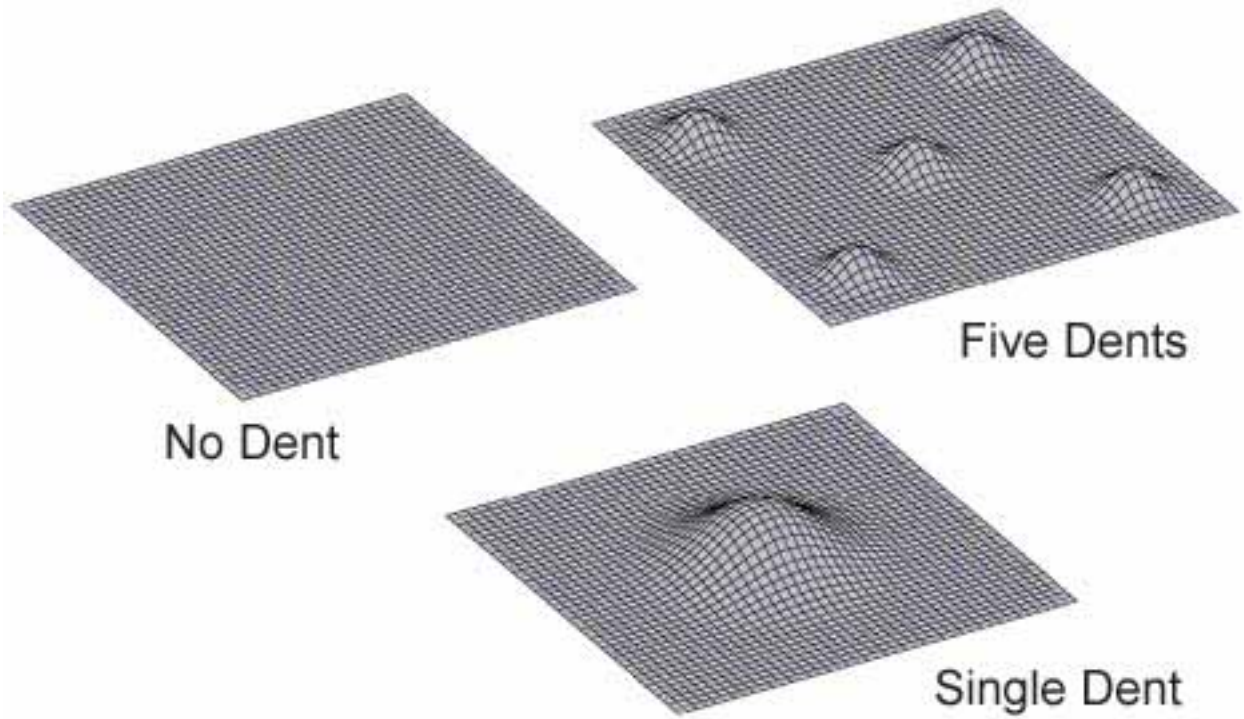


Figure 9.3-9 Dent Geometries Generated Through User-written Subroutines

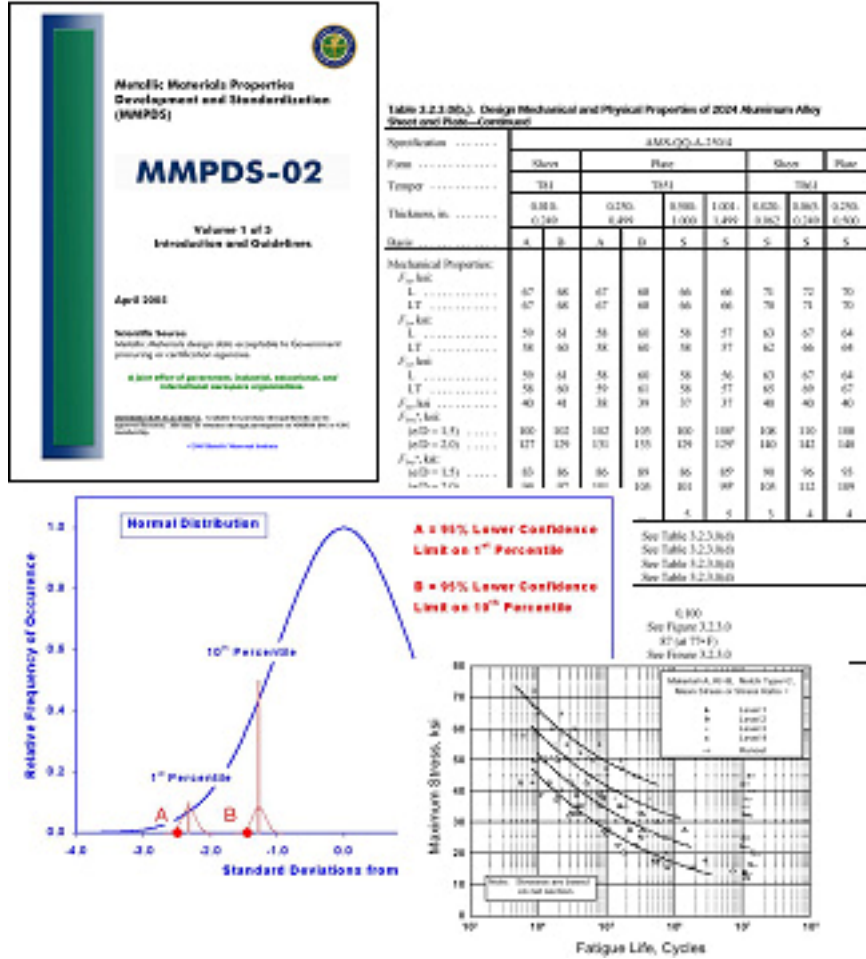


Figure 9.3-10 Metallic Materials Properties Development and Standardization

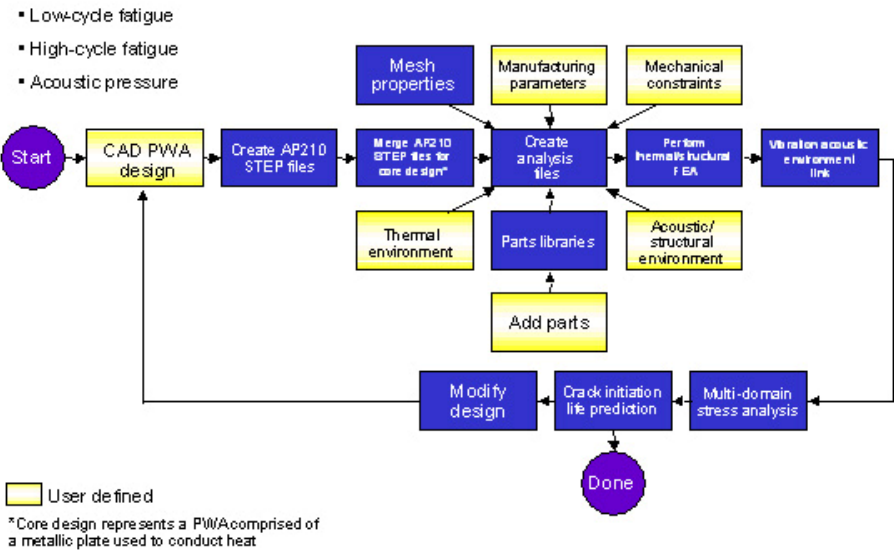


Figure 9.3-11 Durability Analysis Process for Environment Modeling

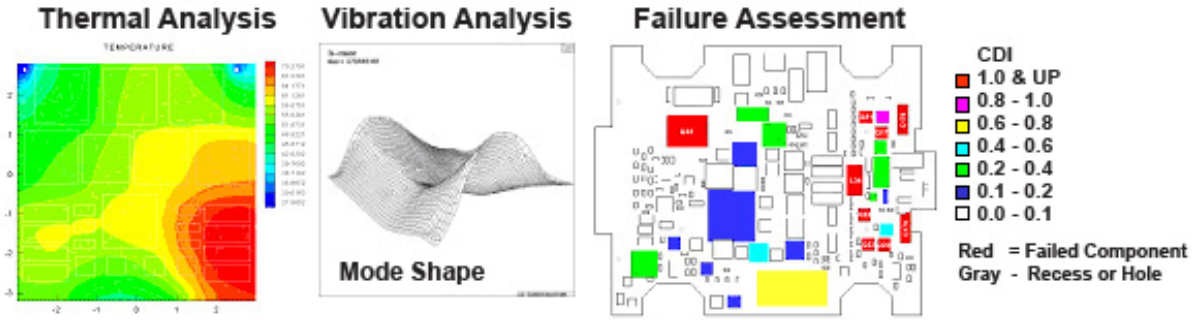


Figure 9.3-12 COTS Performance and Life Assessment

Table 9.4-1 Split Sleeve Cold Hole Expansion Test Conditions and Results

Alloy	Product Form	Original Product Thickness (mm)	Specimen location	Specimen Thickness (mm)	Specimen Width (mm)	Starting hole diameter (mm)	Applied expansion (%)	Angle of split from L	FTI tool code	Ave. Retained Cx (%)	Visual Observations	
2099-T83	Extruded ISP	18.7	Web, T/2	15.2	50.8	14.81-14.88	4	45	18-3-N	1.9	No cracks. Small surface perturbations at location of split in sleeve.	
		16.5	Hat, T/2	15.2	38.1	8.74-8.81	4	45	10-3-N	2.0		
		16.7	Stiffener, T/2	15.2	38.1	8.74-8.81	4	45	10-3-N	2.1		
2099-T8E67	Extruded ISP	18.7	Web, T/2	15.2	50.8	14.81-14.88	4	45	18-3-N	2.2		
		16.5	Hat, T/2	15.2	38.1	8.74-8.81	4	45	10-3-N	2.4		
		16.7	Stiffener, T/2	15.2	38.1	8.74-8.81	4	45	10-3-N	2.4		
2199-T8E80	Thin Plate	38	L-LT, T/4	19.1	50.8	14.81-14.88	4	45	18-3-N	2.2		
Al-Li-X	Thin Plate	28	L-LT, T/4	19.1	50.8	14.81-14.88	4	45	18-3-N	1.9		
2099-T8E77	Thick Plate	76	L-LT, T/4	19.1	50.8	14.81-14.88	4	45	18-3-N	2.0		Small crack at location of split in sleeve (45 deg) in three of the four holes.
		76	L-ST, T/2	19.1	50.8	14.81-14.88	4	45	18-3-N	2.0		
		76	L-ST, T/2	19.1	50.8	14.81-14.88	4	90	18-3-N	2.3	No cracks. Small surface perturbations at location of split in sleeve.	

Average Fatigue Life, With and Without SSCx

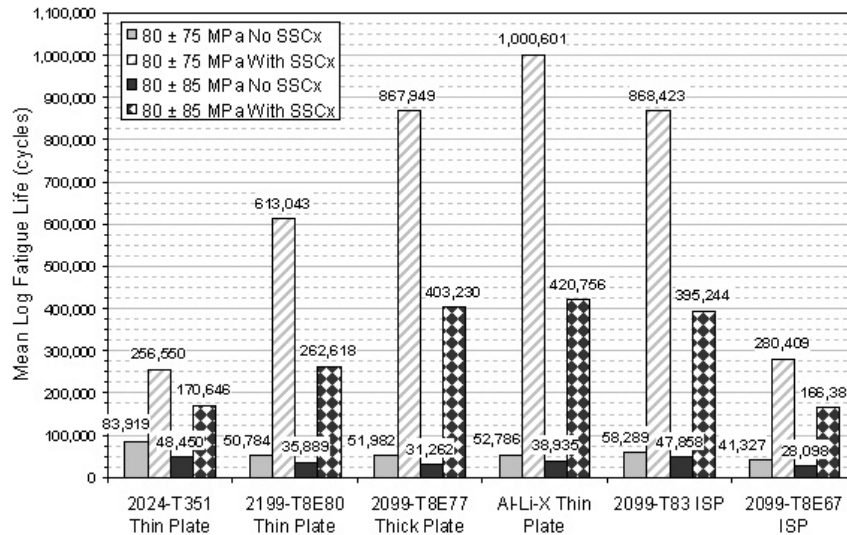


Figure 9.4-1 Mean Log Fatigue Life With and Without Split Sleeve Cold Hole Expansion for All Alloys Tested

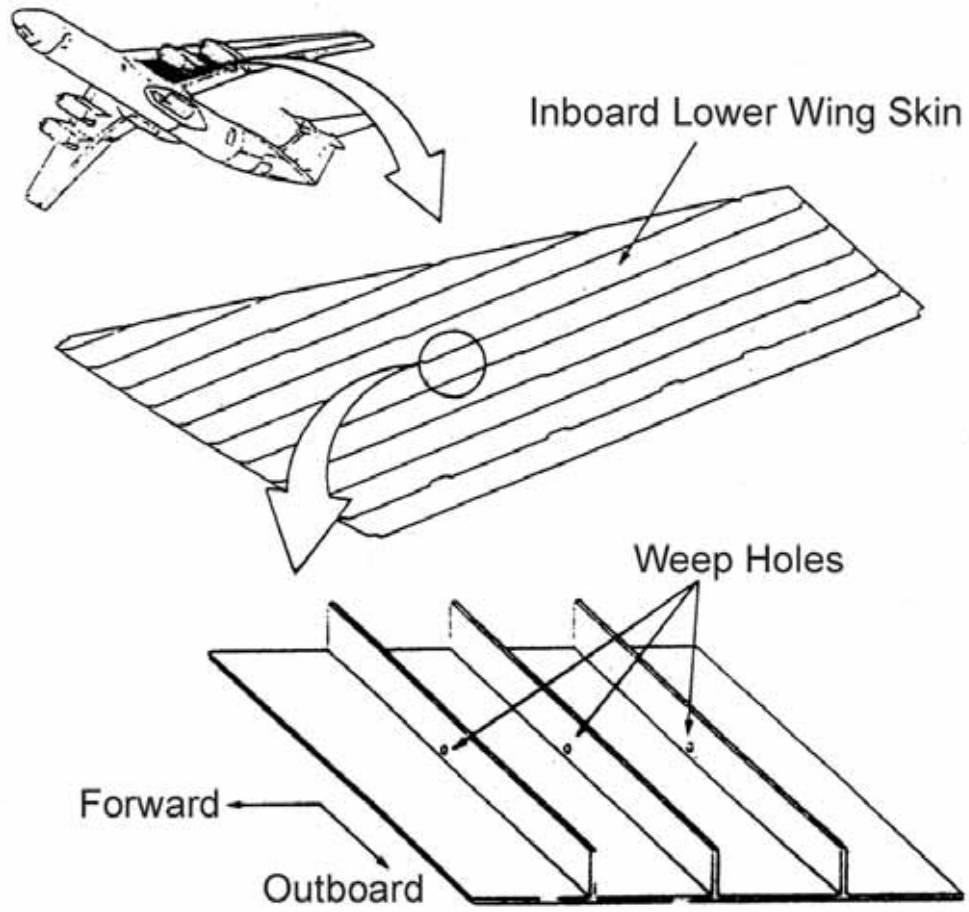


Figure 9.4-2 C-141 Lower Wing Skin and Weep Holes

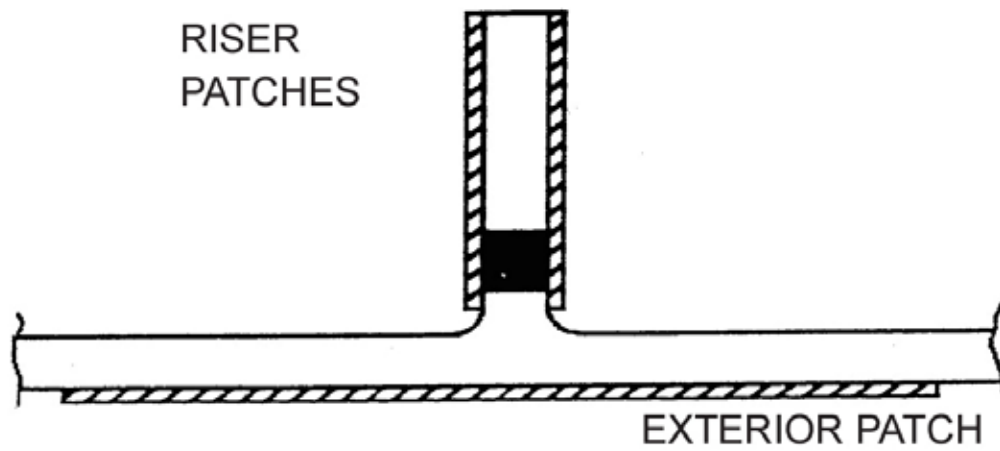


Figure 9.4-3 Cross Section of Typical Weep Hole Repair



Figure 9.4-4 Typical Dents in Fuselage Structure

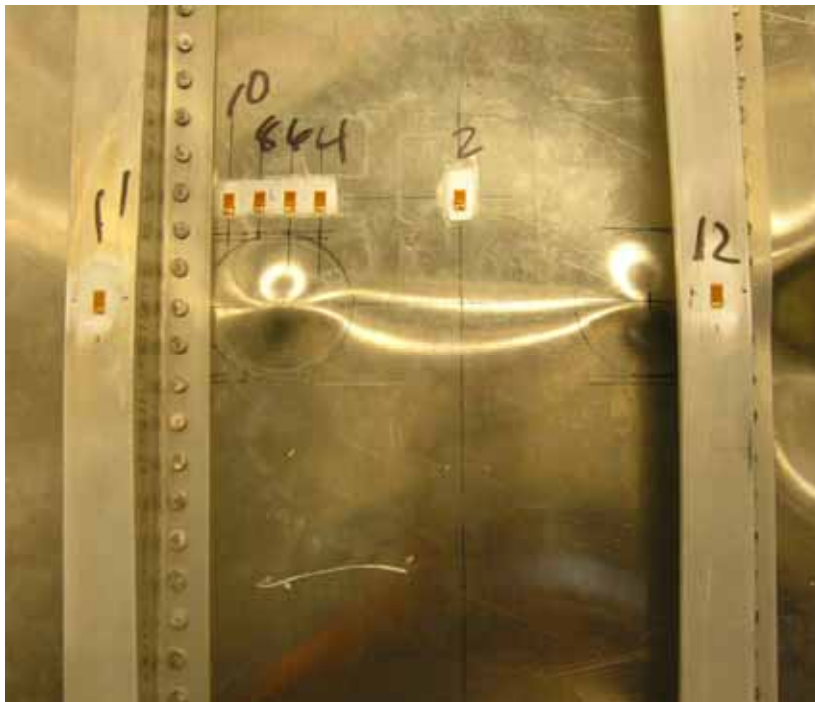
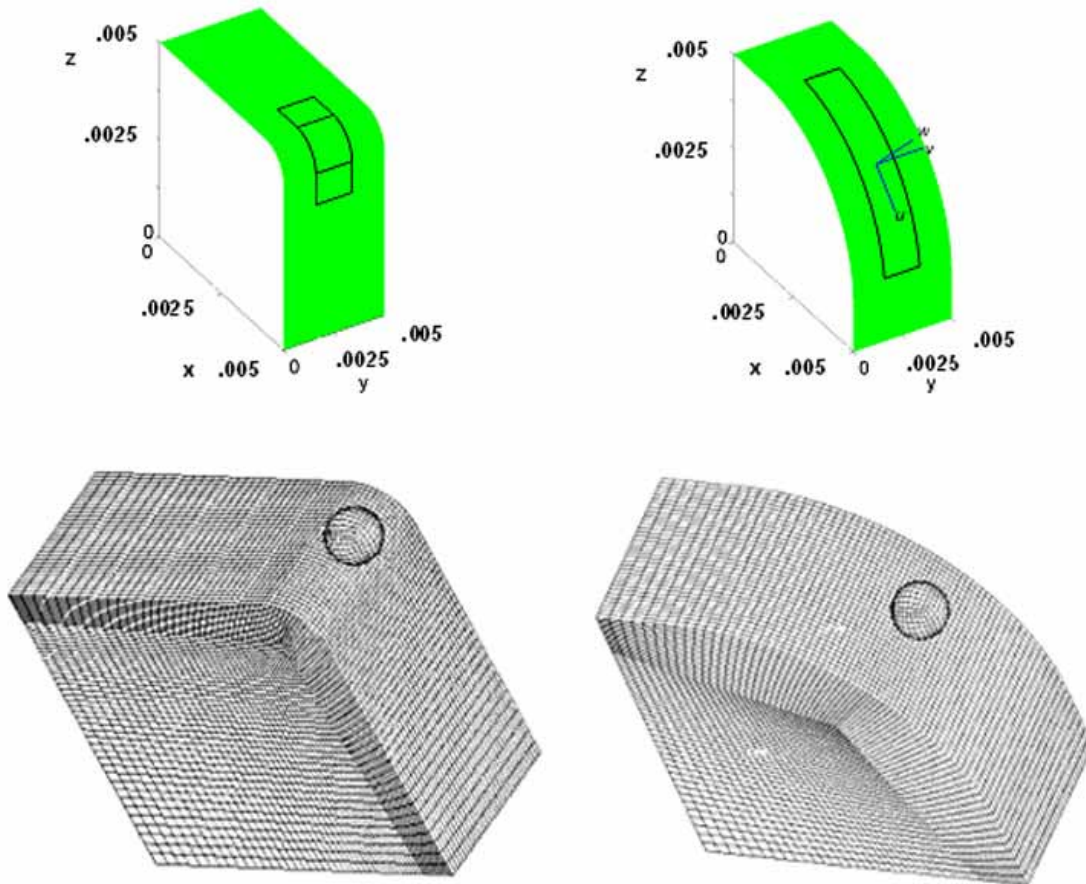


Figure 9.4-5 Dented Compression Panel



(a) Work-piece with edge radius $7.62E-4$ m. (b) Work-piece with edge radius $3.81E-3$ m.

Figure 9.4-6 Geometry Models and Finite Element Meshes for the Work-pieces With Rounded Edges

Table 9.4-2 Material Constitutive Law for the Work-piece.

True Stress (MPa)	0.	381.22	452.11	491.11	541.82	632.29	3.041E3	4.543E4
Plastic Strain	0.	7.08E-5	2.59E-3	1.07E-2	3.93E-2	1.28E-1	1.49	3.47

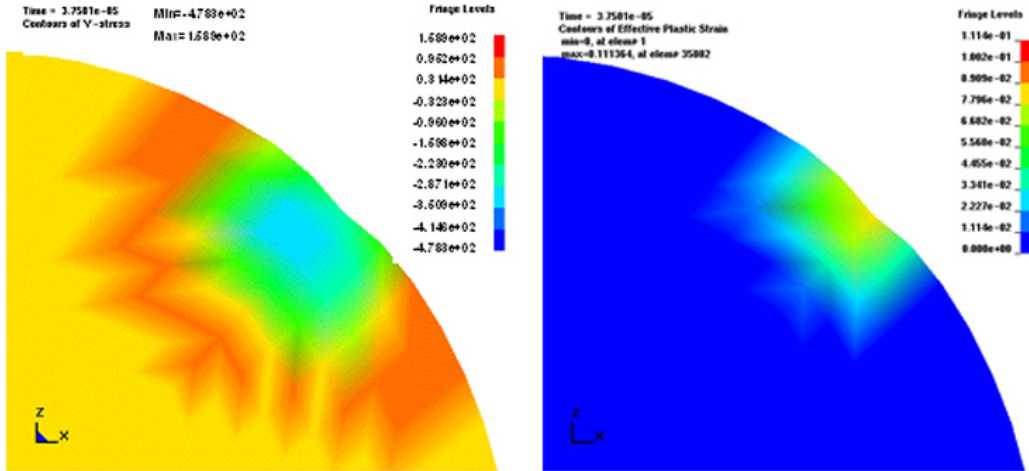


Figure 9.4-7 Mid-plane (Normal to y) Cross Sections of Axial Residual Stress σ_w and Plastic Strain ϵ^p Experienced by the Work-piece With Edge Radius 7.62E-4m

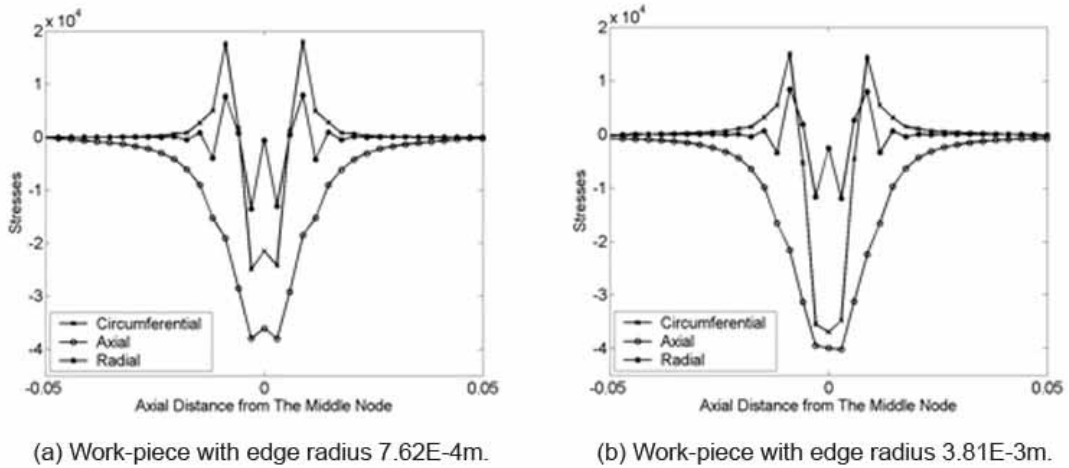


Figure 9.4-8 Stress State Along the Axial Line Through the Impact Center

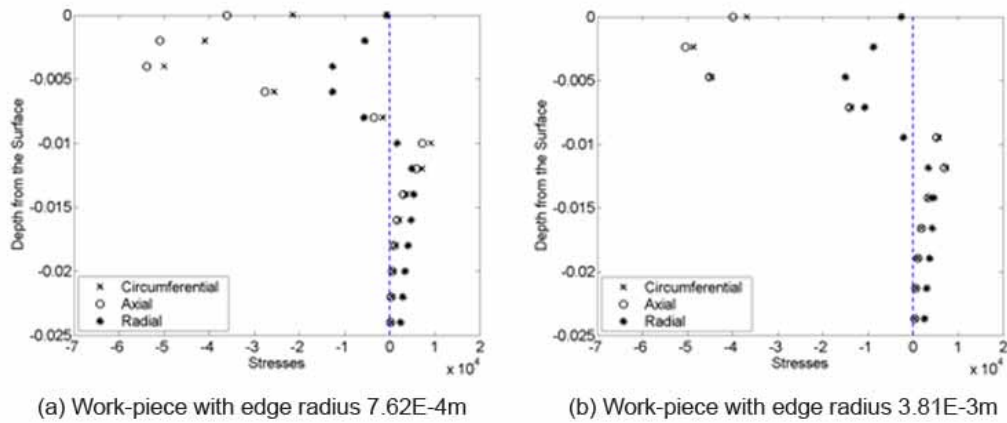


Figure 9.4-9 Circumferential, Axial and Radial Residual Stresses Beneath the Center Line of the Shot

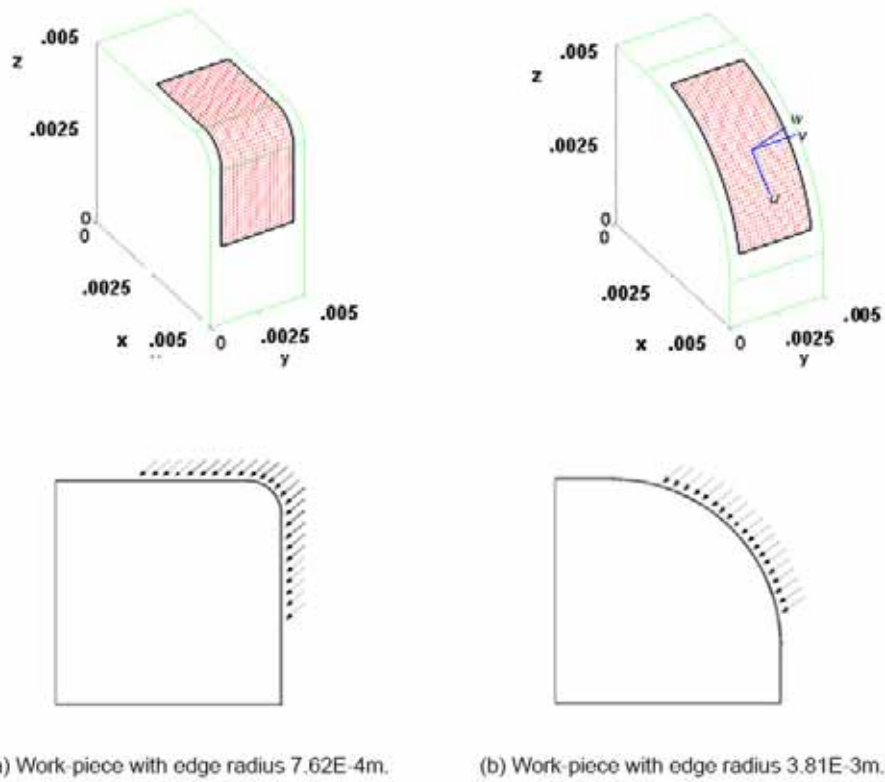


Figure 9.4-10 Coverage Areas and Impact Angles for the Multiple Impact Model

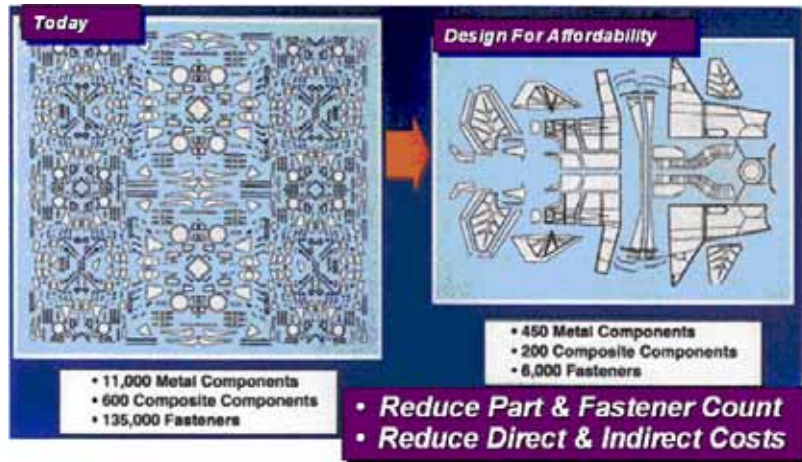


Figure 9.5-1 Composites Affordability Initiative's Technical Approach

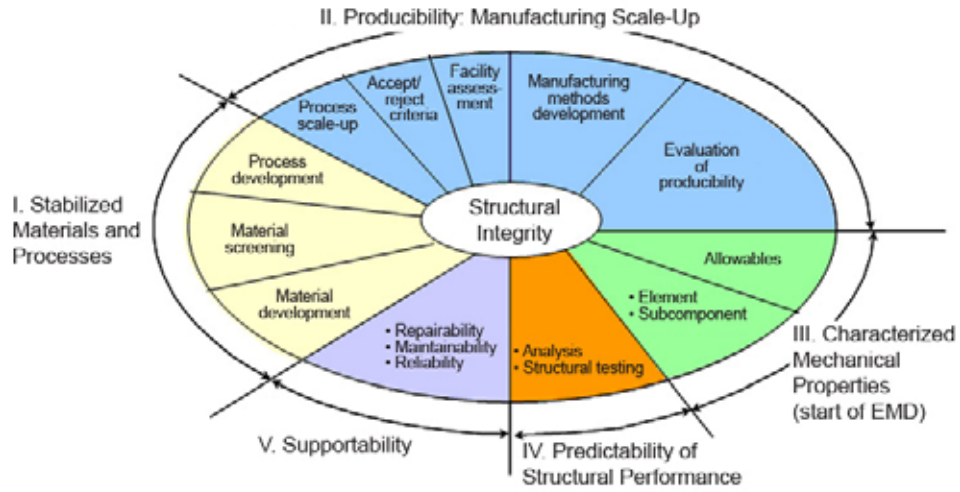


Figure 9.5-2 Structural Integrity Areas

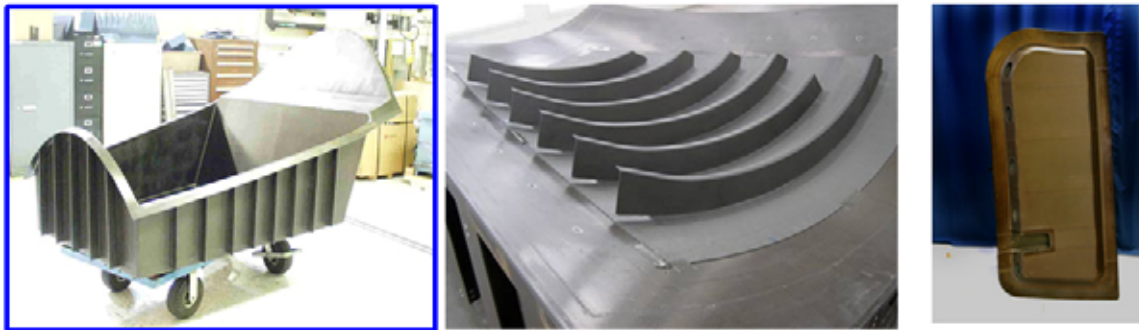


Figure 9.5-3 Aerospace VARTM Demonstration Parts

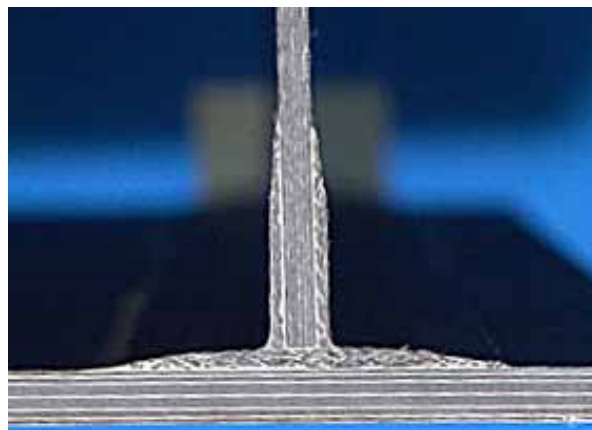


Figure 9.5-4 Cross Section of the Pi Joint

Table 9.5-1 Full-Scale Structural Testing of Pi-Joints

Test Article	Testing Performed
F-35 like wing (Figure 9.5-5, upper left)	Static and ballistic tolerance
F-35 like vertical tail (Figure 9.5-5, upper right)	Static, damage and fatigue
X-45A like wing carry through (Figure 9.5-5, lower left)	Static
X-45 wing (Figure 9.5-5, lower right)	Static, damage and fatigue (2 lifetimes)



Figure 9.5-5 Full-Scale Bonded Structure Demonstration Articles

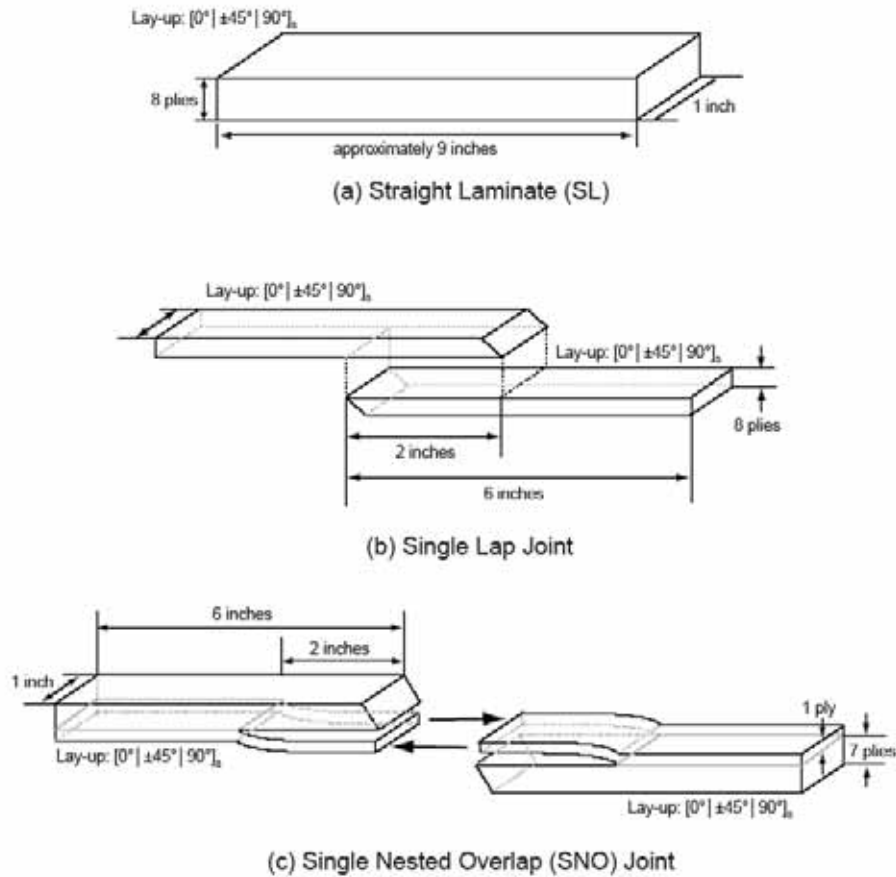


Figure 9.5-6 Illustration of Three Joint Configurations and Their Geometries

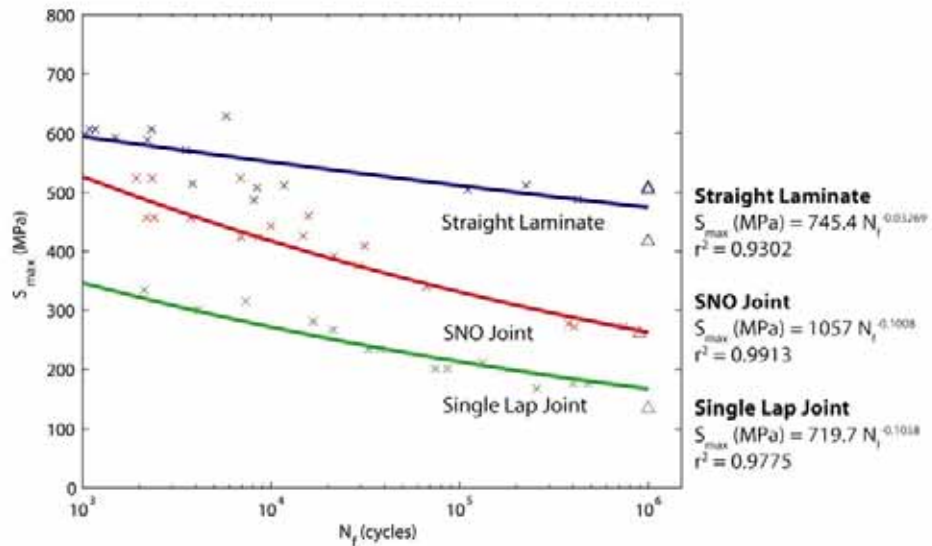


Figure 9.5-7 S-N Curve Comparison (Power Fit) for Three Joint Configurations

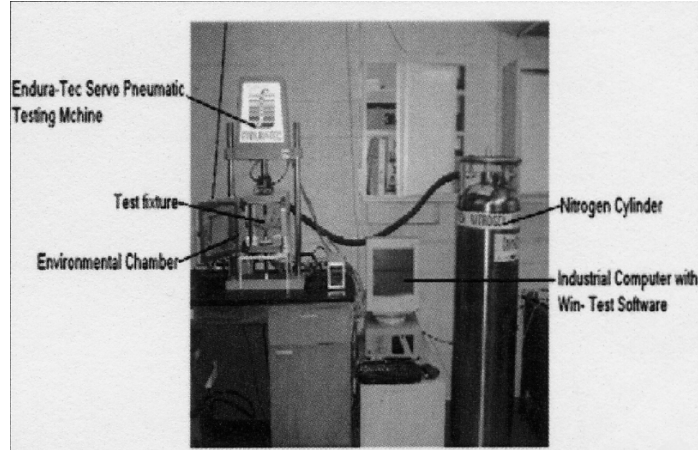


Figure 9.5-8 Experimental Set up for Four Point Static and Fatigue Testing

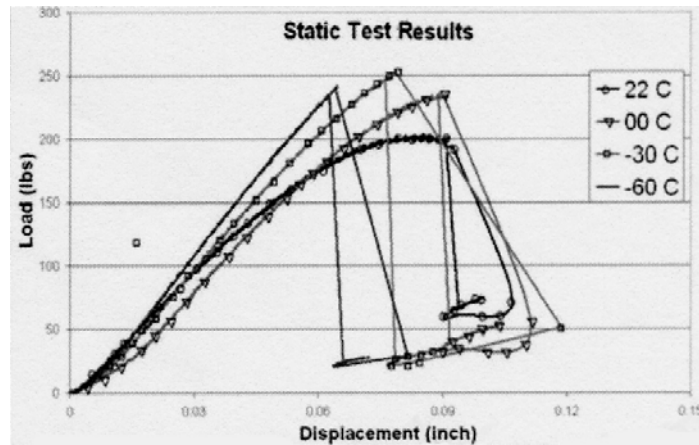


Figure 9.5-9 Static Flexure Test Results of CS Beams

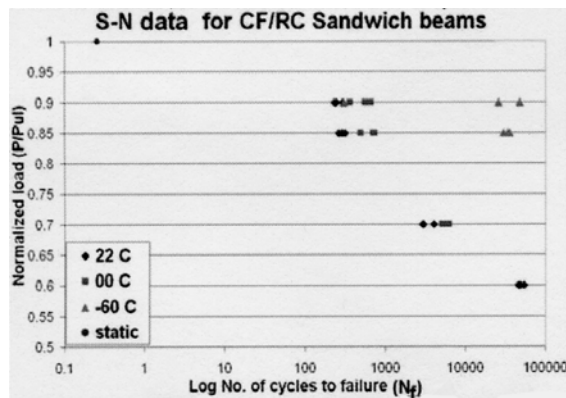


Figure 9.5-10 S-N Data for CF/RC Beams Showing Effects of Low Temperatures on Fatigue Life

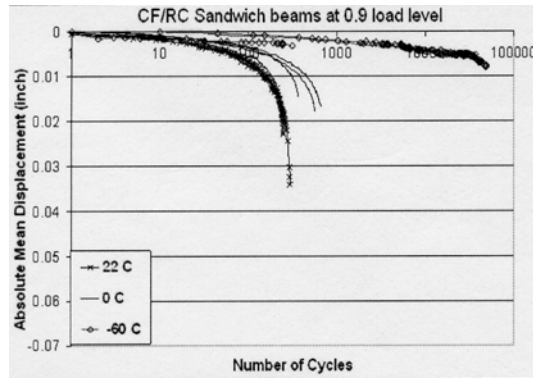


Figure 9.5-11 Absolute Mean Displacement vs. Number of Fatigue Cycles for CF/RC Beams at 0.9 Load Level and Different Temperatures

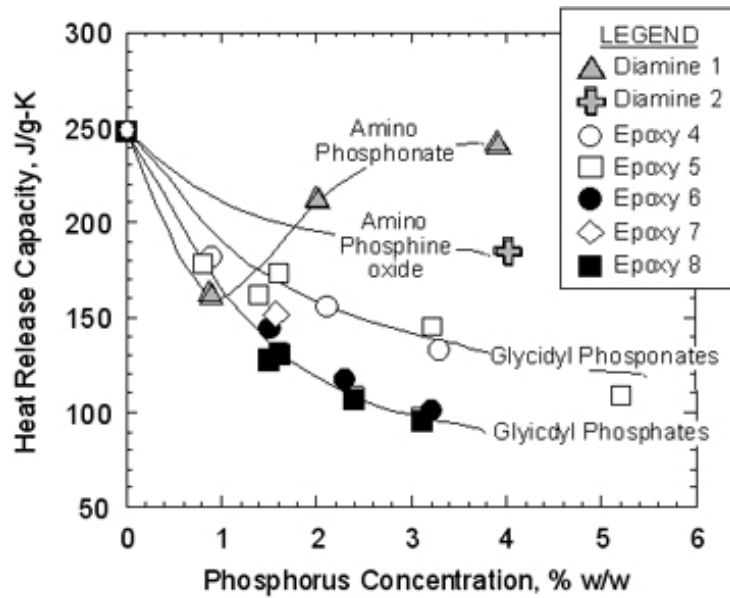


Figure 9.5-12 Heat Release Capacity vs. Phosphorus Concentration



Figure 9.6-1 US Coast Guard HC-130H Aircraft No. 1707

Table 9.6-1 Parameters and Their Sample Rates

Parameter	Sample Rate (Hz)	Record Rate (Hz)
Acceleration, N_z	32	32
Strains	32	32
RTDs	8	4
Pressure (PPT, RS-232)	4	4
Pressure (PTU200, RS-232)	4	4
GPS Data (RS-232)	4	4
True Airspeed	8	4
Weight on Wheels	8	4
Ramp Door Position	8	4
Flap Position Sensor	1024	1024

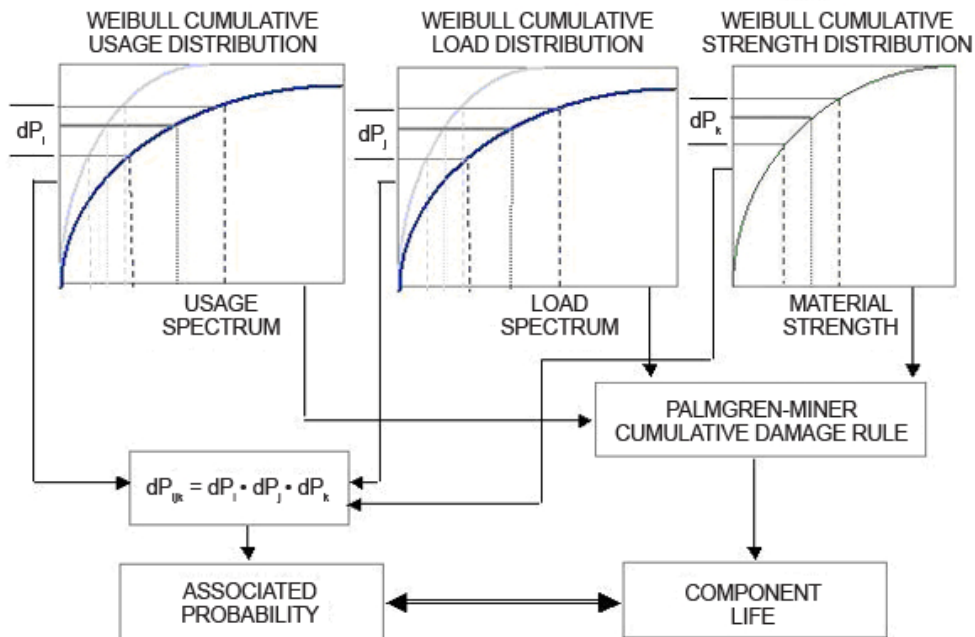


Figure 9.6-2 Life and Associated Probability

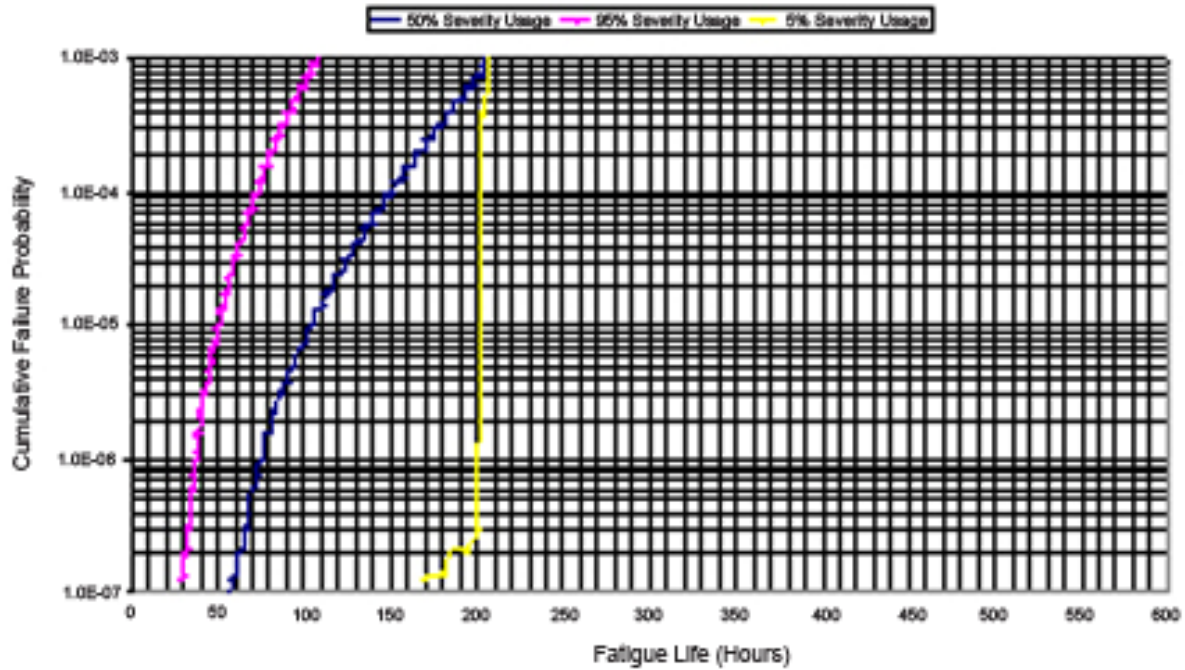


Figure 9.6-3 Cumulative Failure Probability Variation

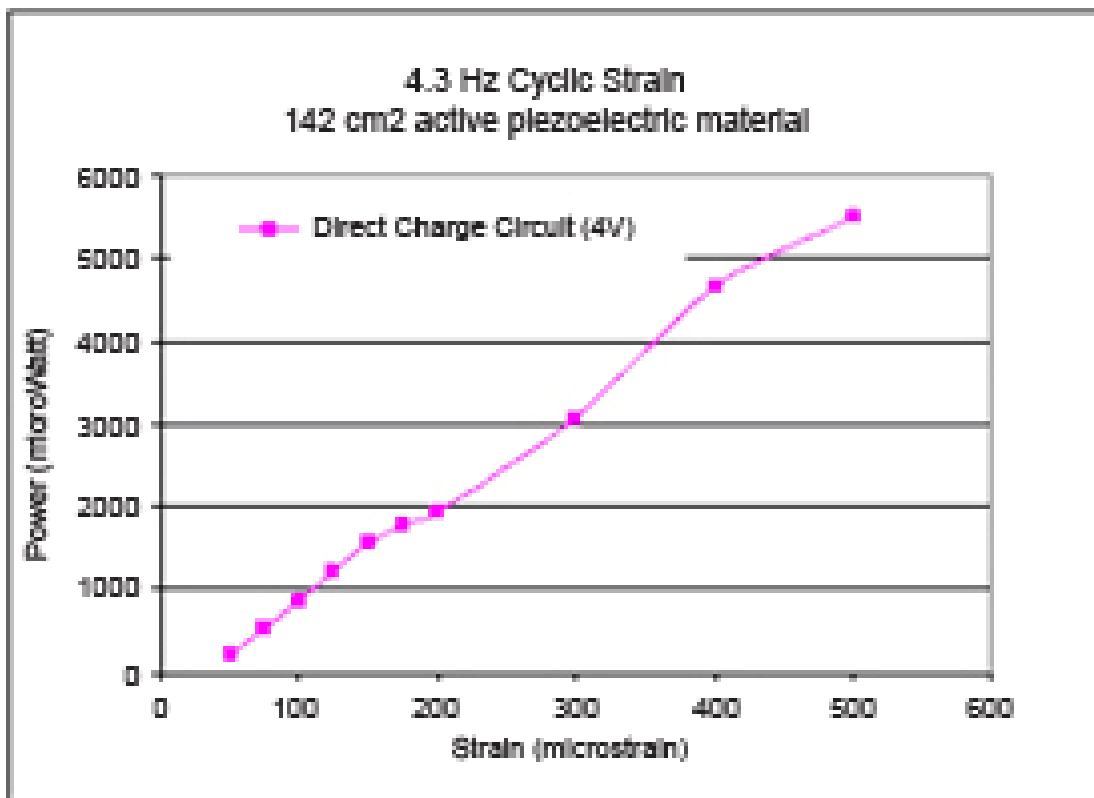


Figure 9.6-4 Power Output vs. Strain Amplitude



Figure 9.6-5 Bell Model 412 Experimental Rotorcraft

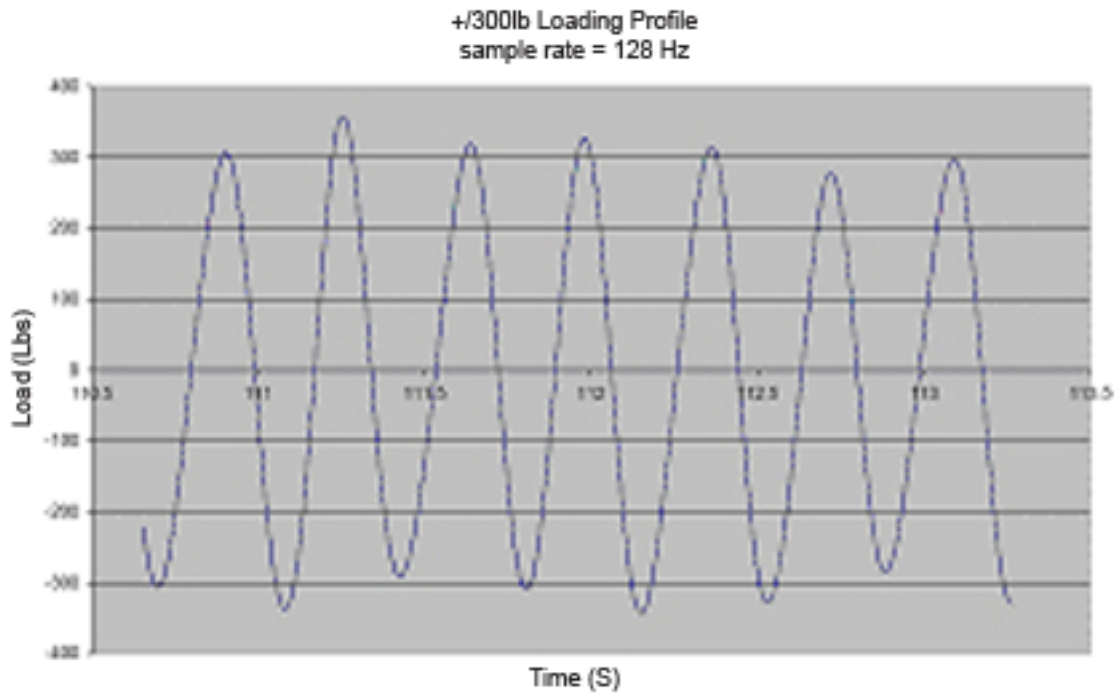


Figure 9.6-6 Pitch Link Measured Load

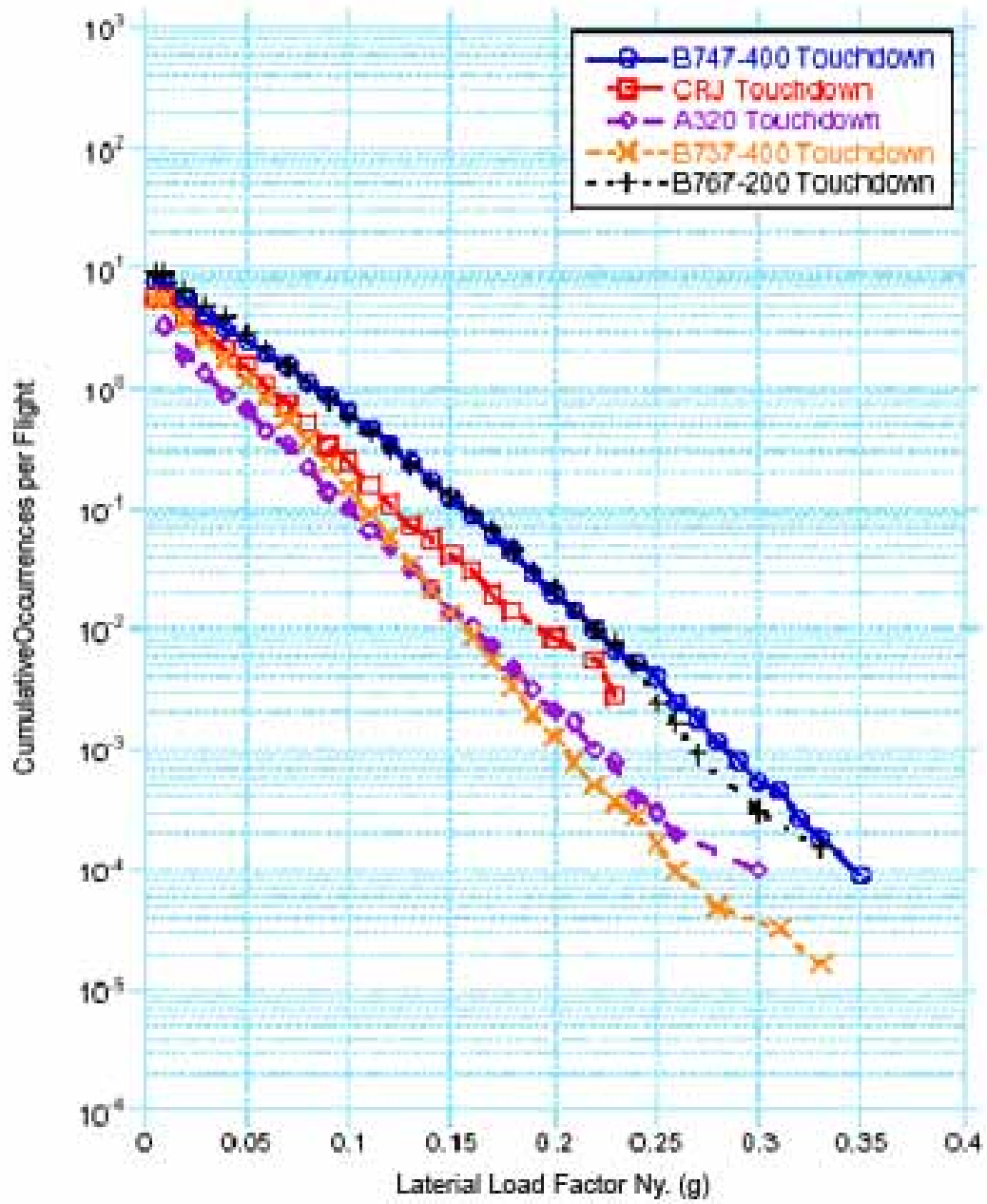


Figure 9.6-7 Cumulative Occurrences of Lateral Load Factor Per Flight During Touchdown

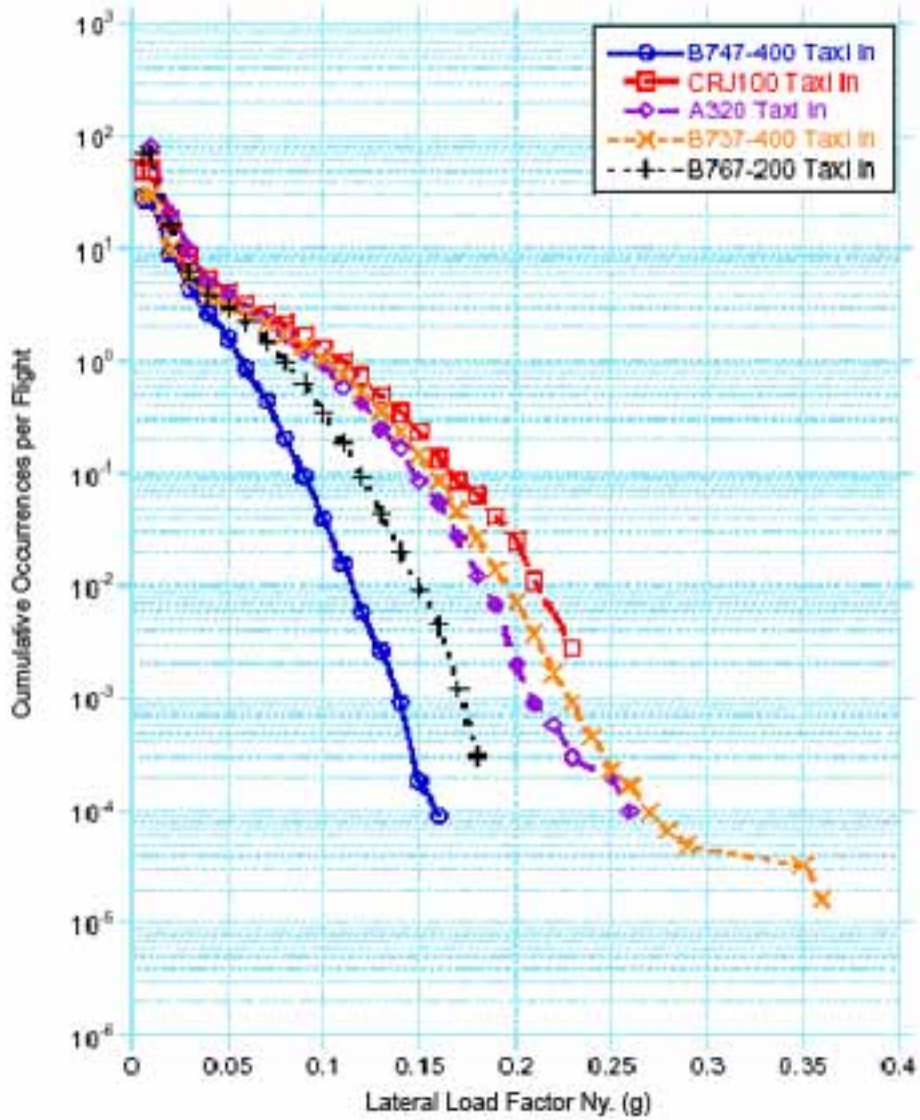


Figure 9.6-8 Cumulative Occurrences of Lateral Load Factor Per Flight During Taxi-in



Figure 9.7-1 SCC and Exfoliation Damage Findings From T-37B Teardown Program Phase I



Figure 9.7-2 Delivery of Phase II Aircraft to CASTLE

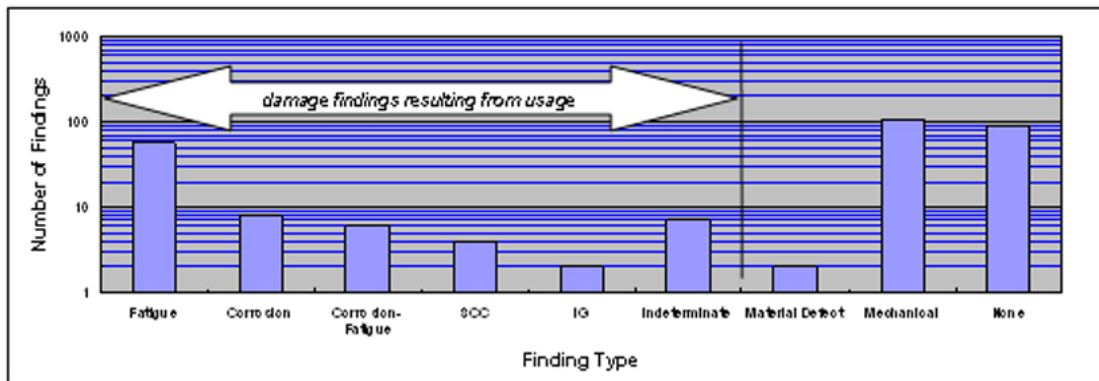


Figure 9.7-3 Summary of the Results of All NDI Indication Evaluations Shown by Finding Category



Figure 9.8-1 Example of POD Test Specimens Used in Blind Study



Figure 9.8-2 Crack Detection Application on 206 Tail Boom Using Modified Eddy Current Sliding Probe (Walking Probe) to Inspect Lap Joint

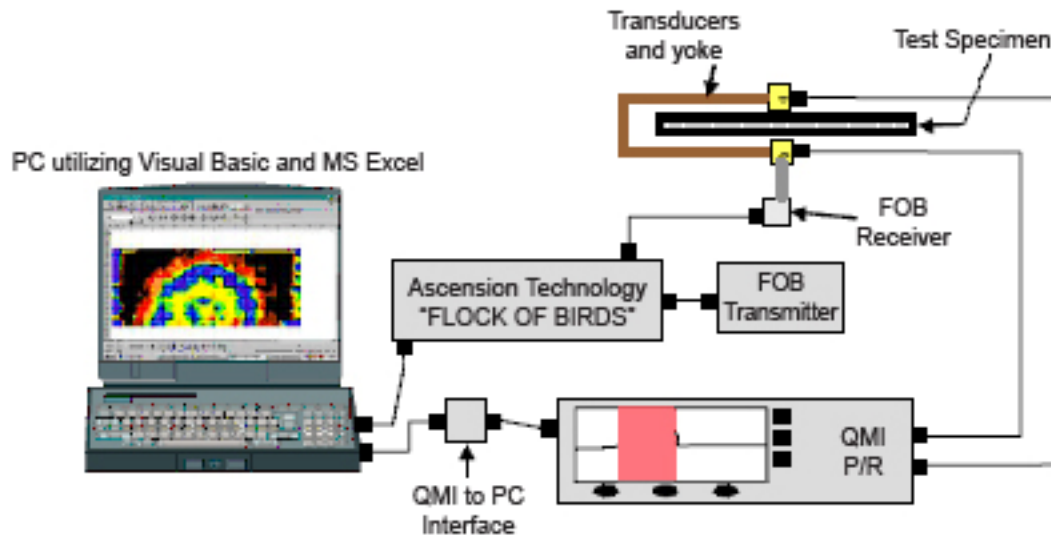


Figure 9.8-3 System Configuration of Air Coupled Ultrasound System

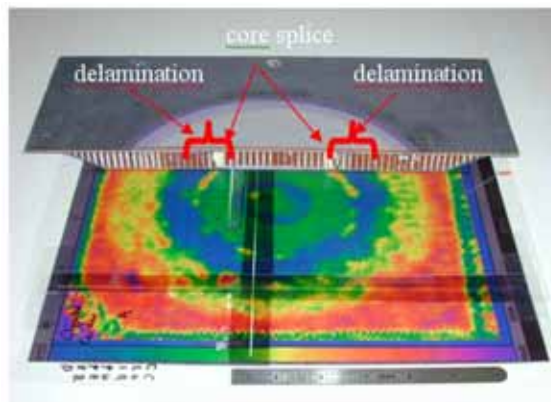


Figure 9.8-4 ACUT Image of Repaired Honeycomb Panel Compared to Actual Sectioned Repair

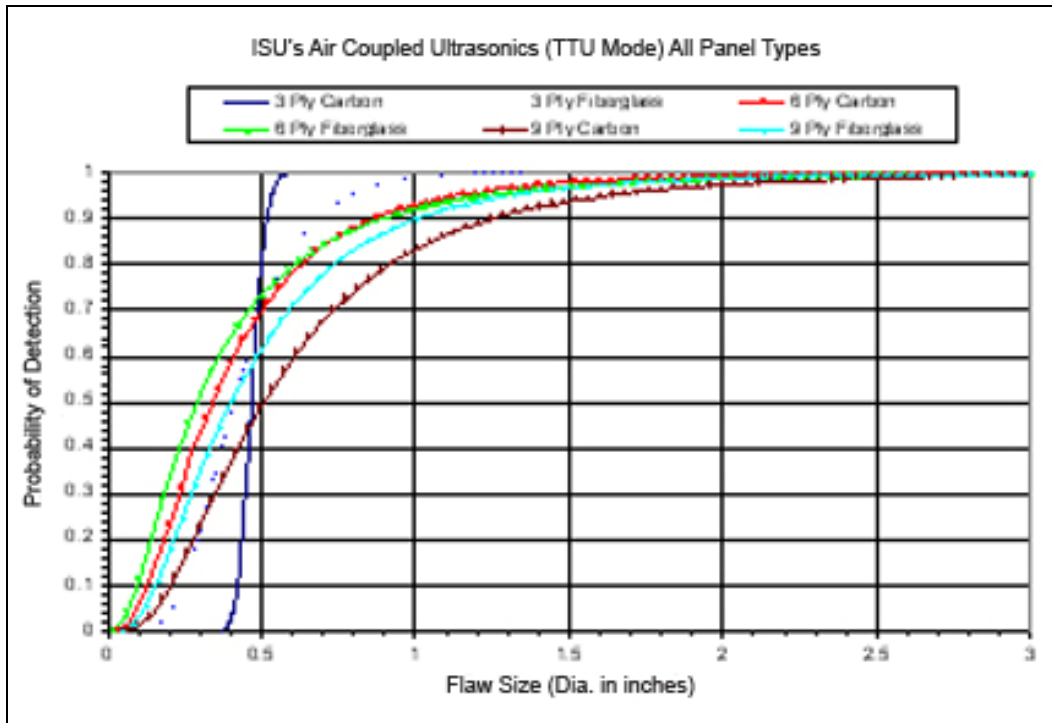


Figure 9.8-5 POD Curves of ACUT System Based on Honeycomb Reliability Experiment Panels



Figure 9.10-1 Crack in Rear Fairing

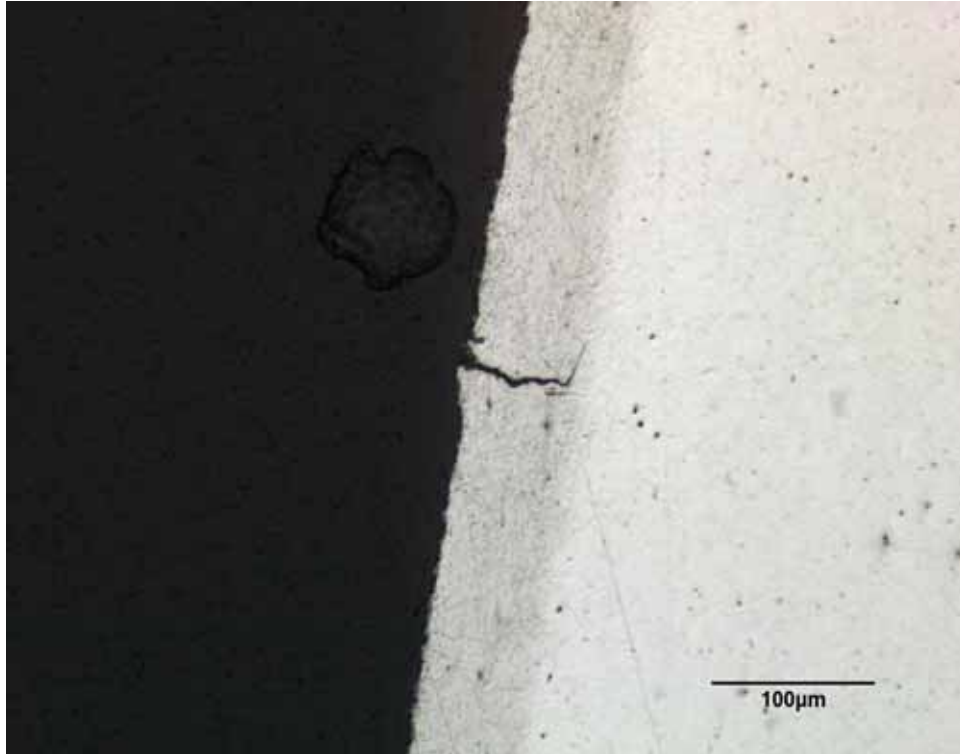


Figure 9.10-2 Surface Crack - Magnification 250X

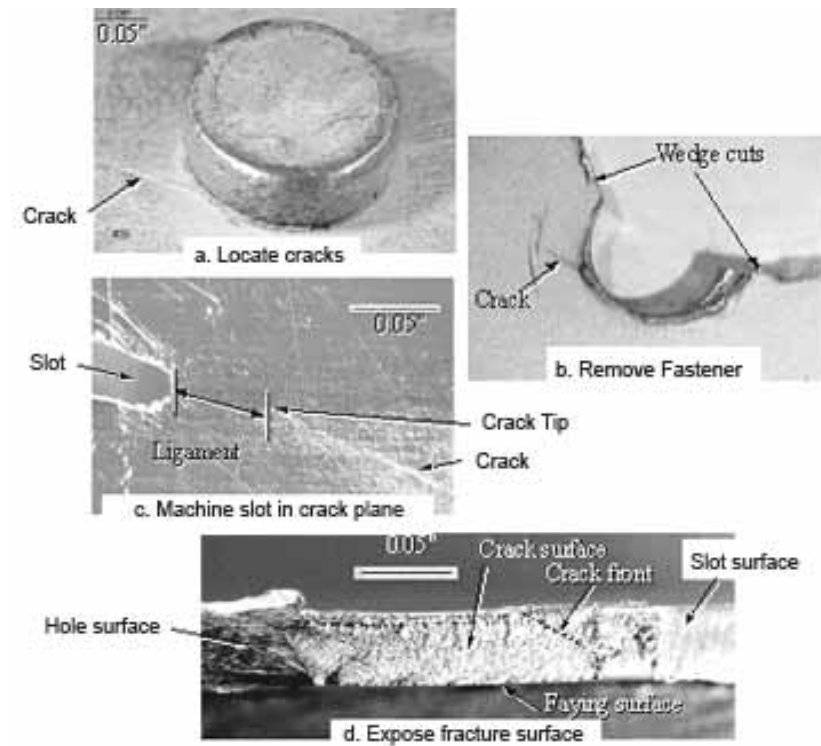


Figure 9.11-1 Steps in Teardown Procedure

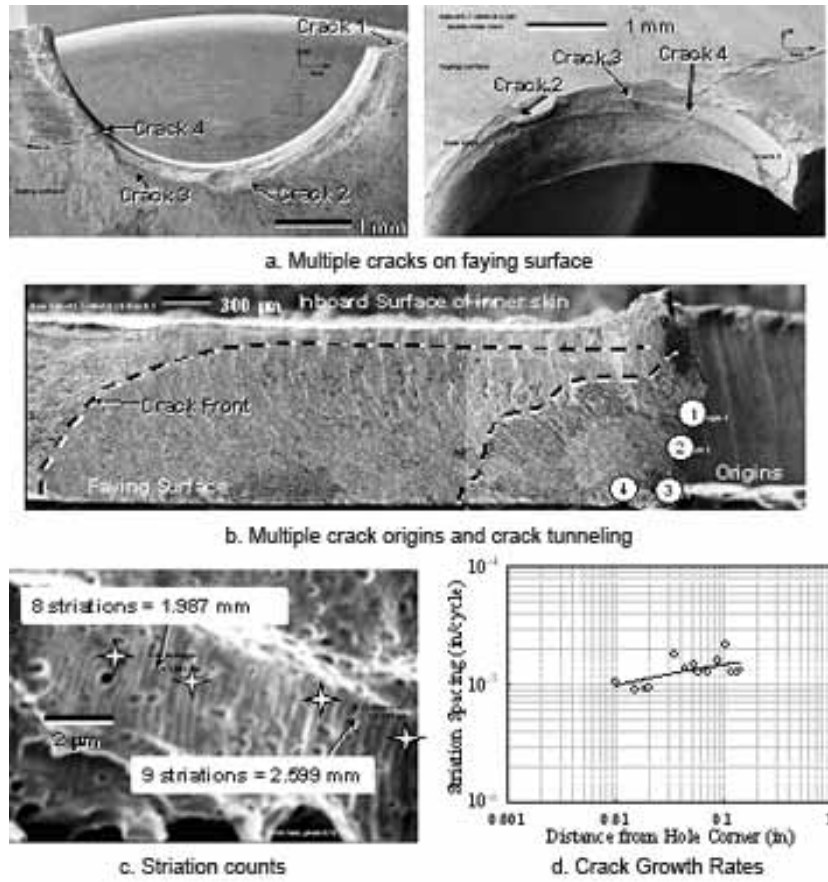


Figure 9.11-2 Typical Crack Information Obtained in Study

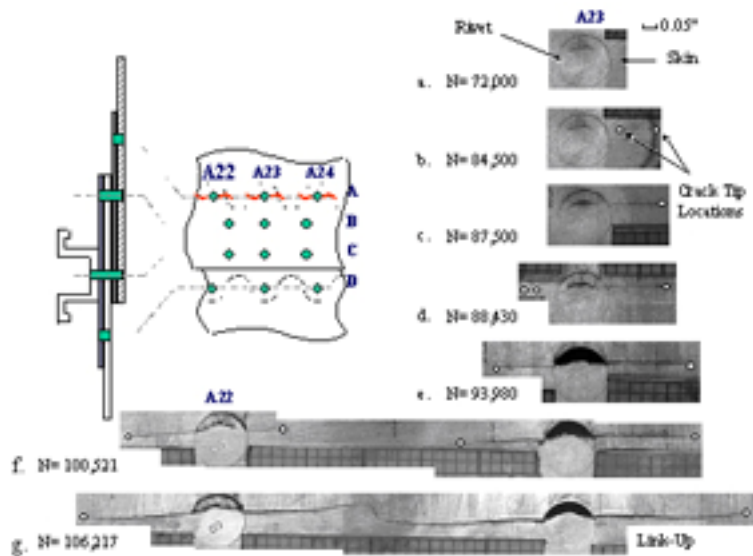


Figure 9.11-3 Damage Growth to First Link-up

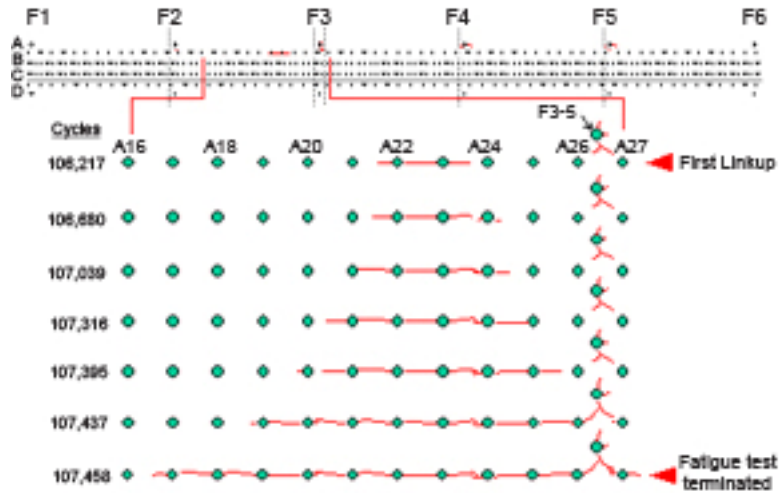


Figure 9.11-4 Damage Evolution After First Link-up

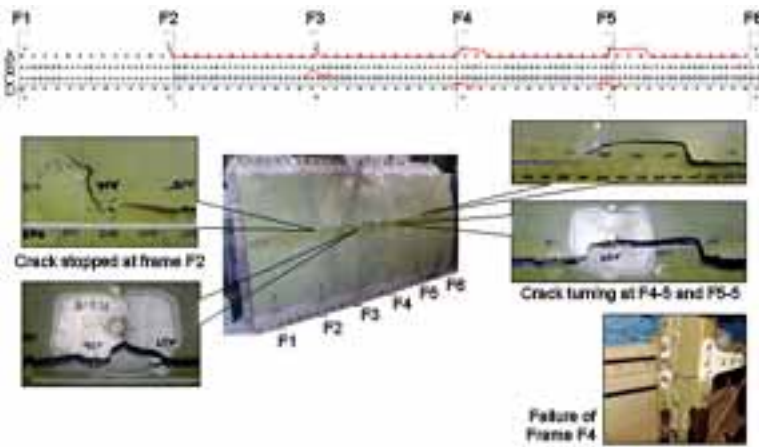


Figure 9.11-5 Final State of Damage at End of Residual Strength Test

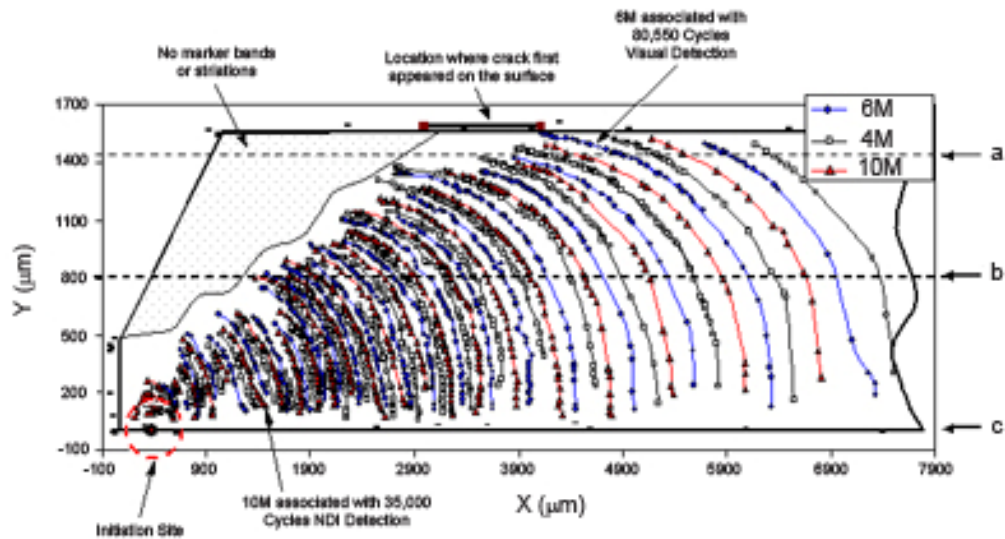


Figure 9.11-6 A Plot of Marker Band Locations

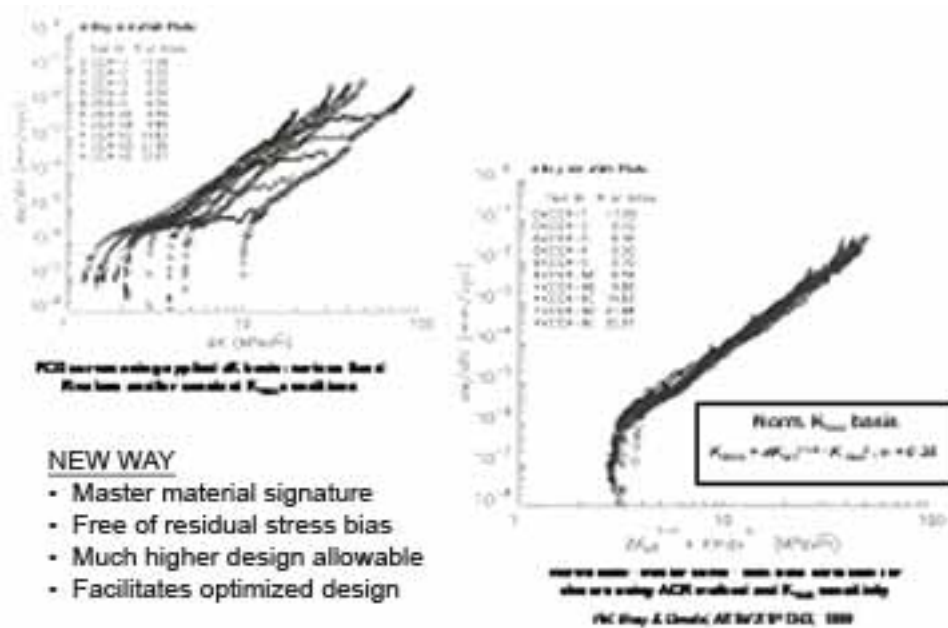


Figure 9.12-1 Concept of “Master FCGR Curve” Using ΔK_{acr} (ACR) & K_{max} Sensitivity to Collapses All Test Data

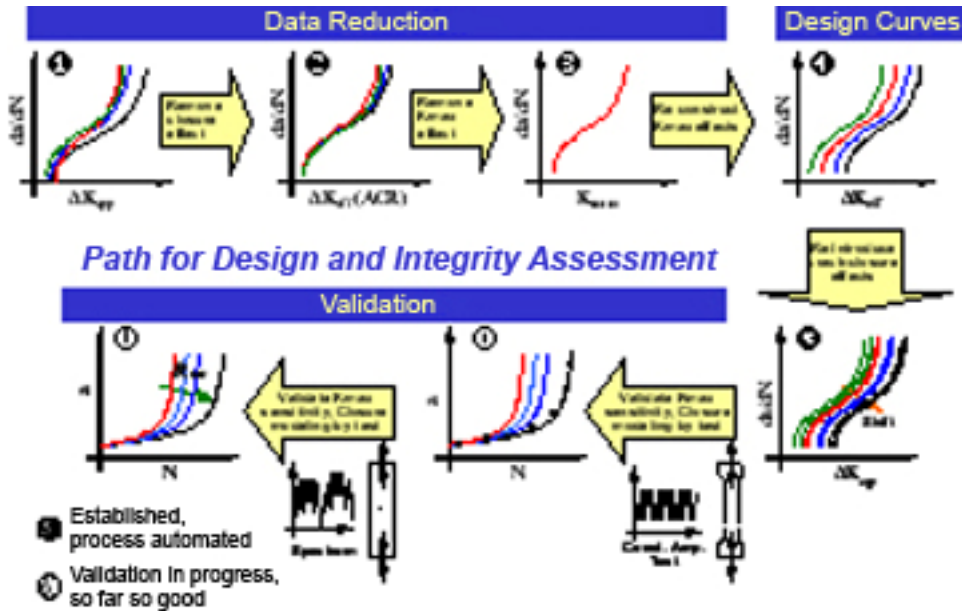


Figure 9.12-2 Proposed Data Reduction and Analysis Methodology, Including Validation Path to Account for Residual Stress Effects in Design of Large Monolithic Components

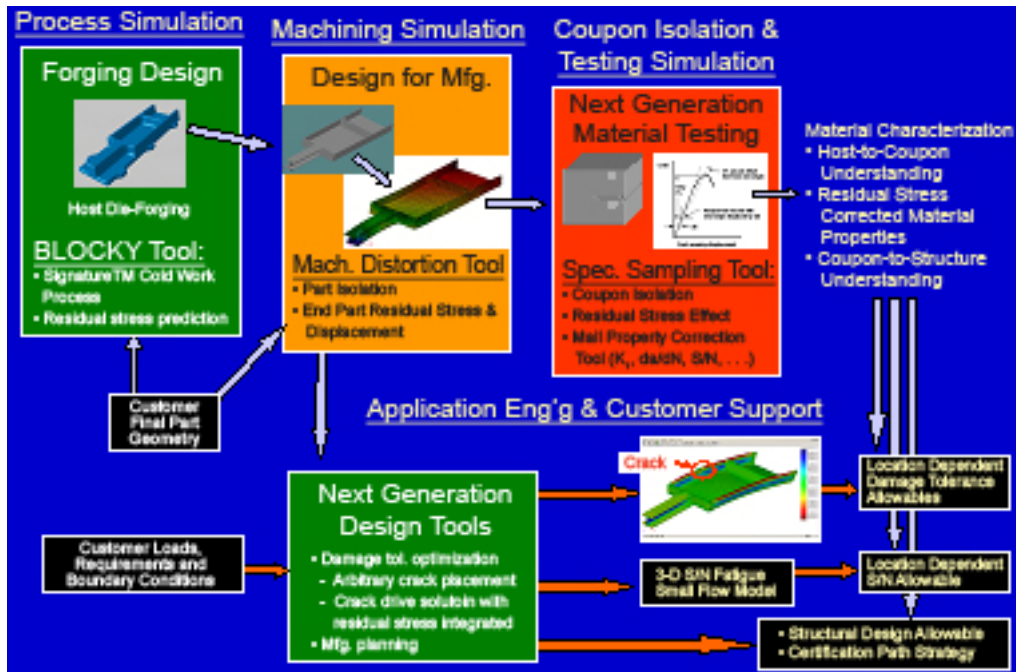


Figure 9.12-3 Alcoa Vision - Virtual Design Support for Monolithic Parts (Forging Example)

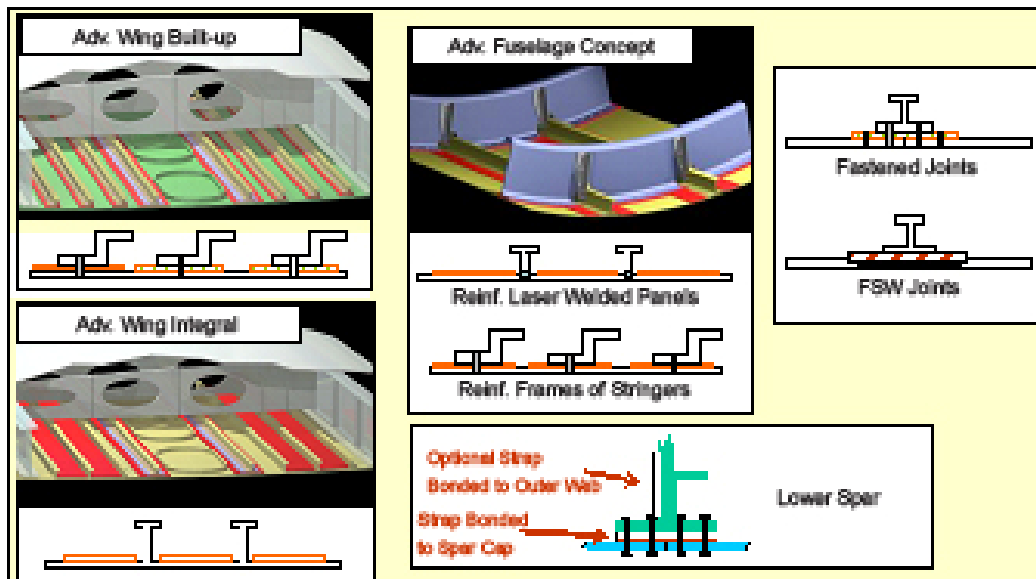


Figure 9.12-4 Selective Reinforcement Concept

- Bonding of crack resistant straps - Fiber Metal Laminate (e.g., GLARE)
- Applied only to “problem” areas to improve structure performance
 - Improves static & residual strength, *the latter especially for integral stiffening*
 - Greatly slows crack growth through fiber bridging
- Under development: high modulus strap mat to offload skin & stiffeners

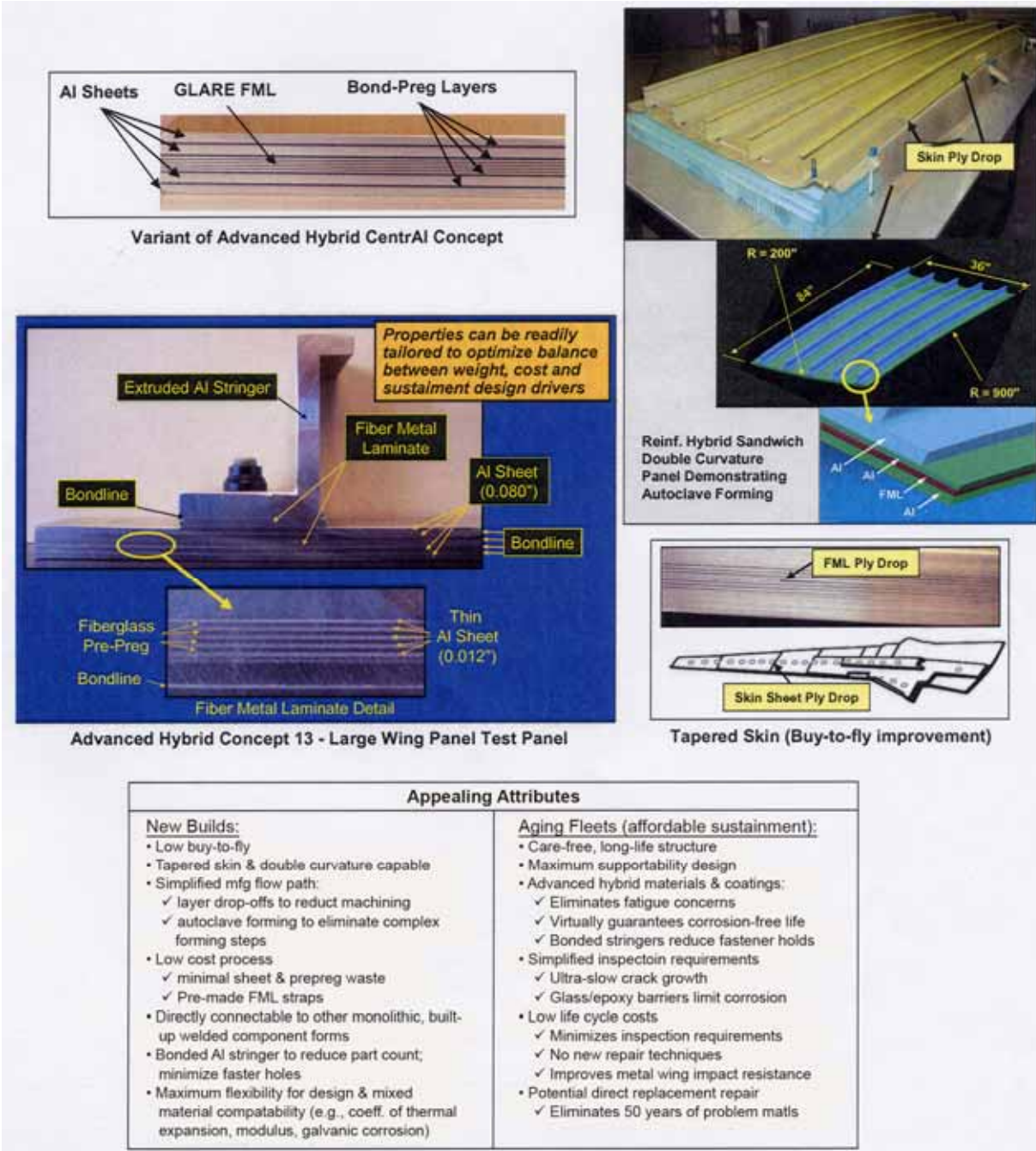


Figure 9.12-5 Further Opportunities - Alcoa Advanced Hybrid Laminate



Figure 9.12-6 Alcoa Large-Scale Proof-of-Concept Testing - Adv. Lower Wing

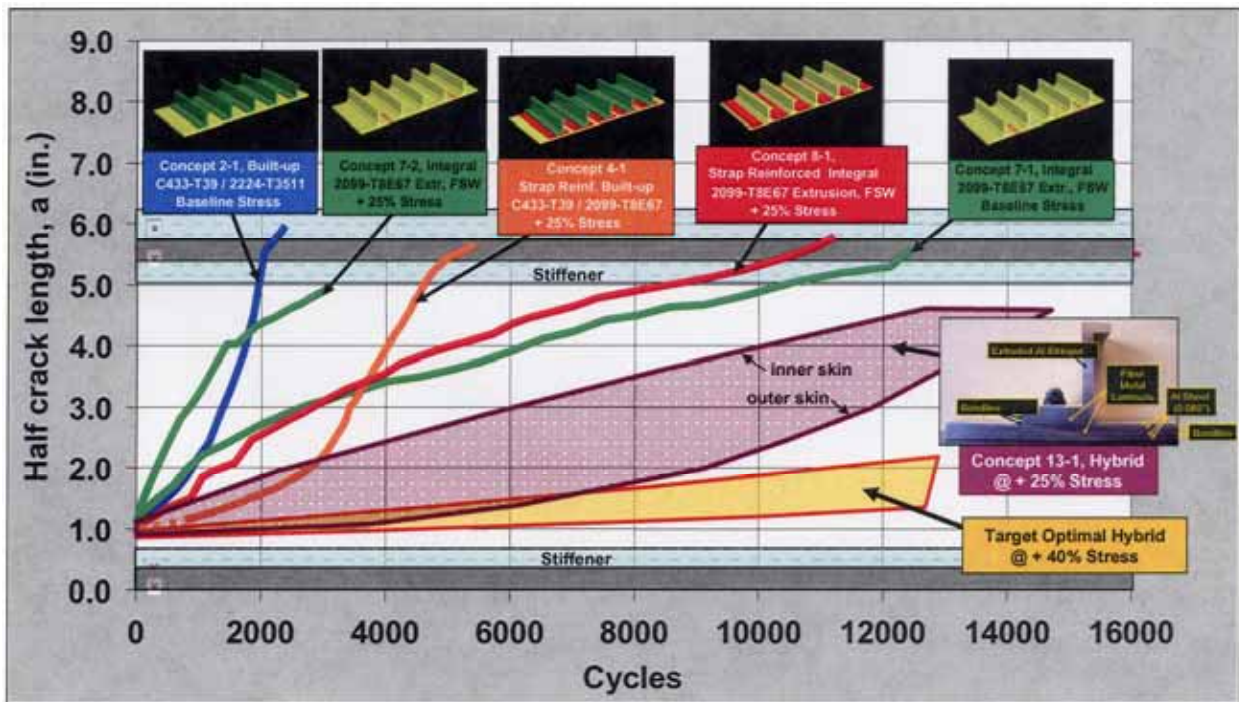


Figure 9.12-7 Alcoa Adv. Lower Wing Concept FCG Test Program
 Central Crack 30"x90" Stiffened Wing Panel
 Baseline: $S_{max} = 17$ ksi, $S_{min} = -6$ ksi (mimics GAG cycle); RH > 90%

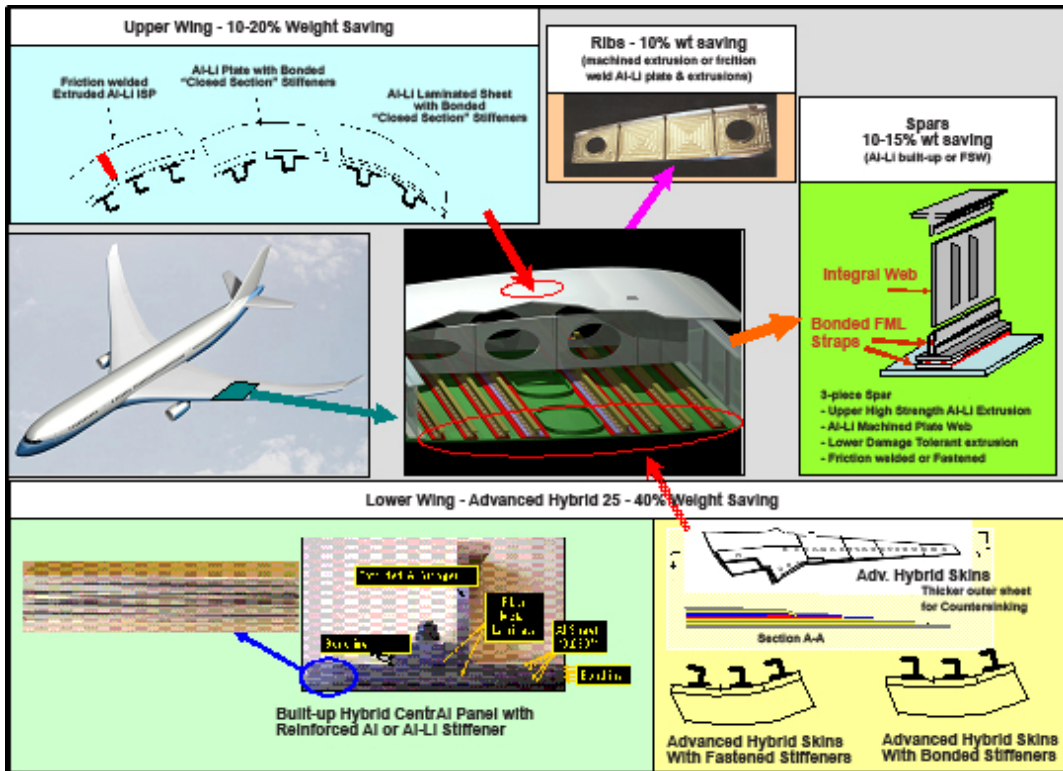


Figure 9.12-8 Alcoa “Best Wing Box” Concept

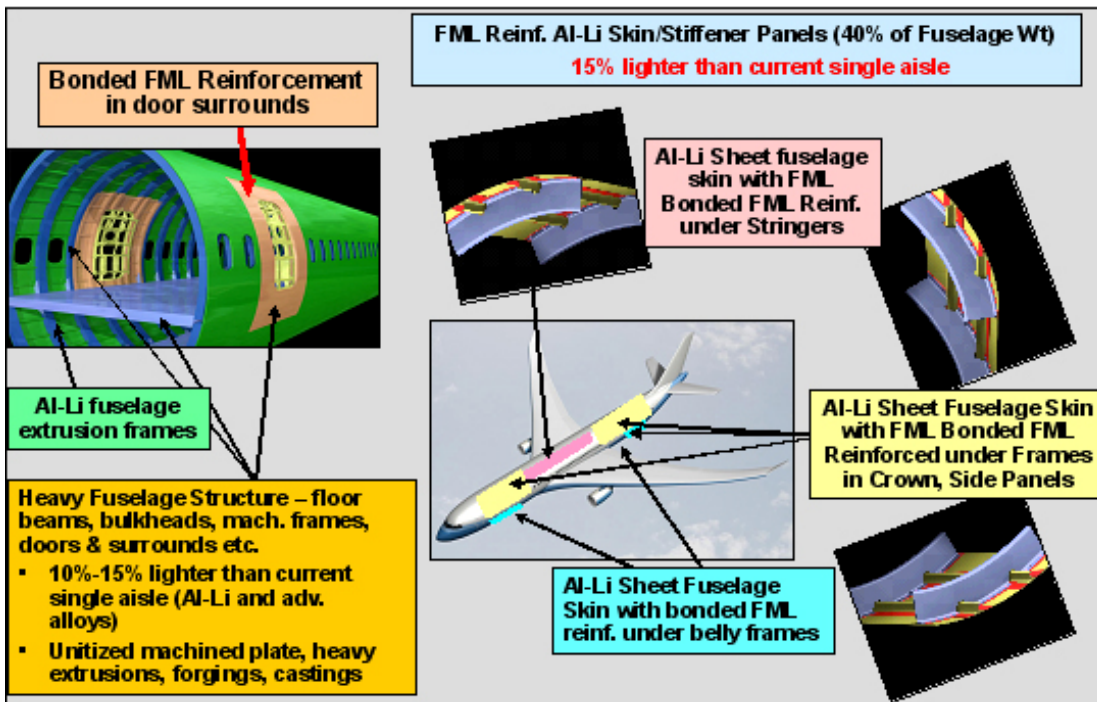


Figure 9.12-9 Alcoa “Best Fuselage Barrel” Concept